Traitement Endovasculaire des Malformations Artérioveineuses Cérébrales par Voie Veineuse : Développement d'un Nouvel Modèle in Vitro

Rodrigo Rivera Miranda

PhD Thesis

Université de Limoges

ED 652 - Biologie, Chimie, Santé (BCS)

CNRS XLIM UMLR 7252

A thesis submitted to University of Limoges in partial fulfillment of the requirements of the degree of Philosophy Doctor (PhD).

Innovation Technologique et Thérapeutique

Presented and defensed by

Rodrigo RIVERA

On December 11, 2023

Traitement Endovasculaire des Malformations Artérioveineuses Cérébrales par Voie Veineuse. Développement d'un Nouvel Modèle pour la Embolisation par Voie Veineuse

Transvenous Embolization of Brain Arteriovenous Malformations. Development of a Novel Model for Transvenous Embolization

Thesis supervisor: Prof. Charbel MOUNAYER et Prof. Aymeric ROUCHAUD

President of jury: M. Jean Christophe Gentric, Professor, Service de Neuroradiologie, Université de Brest, France.

JURY:

President of jury

M. Jean Christophe Gentric, Professor, Service de Neuroradiologie, Université de Brest, France.

Reporters

M. Frédéric Clarençon, Professor, Service de Neuroradiologie Interventionnelle, Hôpital La Pitié Salpetrière, Paris, France.

Mme. Christina Iosif, Professor, CHU de Martinique, France.

Examiners

M. Charbel Mounayer, Professor, Service de Neuroradiologie, CHU Limoges, France

M. Aymeric Rouchaud, Professor, Service de Neuroradiologie, CHU Limoges, France

Mme. Chrysanthi Papagiannaki, CHU Charles Nicolle, Rouen France.

To my three boys, Lucas, Agustin, and Santiago. Keep learning, question all, be uncomfortable, be humble.

To Catalina, my love, for pushing me to be here. Without you, I would not have even started this journey.

To my parents, who always taught me to give my best and brought me the opportunities of my earliest education and growth.

All models are wrong, but some are useful.

George E.P.Box

A person who never made a mistake never tried anything new.

Albert Einstein

TABLE OF CONTENTS

List of Figures

List of Tables

Acknowledgements

I would like to thank my teachers and guides, Prof Charbel Mounayer and Prof Aymeric Rouchaud for being a strong support during complicated times. For conducting my thesis and for being a real role model for research in interventional neuroradiology.

Thanks to Alvaro Cespedes, for managing all computer designs of BAVM models. For translating ideas to great designs.

A sincere thanks to Juan Pablo Cruz, for the support in writing and reviewing all the manuscripts, but also for all the friendship advice.

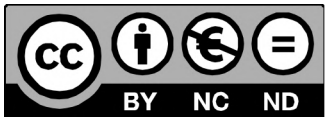

ABSTRACT

Brain Arteriovenous Malformations (BAVM) are rare but significant vascular anomalies that can lead to severe neurological consequences. Managing them has been challenging, and endovascular treatment has emerged as a cornerstone approach. Endovascular embolization, involving the use of liquid materials that solidify inside the vessels, can partially or completely occlude a BAVM. The arterial route has traditionally been the primary access point for treating BAVMs. However, in recent years, transvenous embolization (TVE) has revolutionized the treatment of selected cases, yielding excellent curative results. This approach, involving endovascular embolization from the venous side in a counterflow manner, demands advanced operator skills.

When we initiated this study, there were no BAVM models suitable for teaching or training in TVE. The objective of our thesis was to develop a new BAVM model for TVE. Our central research question was whether it was possible to create a new BAVM model for transvenous embolization.

As an initial part of the thesis, we conducted extensive research, were we systematically examined all the models employed in BAVM studies. We observed that endovascular models predominantly featured the utilization of the rete mirabile in swine, and that in vitro models had not been widely utilized for this purpose. Three-dimensional printing appeared to be an attractive technique for creating new models, cheaper and more accessible than animals; however, no effective models with hollow channels had been developed using this technology.

We discovered that a specialized 3D printing technique known as Stereolithography (SLA) had been used to create objects with small channels for a field called Millifluidics. Given that creating small hollow channels has been a technological challenge and achievement in millifluidic, we chose to utilize SLA to develop a novel vascular model. We began with simple

container designs, which we referred to as 'chips,' featuring inner hollow tubes. Over time, we incorporated softer curves and more organic structures to simulate a BAVM, with the classical elements of arterial feeders, nidus, and draining veins.

On a second phase of our research, we tested our initial BAVM chip model using the transarterial route embolization within a closed circuit and we were able to confirm its structural and functional reliability. This study was used as a proof of concept that the model could be employed for training, teaching, and research in BAVM embolization.

Through an iterative design process, we reached the final evolution of the BAVM model, where we were able to transfer real patient image data into a computational design and 3D print it. This model was connected to a system with a pump, enabling us to replicate the vascular environment of transvenous embolization. We successfully demonstrated the feasibility of TVE using microcatheters and liquid embolic agents. This accomplishment marked the creation and testing of the first in vitro BAVM model for TVE using 3D printing, successfully answering our research question.

This unique and innovative model opens new possibilities for teaching, learning, training, and research in endovascular treatment for BAVMs.

RÉSUMÉ.

Les malformations artérioveineuses cérébrales (MAVC) sont des anomalies vasculaires rares mais significatives pouvant entraîner de graves conséquences neurologiques. Leur prise en charge a été un défi, et le traitement endovasculaire s'est imposé comme une approche essentielle. L'embolisation endovasculaire, impliquant l'utilisation de matériaux liquides qui se solidifient à l'intérieur des vaisseaux, peut partiellement ou complètement obstruer une MAVC. La voie artérielle a traditionnellement été le principal point d'accès pour traiter les MAVC. Cependant, ces dernières années, l'embolisation transveineuse (ETV) a révolutionné le traitement de certains cas, obtenant d'excellents résultats curatifs. Cette approche, impliquant l'embolisation endovasculaire du côté veineux de manière à contre-courant, exige des compétences avancées de l'opérateur.

Lorsque nous avons lancé cette étude, il n'existait aucun modèle de MAVC adapté à l'enseignement ou à la formation en ETV. L'objectif de notre thèse était de développer un nouveau modèle de MAVC pour l'ETV. Notre question de recherche centrale était de savoir s'il était possible de créer un nouveau modèle de MAVC pour l'embolisation transveineuse.

Dans une première partie de la thèse, nous avons mené des recherches approfondies, examinant systématiquement tous les modèles utilisés dans les études sur les MAVC. Nous avons observé que les modèles endovasculaires utilisaient principalement le rete mirabile chez le cochon, et que les modèles in vitro n'étaient pas largement utilisés à cette fin. L'impression 3D semblait être une technique attrayante pour créer de nouveaux modèles, moins chère et plus accessible que les animaux ; cependant, aucun modèle efficace avec des canaux creux n'avait été développé en utilisant cette technologie.

Nous avons découvert qu'une technique d'impression 3D spécialisée appelée stéréolithographie (SLA) avait été utilisée pour créer des objets avec de petits canaux pour un domaine appelé millifluidique. Étant donné que la création de petits canaux creux était un défi technologique et une réalisation en millifluidique, nous avons choisi d'utiliser la SLA pour développer un nouveau modèle vasculaire. Nous avons commencé avec des conceptions de conteneurs simples, que nous avons appelées « puces », comportant des tubes internes creux. Au fil du temps, nous avons incorporé des courbes plus douces et des structures plus organiques pour simuler une MAVC, avec les éléments classiques des artères d'alimentation, du nidus et des veines de drainage.

Dans une deuxième phase de nos recherches, nous avons testé notre modèle initial de puce de MAVC en utilisant l'embolisation par voie transartérielle dans un circuit fermé et nous avons pu confirmer sa fiabilité structurelle et fonctionnelle. Cette étude a servi de preuve de concept que le modèle pouvait être utilisé pour la formation, l'enseignement et la recherche en embolisation de MAVC.

Grâce à un processus de conception itératif, nous sommes parvenus à la dernière évolution du modèle de MAVC, où nous avons pu transférer des données d'image de patients réels dans une conception informatique et l'imprimer en 3D. Ce modèle était connecté à un système avec une pompe, nous permettant de reproduire l'environnement vasculaire de l'embolisation transveineuse. Nous avons réussi à démontrer la faisabilité de l'ETV en utilisant des microcathéters et des agents emboliques liquides. Cette réalisation a marqué la création et le test du premier modèle in vitro de MAVC pour l'ETV utilisant l'impression 3D, répondant ainsi avec succès à notre question de recherche.

Ce modèle unique et innovant ouvre de nouvelles possibilités pour l'enseignement, l'apprentissage, la formation et la recherche dans le traitement endovasculaire des MAVC.

Chapter I. Introduction to Brain Arteriovenous Malformations

Brain arteriovenous malformations (BAVMs) are complex vascular lesions, implying an abnormal connection between arteries and veins with an interposed tangle of disorganized vascular vessels, the so-called nidus, by-passing the normal capillary system, leading to an arteriovenous shunt[1] (Figure 1).

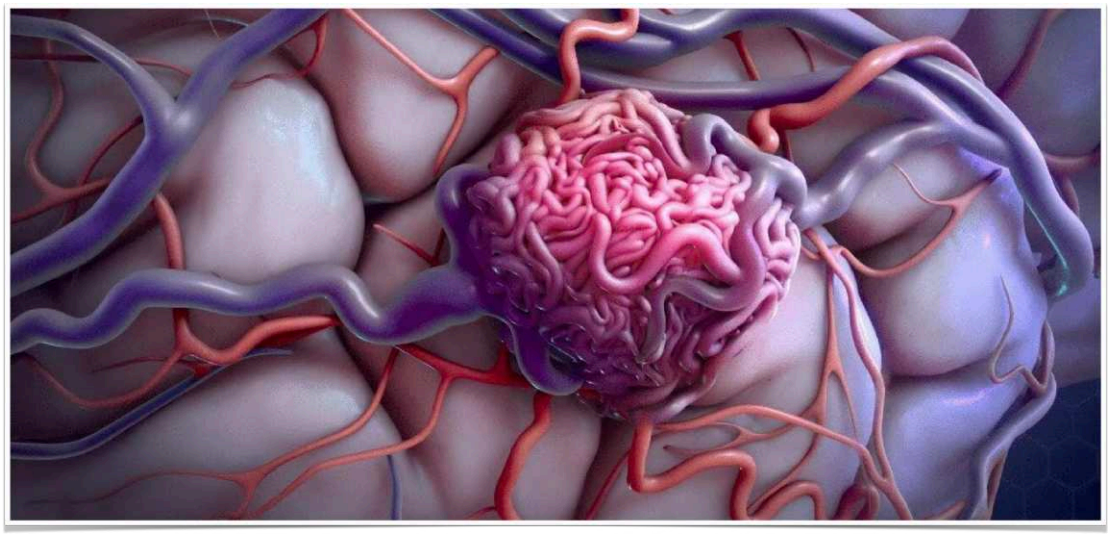

Figure 1. A BAVM scheme showing in red the feeding arteries, the nidus and veins in purple.
Image Source: Barrow Neurological Institute.

I.1. Etiology.

Brain arteriovenous malformations have been considered a congenital disease for a long time. The precise mechanism of its origin and formation has yet to be elucidated, thus, there is growing evidence nowadays that most of them are not present at birth and develop during the post-natal period, because of a genetic predisposition and exposure to secondary triggers during life[2,3]. They represent a complex endothelial cell dysfunction, triggered by still unknown factors[4]. Most of these malformations are sporadic, with no clear genetic mutation, thus, familiar studies have determined single nucleotide polymorphisms in some genes as the activin-

like kinase receptor 1 (Alk-1), interleukin-6, tumor necrosis factor alpha and NOTCH4 [5,6]. On the other side, syndromic or hereditary BAVMs account for a small percentage of these vascular lesions etiology. In this group, patients with hereditary hemorrhagic telangiectasia type 1 and 2 (HHT1 and HHT2), an autosomal dominant genetic disorder, are prone to develop capillary telangiectasias, arteriovenous fistulas and arteriovenous malformations (AVMs) in several organs including the brain. The genetic defect is a mutation in endoglin and Alk-1 genes for HHT1 and HHT2 respectively, compromising the codification and signaling in the vasculogenesis process[7]. Brain AVMs behave more as a dynamic disease during lifetime than a static disorder. The development of the vascular system does not stop at birth, with maturation and remodeling occurring as far as early adulthood. In this sense BAVMs can be triggered and affected by this process in a susceptible vascular bed for a long period until adulthood which explains in part their presentation and behavior[3].

I.2. Epidemiology and risks.

Brain arteriovenous malformations are infrequent, with a prevalence of 15-18 per 100.000 inhabitants and annual detection rate of 1 per 100.000 adults[8,9]. Although their incidence is low, half of the patients could present as an intracerebral hemorrhage, with high clinical impact and disabilities[8,10]. On the other hand, BAVM can be totally asymptomatic and never be detected during lifetime or be diagnosed as an incidental finding in noninvasive studies with magnetic resonance imaging (MRI) or computer tomography (CT) [11]. Furthermore, in some patients it can be diagnosed with imaging studies after different clinical manifestations as:

- Intracerebral hemorrhage
- Seizures

- Headaches
- Neurological deficits

Intracerebral hemorrhage (ICH) is the most common and severe form of clinical manifestation in BAVMs (Figure 2). Hemorrhagic presentation usually presents in these patients between 20 and 40 years of age[12,13], with an annual bleeding risk of approximately 3%[14,15], thus this can range from less than 1% to as high as 33%, depending on different factors as previous bleeding, deep BAVM location or deep single venous drainage. The bleeding risk increases if one or more of these characteristics are present[10]. In the only randomized controlled trial of unruptured BAVM treatment ARUBA (**A** **R**andomized trial of **U**nruptured **B**rain **A**rteriovenous Malformations) the annual rate of bleeding during follow up was 2.2%[16].

The importance of BAVM rupture is that morbidity and mortality can be significant. After first hemorrhage there is a 10% mortality risk which increases up to 20% for recurrent bleeding events[4]. After a BAVM bleeding the risk of re-rupture during the first year is estimated between 6-17%, that will be back to baseline at year 3[14].

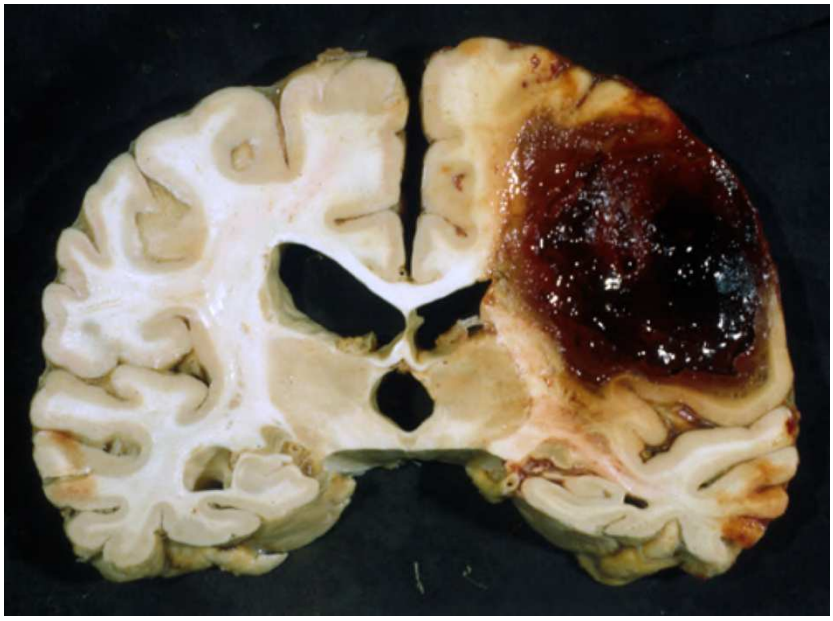

Figure 2. Intracerebral hemorrhage in left brain hemisphere due to a ruptured BAVM.

I.3. Anatomical features.

BAVMs are composed by an abnormal connection between arteries and veins leading to a vascular shunt. The main components of a BAVMs are: One or several feeding arteries, a tangle of abnormal vessels called the “nidus” and one or several draining veins. The nidus is the differential characteristic between BAVMs and other vascular malformations as arteriovenous (AV) fistulas or dural AV fistulas. This aberrant vascular network or nidus has not been well characterized and actual standard vascular imaging modalities such as magnetic resonance angiography (MRA), computer tomography angiography (CTA) or digital subtracted angiography (DSA) with 3D or four-dimensional (4D) images, still present difficulties in defining its microstructure[17]. Since the definitions from Houdart et al[18], BAVMs have been classified as an arteriolovenulous fistula, meaning that the nidus is the sum of the connections between arterioles and venules that will finally drain to bigger collectors or veins (Figure 3).

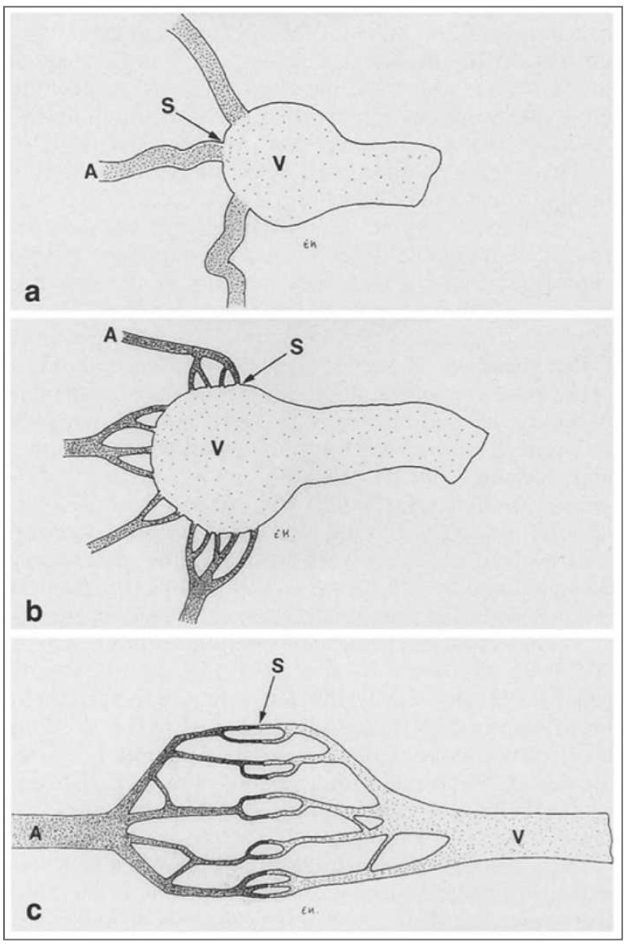

Figure 3. Schematic representation of different AV fistulas as presented by Houdart et al[18].
A) Arteriovenous fistula. No more than three separate arteries (A), shunt (S) to the initial venous compartment (V). B) Arteriolovenous fistula. Multiple arteries shunt to a single vein, giving plexiform arterial appearance on proximal arterial injection. C) Arteriolovenulous fistula. There are multiple shunts between arterioles and venules which face each other. The first identifiable venous compartment is away from the shunts.

Nevertheless, a clearer definition of this intricate connections between arteries and veins have been determined with modern imaging as shown by the work by Keil et al[17], in which a BAVM could have different forms of AV connections: direct AV fistulas, arterial plexiform to vein unions or plexiform arterial to vein shunts, with a superimposition of the anatomical characteristics defined previously by Houdart et al[17,18] (Figure 4). The lack of clear anatomical definition of the nidus will have an important meaning when trying to reconstruct and replicate these structures as will be exposed later in this work.

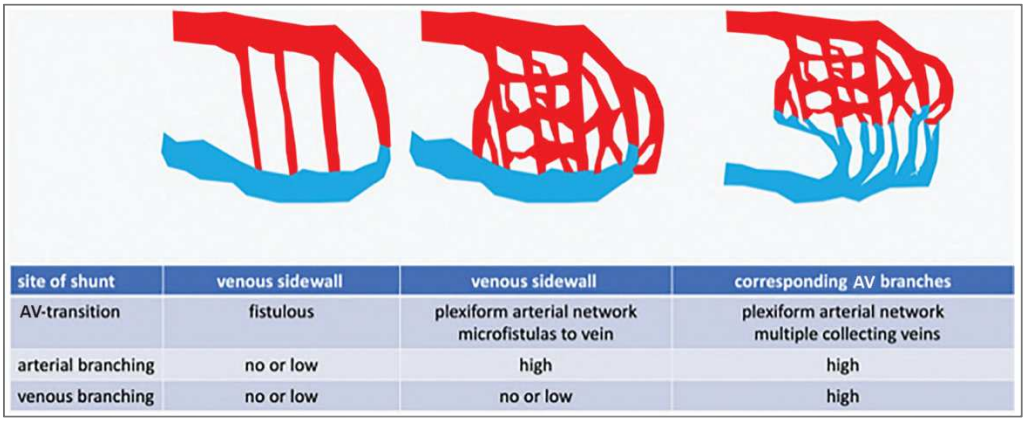

site of shunt	venous sidewall	venous sidewall	corresponding AV branches
AV-transition	fistulous	plexiform arterial network microfistulas to vein	plexiform arterial network multiple collecting veins
arterial branching	no or low	high	high
venous branching	no or low	no or low	high

Figure 4. The three types of shunts in BAVM as described by Keil et al[17].

Schematic drawing of 4D-fPCBCTA findings in cases of AVMs to characterize different types of intranidal AV shunts and intranidal branching patterns (modified according to the classification of Houdart et al).

Other anatomical important characteristics of BAVM can be defined with further imaging methods as CT or magnetic MRI, as topographic brain localization, relationship with brain structures, signs of actual or previous bleeding, and the location or interaction with gyrus or sulcus, ventricles, or the subarachnoid space[4,19,20].

An important feature of anatomical characteristics is their use for defining therapeutic strategies or management. Some anatomical issues have been grouped and used as grading scales. One of the most know and used scale is the Spetzler-Martin (SM). Created for outlining surgical risk[21], it has been widely used as a unified language in other treatment modalities[10]. The SM is a 5-points scale (from 1 to 5) that evaluates three different aspects of BAVMs: size, eloquence, and venous drainage (Table 1), which gives lower surgical risk if score is low (≤3) or high risk if score is equal or greater than 4. Other scales have been described in the literature, thus, because of its simplicity and reproducibility none has been as widely used as the SM scale. More recently and additional scale to SM have been proposed by Lawton and Young, assigning 3 more features to the score: age, previous bleeding (yes/no) and nidus characteristics (compact / diffuse)[22] (Table 2). This scale has demonstrated to be more accurate in predicting surgical risk and outcome than previous ones.

Graded Feature	Points assigned
Size	
Small (<3cm)	1
Medium (3-6cm)	2
Large (>6cm)	3
Eloquence of Adjacent Brain	
Non-eloquent	0
Eloquent	1
Pattern of Venous Drainage	
Superficial only	0
Deep	1

Table 1. The Spetzler Martin Scale. Grade = Size + Eloquence + Venous Drainage

Graded Feature	Points assigned
Age (years)	
<20	1
20-40	2
>40	3
Bleeding	
yes	0
No	1
Compact Nidus	
Yes	0
No	1

Table 2. The Lawton-Young supplemental Scale.

I.4. Management of BAVM.

Brain AVM management is still controversial, and no clear optimal treatment has been defined. For several decades, the best treatment option for BAVM was believed to be any intervention modality as surgery, endovascular occlusion, radiosurgery, or a combination of these therapies. This vision dramatically changed in 2014 after the publication of the ARUBA study, the only randomized controlled trial (RCT) in BAVM comparing interventional treatment to best medical management. The study, that recruited 223 patients, demonstrated that the interventional arm presented a significant increase in the risk of stroke or death versus medical treatment (30.7% vs 10.1%). These results led to early termination of the study by the security interim committee[16]. The impact on the medical community was immediate and significant, resulting in a strong resistance to modify usual practices and sparking controversy about the results, highlighting several methodological flaws[23]. Nevertheless, in several centers, BAVM management strategies were modified turning more to a conservative / medical option. The long-term impact of ARUBA on daily clinical management is still not well determined. Recent data from United States (US) National Impatient Sample described and increase in ruptured BAVM admissions compared to pre-ARUBA era [24]. The debate is not closed. The TOBAS trial (**T**reatment **o**f **B**rain **A**VMs **S**tudy) is an ongoing multicenter clinical research project leaded by Montreal INR group, trying to elucidate the best management strategy for BAVMs. It is a randomized pragmatic study and registry that will follow up patients for 10 years[25]. With this controversial data, there is still place for equipoise in the management of this disease.

Today, the main interventional strategies for treating an unruptured or ruptured BAVM are:

- Surgery

- Stereotactic Radiosurgery
- Endovascular embolization

I.4.1. Surgery / Microsurgery.

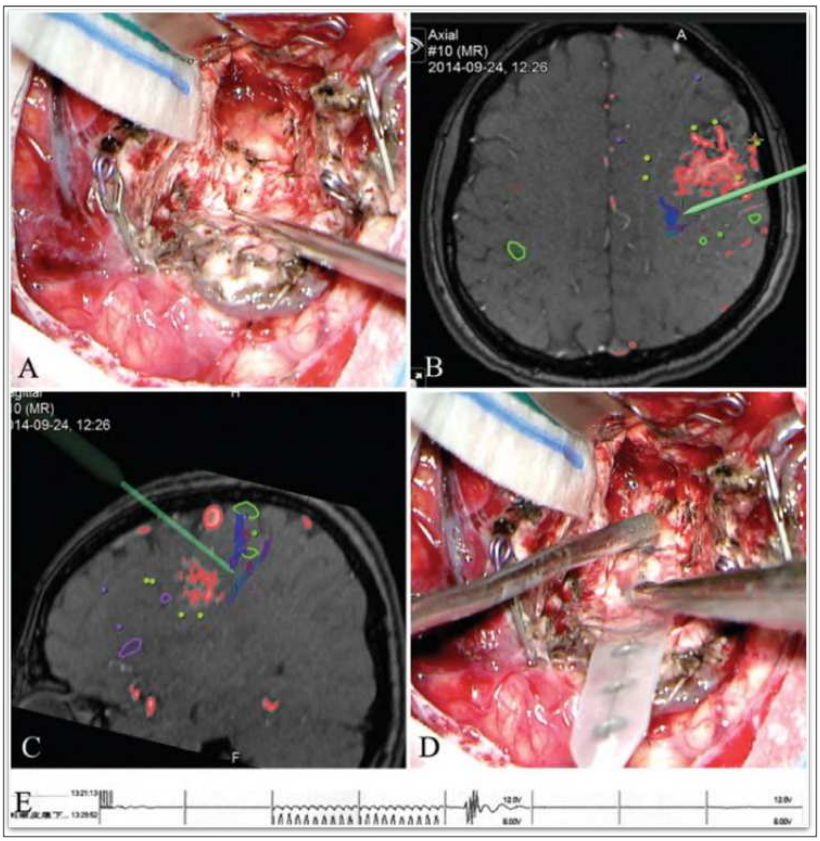

Figure 5. Microsurgery.

A modern microsurgical treatment of a BAVM. Left frontal BAVM resected with a meticulous technique, managing to resect the border, control feeding arteries and extirpate the nidus. Neuronavigation has become nowadays in an important tool that can help better surgical resections. A) and D) Intra-operative images of a BAVM resection. B) and C) neuronavigation images of the AVM at pre-central frontal gyrus.

The first reported attempt to treat a BAVM was described in 1889 by Giordano and Péan[26]. Thus, a more contemporary surgical technique and description for their excision was reported by Harvey Cushing and Walter Dandy in the earlier 1900s[26,27]. With the introduction of cerebral

angiography in 1927 by Egas Moniz it allowed a more precise diagnostic and characterization of BAVM[28], helping neurosurgeons, during the 20th century, to progress and refine their technique, with ongoing less operative morbidity and mortality (MM). One of the greatest advances in BAVM operative management was the introduction of the surgical microscope by MG Yasargil in the late 1960s. He also introduced the use of bipolar coagulation and micro instruments, redefining the art of surgical resection of this illness[29]. Microsurgery has continued its evolution for BAVM excision with MM widely reported, thus showing big differences between experiences and centers, probably due to selection bias (Figure 5). Permanent neurological deficit after surgical resection has been described to be as low as 2% for SM grade 1 and 2, 17% for SM 3 and 45% for SM 4 and 5[10,30]. Van Beijnum et al showed a 7.4% (range 0-40%) rate of permanent neurological deficit after surgical treatment in their systematic review and meta-analysis, and the degree of complete treatment and curation was 96% (range 0-100%)[8]. In a recent review of the ongoing TOBAS trial, the surgical subgroup presented 89% of curative results, mainly in low grades BAVMs, with 56% receiving presurgical embolization. Serious adverse events occurred in 21%, thus only 4% with permanent neurological deterioration with a modified Rankin Scale (mRS) > 2[31].

I.4.2. Stereotactic Radiosurgery (SRS).

SRS for brain AVMs is the use of high dose focal radiation to obliterate and cure the disease. SRS was introduced by Leksell in 1951, as gamma knife, with latter progressive advances and specific improvements for BAVM treatments[10,26] (Figure 6).

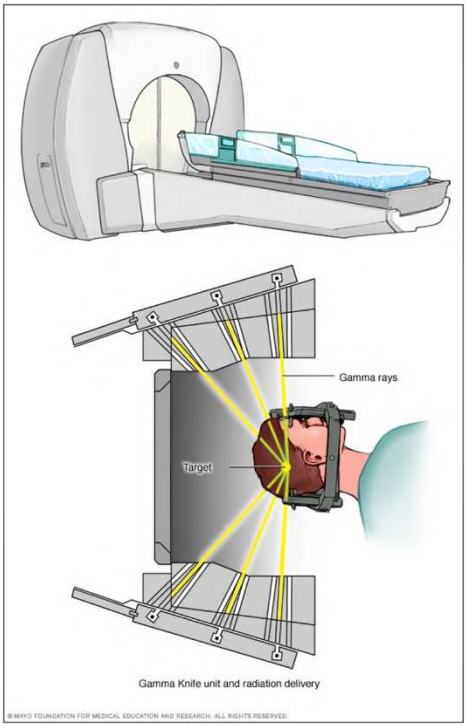

Figure 6. Radiosurgery using Gamma knife.
Image Source: Mayo Clinic Foundation

The biological effect of SRS is the induction of endothelial proliferation and occlusion of the aberrant nidal vessels, leading to thrombosis and cure. The process is not fast, and the obliteration of a BAVM would normally take 2-3 years. The initial radiation source energy was cobalt, thus latter others have been used as stereotactic proton beam or helium. In the past decades the use of linear accelerator was introduced and quickly used to treat this vascular disease[26]. SRS curative results are directly related and depends on nidal size, with better occlusions rates if volume do not exceed 4 cm[332]. A specific scale for grading AVMs was created for SRS, to predict outcome and results. The Virginia Radiosurgery AVM Scale (VRAS) is a 5 points scale that evaluates 3 different features, size (<2 cm^3 = 0 points, 2-4 cm^3 = 1 point, > 4 cm^3 = 2 points), eloquence (1 point) and history of bleeding (1point). Better BAVM cure rates have been related to lower scores in the VRAS[10,32]. In Van Beijnum et al. systematic review and meta-analysis, SRS presented an overall occlusion rate of 38% (range 0-75%) and permanent neurological deficit of 5.1% (0-21%)[8]. A large multicenter cohort study

showed an overall obliteration rate of 64.7% with predictors of better occlusion rate if: younger age, smaller nidus volume, increasing years after SRS and higher margin dose. The annual risk of bleeding was 1.1% with no hemorrhagic complication after angiographic cure[33]. SRS has been used as an adjuvant treatment after partial surgical resection or BAVM reduction by embolization, thus also it could be used as stand-alone therapy specially for small, deep located, or eloquent BAVM[33,34]. Complications derived from SRS that leads to imaging changes and transitory or permanent neurological deficits have been reported to range from 0.4-20.6% of treated patients, and directly related to BAVM location and volume of tissue receiving more than 12Gy[34].

I.4.3. Endovascular Treatment (EVT).

Endovascular treatment embolization which consists of filling the BAVM vessels and nidus with liquid embolic materials to exclude them from the bloodstream, has become one of the preferred options for managing this disease, as a coadjutant for other therapies or as a stand-alone treatment. The advantage of this technique is that it avoids the manipulation of the brain or other neural structures and has few or no restrictions in reaching BAVMs in various locations. When EVT it is used as a curative option, the aim and principles are to occlude the BAVM by filling with embolic materials the arterial feeders, the nidus and the vein at its origin (foot of the vein).

First attempts for embolizing a BAVM were described in 1930 by Brooks who injected muscle particles through an exposed open cervical carotid artery. This technique was repeated 30 years later by Luesssenhop and Spence in the 60s using steel sphere particles covered with methacrylate to treat a BAVM. Thus, a decade later the first embolization procedure using

particles, percutaneous femoral access and a catheter was done by Kricheff[4]. BAVM endovascular treatment development has been absolutely ligated to several advances in other fields as the evolution of neuroimaging, especially angiography: digital subtraction angiography (DSA), 3D rotational images, Flat panel acquisition with Cone Beam computer tomography (Cone Beam CT) capability and other imaging modalities as MRI, MRA, functional MRI, and others[35]. Moreover, the evolution of materials has also been a great coadjutant to embolization development, with the introduction of better guiding catheters and proximal support devices, microcatheters, microguidewires and embolic materials. A great innovation come with the transition from using different kind of free particles to liquid embolic agents (LEA). These products expanded endovascular possibilities by allowing the administration through smaller caliber microcatheters that then solidify by the contact of blood. Smaller catheters allowed distal navigation and intranidal administration of the material. Zanettti and Sherman introduced in 1972 Isobutyl-2-cyanocrylate[36], that was latter replaced by the development of n-butylcyanocrylate (NBCA) (Histoacryl, Braun Meesungen Germany)[26]. NBCA became the preferred embolic material for BAVM, allowing better penetration to the nidus, while using different concentrations / polymerization times, by mixing it with contrast agent Lipiodol (Guebert, France). After this, different cyanoacrylate appeared in the market trying to give a longer or retarded polymerization time for better BAVM nidus filling and curation rates. Nevertheless, one of the more important innovations in endovascular management comes with the introduction of non-adhesive LEA (Figure 7). The first one was Ethylene Vinyl Alcohol Copolymer (EVOH) introduced in the early 90s and named as Onyx (Medtronic, Minneapolis MN USA)[37]. EVOH is diluted in dimethyl sulfoxide (DMSO) and uses tantalum powder for radio-opacity. This product showed substantial differences with previous materials, allowing slower and prolonged injections with nidal filling and greater occlusion rates. A randomized trial comparing EVOH with NBCA for presurgical embolization

showed an equivalence between the two agents in terms of percentage of nidal occlusion rates over 50%, blood loss and surgical time at BAVM resection[38]. Prospective larger series with EVOH have shown an obliteration rate of 51% in endovascular treatment with an intention to cure, with stable long-term results with 7.1% permanent morbidity and 1.4% mortality[39]. A new copolymer, known as PHIL (Precipitating Hydrophobic Injectable Liquid) (Microvention, Aliso Viejo CA USA), has been recently introduced. PHIL copolymer is formed using the monomer hydroxyethylmethacrylate (PHEMA) and works similarly as EVOH, but contains a bonded iodine molecule that gives the compound greater homogeneity compared to tantalum based EVOH.

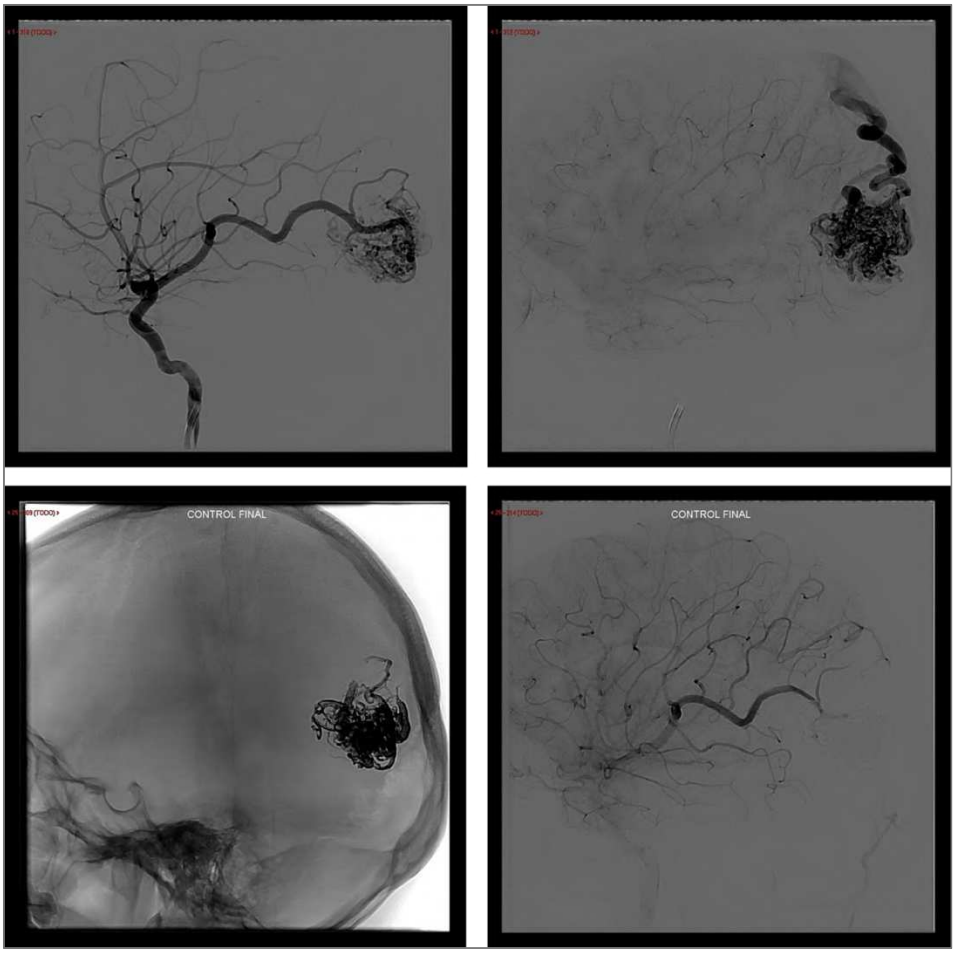

Figure 7. Endovascular treatment.

Parieto-occipital BAVM treated with endovascular embolization using EVOH. A) Arterial phase DSA, B) Late DSA phase, showing superficial venous drainage. C) LEA cast after embolization; D) Final control DSA, after LEA embolization. No BAVM filling, confirming complete exclusion.

As stated, important advances have been made in techniques and technology of BAVM endovascular management over the last decades, nevertheless, the global curative rate of the technique has not been high, reported as low as 13% (Range 0-94%), with acute complications rates ranging between 7.6-55% (cerebral infarcts or brain hemorrhage)[8].

I.4.3.1. Transvenous Embolization (TVE).

Since the begging of BAVM therapies, the dogma was to avoid closing the vein until there was complete arterial control and occlusion. An accidental venous blocking could lead to nidus acute hypertension, rupture, and bleeding[18,40]. The standard route for BAVM endovascular treatment has been the arterial side, with evolving techniques for reaching more nidus and more curative results. Although the arterial or anterograde to flow route has been the standard endovascular access to BAVMs embolization, the transvenous venous approach (TVA) has evolved as a game changer in the last years for treating this disease. TVA consists in accessing the vascular disease through an inverse route, coming counter flow and against pressure from the vein side to the nidus, defying the classic concept of not to alter BAVM output to avoid rupture or bleeding. The concept of TVA was introduced by Tarek Massoud and George Hademenos in 1999[41,42]. Using animal models (swine rete mirabile) they were able to determine that contra-flux contrast injections were feasible using induced systemic hypotension or decreased nidus flow with proximal balloon occlusion and that this concept could be used in the future using sclerosants agents as alcohol to occlude the nidus[41,42]. They proposed several advantages of the TVA over trans-arterial embolization that were lately proved in clinical practice:

- Less ischemic damage to normal brain.
- More curative results with complete nidus exclusion.
- Simpler anatomy and number of draining veins than arterial feeders.
- Access to BAVMs with complex arterial feeders or “in passage” arteries.

A decade later, the concept reached the clinical field with an initial report by Nguyen et al[43], and then followed by several experienced groups and pioneers that explored this technique, proving that under several conditions and considerations it is a safe and efficient technique for treating some human BAVMs[44–48]. Mounayer et al at Limoges France, showed their first experience with 5 cases in 2011, with no procedural complications and complete obliteration in 4/5 cases [48]. The same group published the first large series in TVE with 40 patients, with a cure rate of 92.6%, no mortality related to the procedure and 1 hemorrhagic complication during the procedure[44]. The technique was named “porcelain vein” because the LEA filled the vein in an outer to inside fashion, in slides, emulating porcelain manufacture, leading to a progressive reduction in output flow in a centripetal fashion without an abrupt venous closure[44,49]. Chapot et al published later in 2021 TVE in 45 patients using their variant “pressure cooker technique”[49] in which the venous LEA reflux is controlled by a combination of systemic hypotension and a venous plug using coils and glue for better nidal counter flow penetration. Other less numbered series have also been published with similar encouraging results [47].

Despite of the results, there are still several aspects of this technique that are not totally clear, and their understanding could allow safer and better embolizations in the future:

- Which is the ideal LEA for TVE?
- How can we avoid long LEA reflux into the vein and better nidal penetration?
- How can the nidus be filled by this route and avoid partial filling?
- How does the number of veins and BAVM size affect nidus retrograde filling?

- How hemorrhagic complications could be avoided using this technique?

All these questions remain unclear for the moment, and there is a gap of evidence on how the TVE works. Because of ethical issues it has been difficult to gain knowledge in this field with human BAVM cases.

TVE is a challenging technique and the need for training medical doctors, testing new devices and techniques has become an important requirement. The possibility of training an interventional neuroradiologist in this technique is complex, with limited access to real human cases and few centers performing many these treatments. The swine rete mirabile has been described for TVA in the early theoretical cases by Massoud et al[41,42,50], thus no embolic agent was used in this series. A recent publication has described the first TVE in vivo model, using the swine rete mirabile, showing its feasibility[51]. At the time we started this thesis no animal model or any kind for TVE had been described or published. Moreover, in order to reduce animal use, we thought to develop a novel ex-vivo model.

The main objective of this thesis was to develop a new BAVM model for endovascular TVE. With this purpose we tried to answer the following questions:

I.5. Main Thesis Question.

Is it possible to develop a new BAVM model for transvenous embolization?

I.5.1. Secondary questions.

1. Which are the actual models for BAVM study?
2. Which models have been used for endovascular treatment simulations?

3. How can we develop a new model for endovascular use and TVE?
4. How can we test and prove a novel TVE model for BAVM?

The following chapters will focus on answering these questions, presenting the data we obtained and the different articles we produced with this purpose.

In summary:

BAVMs are an infrequent but important disease due to their bleeding risk and possibility of leading to permanent disability or death.

Evidence points to a genetic susceptibility and development through lifetime by secondary triggers.

Treatment is still not well defined, especially in unruptured BAVMs. Although the only RCT on treatment suggested that any intervention can be more deleterious than observation, there are still trials trying to have better answers in this field.

Endovascular treatment is one of the main options to treat BAVM, and the transvenous embolization (TVE) has become a game changer for the management of some of these vascular diseases. Its technical difficulty has opened an expanding need for adequate training and teaching for safer procedures.

There is no actual BAVM model for TVE. Is it possible to develop a novel BAVM for TVE?

Chapter II. Brain AVM experimental models.

II.1. Context and problem.

“All models are wrong, but some are useful” George E.P. Box.

With the development of new tools and modern surgical and endovascular treatments in the late '70s, the first BAVM models were described and published. Questions such as the mechanisms of normal perfusion pressure breakthrough or the behavior of new embolic agents needed answers and testing. The first models were conducted using small animals, such as cats or rodents, to study the effects of shunting the brain and increasing blood flow [52]. On the other hand, endovascular models began as simple vein grafts connected to a flow circuit to test the effects of an embolizing agent on the vessel [53]. Later, more complex questions needed to be answered, such as the genetic causes of BAVMs or the development of new therapeutic strategies. As a result, models continued to evolve continuously to meet the increasing demands for technology, knowledge, and techniques.

II.2. Presentation of Article 1.

For answering the first of our secondary questions (*Which are the actual models for BAVM study?*), we decided to scope all scientific literature and main databases for having a clear idea which were the BAVM models that have been developed, in the past or actual ones in use. We searched databases for any BAVM model, independent from its use and purpose.

II.3. PDF of article 1.
Interdisciplinary Neurosurgery: Advanced Techniques and Case Management.

Interdisciplinary Neurosurgery: Advanced Techniques and Case Management 25 (2021) 101200

Contents lists available at ScienceDirect

Interdisciplinary Neurosurgery: Advanced Techniques and Case Management

journal homepage: www.elsevier.com/locate/inat

Review Article

Brain arteriovenous malformations: A scoping review of experimental models

Rodrigo Rivera [a,b,*], Juan Pablo Cruz [a], Catalina Merino-Osorio [c], Aymeric Rouchaud [b,d], Charbel Mounayer [b,d]

[a] Neuroradiology Department, Instituto de Neurocirugia Dr. Asenjo, Santiago, Chile
[b] Limoges University, CNRS XLIM, UMR7252 Limoges, France
[c] Facultad de Medicina Clinica Alemana Universidad del Desarrollo, Santiago, Chile
[d] Neuroradiology Department, CHU Limoges, Limoges, France

ARTICLE INFO

Keywords:
Arteriovenous malformations
Animal models
Brain
Neurosurgery
Neuroradiology
Radiotherapy

ABSTRACT

Background: Brain arteriovenous malformations (bAVM) are one of the most complex vascular lesions in humans. Their understanding and treatment have been possible through the use of different experimental models. The aim of this scoping review was to systematically map the existing experimental models used for bAVM research and training.

Methods: A scoping review was conducted, and a search process was performed in 7 electronic databases from inception to April 30th, 2020. Study selection included all types of research articles that used any kind of experimental model for AVM study. Selection and data extraction were performed by independent reviewers.

Results: The initial search retrieved 942 articles which were reduced to 177 articles after the whole inclusion / exclusion process. We identified 9 main AVM experimental models, divided in *in vivo*: transgenic, rete mirabile, carotid-jugular fistula, carotid-jugular plexus fistula, arteriovenous shunt and cornea; or *in vitro*: 3D cast, computer generated and biological graft. First developed models were dedicated to study the hemodynamic effects and then followed by endovascular testing using the swine rete mirabile. The latest developments have come with transgenic models, allowing the manipulation and creation of AVMs in rodent brains, giving a huge step in the understanding of genetic origin, angiogenic mechanisms or potential therapeutic targets for the future.

Conclusions: There is no unique model that could account for all features of bAVM. We expect a continuous development of more accurate models that could lead to optimize and develop new treatment strategies for increasing the cure rate of this disease.

1. Introduction

Brain arteriovenous malformations (bAVM) are vascular lesions composed of complex abnormal connections between arteries and veins. They do not follow the standard vascular structure, so arteries and veins are connected by a tangled vessel configuration known as the "nidus" [1,2]. Although they are rare, with a prevalence estimated in 15–18 per 100.000 adults [3,4], bAVMs can result in severe clinical consequences and neurological impairment due to chronic venous congestion or rupture leading to intracerebral hemorrhage (ICH) [1,5].

Brain AVM management is difficult and there is no consensus regarding which is their ideal treatment. Interventional treatments options are open microsurgery, endovascular embolization and radiosurgery [4]. Thus, clinical observation with no intervention might be an option for unruptured bAVMs, according to ARUBA trial in which conservative management showed to be safer on the midterm than any type of intervention [6]. Until now, treatment decisions frequently rely on the neurovascular center or physician's experience, with a difficult and potentially biased decision-making process [7].

Experimental models have been used for decades in several brain vascular diseases as stroke and cerebral aneurysms [8] and their contribution has had a tremendous impact in the understanding of the pathophysiology and molecular mechanisms through basic sciences research and therapeutic drug and device development. Since the

* Corresponding author at: Neuroradiology Department, Instituto de Neurocirugia Dr. Asenjo, Santiago, Chile. Limoges University, CNRS XLIM, UMR7252 Limoges, France.
E-mail address: rodrigorivera@me.com (R. Rivera).

https://doi.org/10.1016/j.inat.2021.101200
Received 22 March 2021; Received in revised form 24 March 2021; Accepted 28 March 2021
Available online 1 April 2021

beginnings of bAVM treatment, physicians began looking for models that could allow development, testing and training in new therapeutic tools and acquiring knowledge to improve the understanding of the disease[9]. Because of their complex structure and physiology, it has been challenging to adequately replicate a bAVM in an *in vivo* or *in vitro* model. Moreover, there are other special features that are difficult to replicate, like complex intertwined flow dynamics, arteriovenous (AV) shunts, AVM angioarchitecture or the biological interaction between the malformation and the surrounding brain tissue.

Because there is disperse information about all bAVM models, we decided to perform a general systematic search as a scoping review with the objective of comprehensively mapping and summarizing the current status and function of the *in vivo* or *in vitro* models of bAVMs.

2. Methods

2.1. Study design

A study design was conducted to identify all the published bAVM models. We performed a scoping review using the Joanna Briggs Institute (JBI) method [10,11], as initially conceived by Arksey and O'Malley [12]. For quality control of this review, we used the Preferred Reporting Items for Systematic Review and Mata-Analysis (PRISMA) extension for Scoping Reviews Checklist [13].

2.2. Research question

- Which are the *in vivo* or *in vitro* bAVM models and their clinical or research applications?

2.3. Data sources and systematic search

A systematic search was performed by two authors (RR and CMO) in PubMed (NCBI), CINHAL Plus with Full Text (EBSCO), Embase, Epistemonikos, Clinical Trials and Cochrane Library. We used as strategy the terms 'Arteriovenous Malformations', 'Intracranial Arteriovenous Malformations', 'Animal Models', 'Biological Models', 'Anatomic Models' 'Endovascular Procedures', 'Neurosurgical Procedures', 'Radiotherapy' and 'Neurosurgery'. Language filters (English and Spanish) were applied. All kind of articles were considered, research articles or conference abstracts. The grey literature was consulted using Open Grey. Finally, a manual selection of the reference list of relevant papers was performed. We used Mendeley (version 1.19.4) as a bibliography software to manage all references. The last search was done on April 30th, 2020.

2.4. Selection of articles

The selection of articles was done by two researchers (RR and JPC) that independently carried out the article selection in three stages: filter by title, abstract and full text according to the selection criteria. Potential disagreement about inclusion or exclusion of articles was discussed, and if the discrepancy persisted a third one (CMO) decided. We used the 'include' rather than the 'exclude' criteria to select by title, abstract and full text in order not to lose relevant information. The following inclusion criteria were used, based on the components of Population, Concept and Context method (PCC) [11,14]: Population: brain Arteriovenous Malformations models; Concept (Intervention): none; Concept (outcomes): for therapeutic, anatomical or biological studies; Context (studies): All type of articles, original studies, conference abstracts, protocols and trials. The following exclusion criteria were used: language other than English or Spanish, models used not for AVM studies, review papers, full manuscript not available for analysis. We reported using the PRISMA flow chart [15].

2.5. Data extraction

The included articles were collated in a Microsoft Excel data extraction spreadsheet by the author RR. Coauthor JPC performed a quality control randomly selecting 10% of articles for extraction and comparing the data to determine if the extraction process was consistent to answer the study question. Data were extracted by using the Peters et al recommendations [11], compiled using PCC nomenclature and organized using Covidence software platform (Melbourne, Australia). The extracted fields were author, year of publication (inception to 1999, 2000–2009, 2010–2020), title, digital object identifier (DOI), Journal, Country of main author, study objective, study design (Experimental/Review), Type of model (*in vivo* or *in vitro*), AVM model, model specifications, purpose of model use and details of use.

This Scoping review did not require experimental participation of human subjects, nor patient's data, therefore did not require ethical committee approval.

2.6. Patient and public involvement

Patients or the public were not involved in the design of our research. They were not involved in the conduct, reporting or dissemination of the proceeding scoping review.

3. Results

The initial data base search yielded 942 results, with 14 other references added manually in a later search. This led to 811 citations after removal of duplicated articles. Following a process of screening and eligibility, 177 articles were used for data extraction. The flow search process of article selection is presented in Fig. 1.

3.1. Characteristics of included articles

General characteristics of eligible articles are summarized in Table 1. Studies were published between 1978 and 2020. There was a clear increase in the number of publications over the decades, with 55% of the citations published between 2010 and 2020. The main source of publications were journal articles (90%) and the remaining 10% from conference proceedings. We found no citation from other sources like thesis dissertation or research protocols. Most of the published literature came from institutions from USA, followed by Australia, Germany and China.

3.2. Title. Biometric information of included articles

We detected 9 main different kinds of bAVM models, with a dominance of *in vivo* (81%) vs *in vitro* (19%) (Table 2).

3.3. Title. Main bAVM models

The use and purpose of the bAVM model's publications has evolved during the past decades. Hemodynamic changes were the early scope of publications, changing to a clear dominance of transgenic models in the last decade (Fig. 2).

We detected different uses and purposes of the experimental bAVM models, that we classified and organized in 5 types: 1) Hemodynamic and Normal Perfusion Pressure Breakthrough, 2) Endovascular and embolic materials, 3) Angiogenesis and AVM development, 4) Radiotherapy and 5) Anatomy / Education.

3.4. Hemodynamics/Normal Perfusion Pressure Breakthrough

The first model developed for bAVM was created by the group of Dr. Robert Spetzler [9] to study and emulate the chronic hemodynamic effects of bAVM in the surrounding tissue. For this purpose, they created a vascular anastomosis between the common carotid artery and the

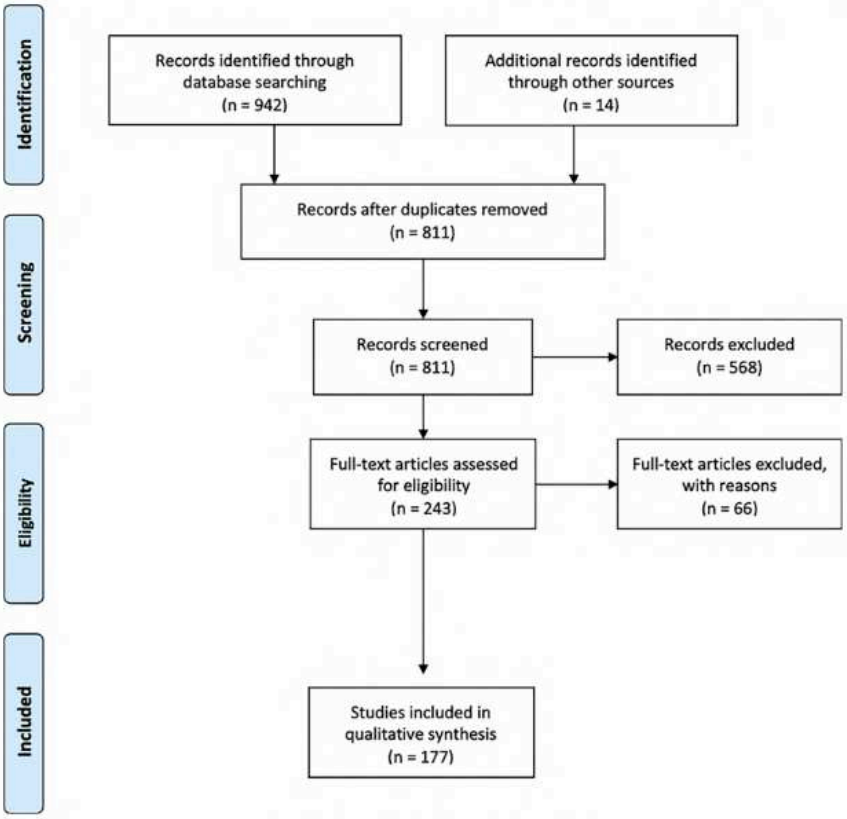

Fig. 1. The PRISMA flow chart of the search process.

Table 1
The biometric information of included articles is displayed: Year of publication, Type of publication and country of main author.

Characteristics	n	%
Year of publication		
1978–1999	37	20.9
2000–2009	44	24.9
2010–2020	96	54.2
Publication Type		
Journal article	159	89.8
Conference proceeding	18	10.2
Main Authors Institution Country		
USA	98	55.4
Australia	19	10.7
Germany	10	5.6
China	10	5.6
Japan	7	4
Canada	5	2.8
France	4	2.3
N/A	7	4
Others	17	9.6

external jugular vein in cats, generating an AV shunt using the circle of Willis (Fig. 3). They reproduced the autoregulation disfunction that chronic hypoperfusion generates in the normal brain with a bAVM, known as Normal Perfusion Pressure Breakthrough (NPPB). This model did not include an AVM nidus, nor an intracranial AV shunt, thus it only indirectly showed one of the effects of bAVM caused by the redistribution of blood and changes in pressures in the brain. Later, other authors modified this model by performing different anastomosis [16,17], for better understanding and replication of NPPB.

The carotid-jugular fistula (CJF) has been a preferred model in different animals for studying these sustained hemodynamic changes and their effects. Early experiments were done with cats, but then progressively switched towards rodents [17–20].

Two direct intracerebral hemodynamic models were created to simulate the local intracerebral effects of AVMs: a first one uses a surgical arteriovenous bypass forming a shunt between cerebral arteries and the venous sinus, with an interposed "nidus" using temporal muscle; the other uses a vein graft bypass between a middle cerebral artery (MCA) branch and the sagittal sinus [21,22].

When looking for other hemodynamic characteristics of AVMs, we found several computer or mathematical models developed for simulating these dynamics. These *in vitro* simulations have aimed to understand how the flow behaves within the nidus and the whole vascular malformation. Some of them have used patient derived data from imaging studies to recreate the vascular environment using Computer Flow Dynamics (CFD)[23], in which through specific software, flow simulations can emulate the complex circulation within an AVM [24,25]. Other simulations have used mathematical models approaching the AVM vessel network as an electrical circuit [26–29].

Table 2
bAVM models. Main division of *in vivo* or *in vitro*, and the specific models with their publication's total number and frequency (%).

	Model Type		
In Vivo	Transgenic = 52 (29.4%)	Rete mirabile = 46 (26%)	Carotid-Jugular Fistula = 21 (11.9%)
	Carotid-Jugular Plexus Fistula = 19 (10.7%)	AV Shunt Bypass = 3 (1.7%)	Cornea model = 3 (1.7%)
In Vitro	Computational = 23 (13%)	3D Cast = 9 (5.1%)	Biological Graft = 1 (0.6%)

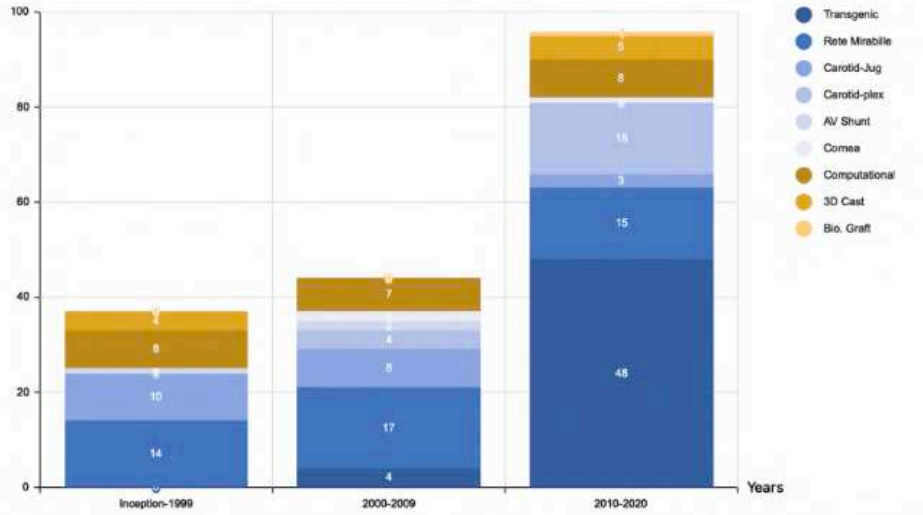

Fig. 2. Number of published bAVM models in different decades: Inception-1999 (just one publication outside range –1979-), 2000–2009 and 2010–2020.

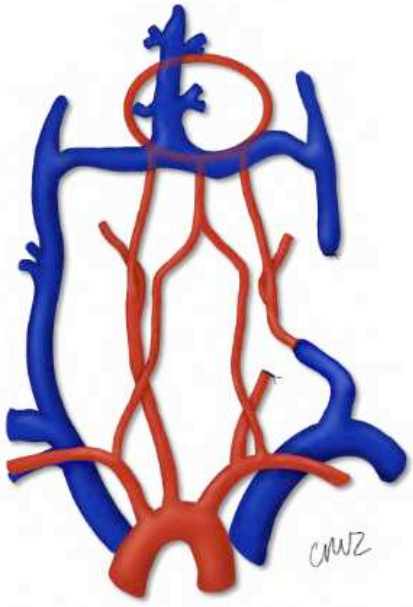

Fig. 3. Schematic image of the carotid-jugular fistula model as developed by Spetzler et al. [9]. A surgical anastomosis between the common carotid artery and the caudal external jugular vein, creating a right to left shunt using the circle of Willis.

3.5. Endovascular/embolic materials models

The main model for endovascular treatment and material testing has been the swine rete mirabile (RM). The RM is a particular vascular structure which is not present in normal conditions in humans [30] but seen in some animals, in which a tangle of arteries forms a pre cerebral arterio-arterial plexus with unknown evolutionary advantage. The swine RM is located invariably in the skull base and it is formed by a plexiform division of the ascending pharyngeal artery (APA), which continues intracranially as the internal carotid artery. It also connects with the contralateral RM crossing the midline, acting as one single nidus type structure. Because of its size and resemblance to an AVM nidus it has been used as a bAVM model with vessels ranging from 70 to 275 μm [31]. The first described use of the RM as an AVM model was published by Lee et al in 1989 [31]. Because this rete is an arterial-arterial connection, several modifications were performed later by other authors in order to create a real arterial to venous shunt: using the cavernous sinus [32] or with a surgical anastomosis from one carotid artery to the jugular vein to reverse the flow direction on that side [33]. This last model (Fig. 4) has become the model of choice in the recent years for testing liquid embolic materials [34–37], new endovascular techniques [38,39] or radiotherapy/radiosurgery protocols [40]. The main advantages of this model are that size of vessels are suitable for testing materials, vascular access, catheters, microcatheters and embolization materials designed for human use.

3.6. Angiogenesis / AVM development

This group of models is dominated by the transgenic work in mice, and has been developed mainly in the last decade, leading to multiple recent publications. Hereditary Hemorrhage Telangiectasia (HHT) is a genetic autosomal vascular disease that affects humans leading to several vascular anomalies in different target organs such as

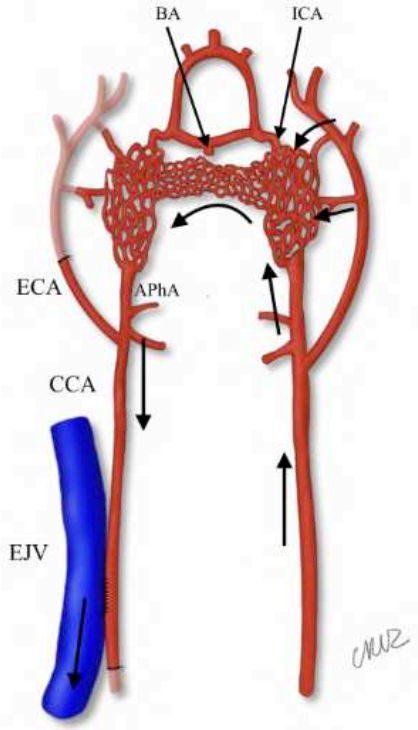

Fig. 4. Schematic image of a modified swine rete mirabile (RM) model. The RM originates as a continuation of the ascending pharyngeal arteries and continues cranially as the internal carotid artery. In this model a surgical anastomosis was done between de common carotid artery and external jugular vein. This created an arterial to venous shunt that emulates an AVM nidus flow direction. Abbreviations: Common Carotid Artery (CCA), Ascending Pharyngeal Artery (APhA), External Carotid Artery (ECA), External Jugular Vein (EJV), Internal Carotid Artery (ACI), Basilar Artery (BA). Curved arrow shows the flow direction.

mucocutaneous telangiectasias in nasal/oral area and AVM formation in brain and other organs as lungs or liver [41]. Research on this disease has shown that it is caused mainly by the mutation of two genes: Endoglin (*Eng*) and Activin Receptor Like Kinase 1 (*Alk1*), causing the HHT type 1 (HHT1) and HHT type 2 (HHT2) phenotype respectively [42].

Early genetic modifications in mice with null *Eng* and *Alk1* gene expression were incompatible with life[42]. Further researchers were able to generate heterozygous *Eng*+/- and *Alk1*+/- mice. These living mice models were capable of producing vascular anomalies in several organs, but not brain AVM [43]. Further advances using Cre-Lox technique were able to create target inducible knock-out *Eng*-iKO or *Alk1*-iKO mice that together with an external noxa or stimuli could develop vascular malformations [44]. bAVMs were induced by injecting directly in the brain a Cre expressing adenovirus at the basal ganglia carrying floxed *Eng* ($Eng^{fl/fl}$) or floxed *Alk-1* ($Alk\text{-}1^{fl/fl}$) alleles with focal angiogenesis (the stimuli) triggered by local injection of adeno-associated viral vector expressing Vascular Endothelial Growth Factor (VEGF) [45,46]. The impact of VEGF in the genesis of bAVM in these models allowed to test anti-angiogenic therapies like bevacizumab as a novel treatment of this disease [46]. Other genetic mechanisms have also been involved as bAVM generators as the Notch pathway with receptors 1 and 4. These transmembrane receptors induce angiogenesis and AVM development [47–49]. Different transgenic mice models are presented in table 3.

Finally, other models have also served for angiogenesis studies, like the swine RM [50], the cornea model in rats: where implanted human bAVM tissue is harvested in the animal eye [51–53], and the zebrafish [54–57]. A special bypass model developed by Lawton et al used a transgenic graft from the aorta to connect the carotid artery to jugular vein for evaluating different cell markers [58].

4. Title. Main transgenic AVM models

4.1. Radiotherapy

Radiation therapy uses ionization energy for bAVM treatment by inducing the nidus obliteration in selected cases by 2–3 years. Yassari et al introduced in 2004 a modification of the carotid jugular fistula model

Table 3
Main Transgenic AVM Models. Abbreviations: Adeno-associated viral vectors (AAV), Adeno-associated viral vector expressing vascular endothelial growth factor (AAV-VEGF), Adenovirus-Cre (Ad-Cre), Activin Receptor Like Kinase 1 (Alk1), Basal Ganglia (BG), Bone Morphogenetic Protein (BMP), Endoglin (Eng), Inducible Endothelial Cell Knock out (iECKO), Hereditary Hemorrhagic Telangiectasia (HHT), Matrix Gla Protein (MGP), Sonic Hedgehog (SHH), Vascular Endothelial Growth Factor (VEGF).

Author / year	Animal	Characteristics / Use
Satomi et al., 2003 [19]	Mouse	Endoglin Heterozygous. Eng+/−. Cerebral vasculature analysis. HHT
Wang et al., 2010 [59]	Mouse	Notch 4 repression. Cranial window to evaluate AVM evolution
Walker et al., 2011 [60–63]	Mouse	$Alk1^{2f/2f}$ (exons 4–6 flanked by loxP sites) + basal ganglia (BG) injection of Cre recombinase + Adeno-associated viral vectors expressing VEFG. Analysis of AVM like vessel formation in BG
Walker et al., 2012 [40,64]	Mouse	Adeno associated viral vector injection in BG in wild type mice and $Alk1^{2f/2f}$ + Cre recombinase mice. Anti-angiogenic treatment testing with Bevacizumab.
Yao et al., 2013[65]	Mouse	Matrix Gla protein (MGP) null mice (MGP -/-). Increased Bone Morphogenetic Protein (BMP) activity due to the lack of MGP induces expression of Alk1, which enhances expression of Notch ligands Jagged 1 and 2, which increases Notch activity and alters the expression of Ephrin B2 and Ephrin receptor B4, arterial and venous endothelial markers, respectively. Test the balance between the Alk-1 and Notch signaling.
Walcott et al., 2014 [66–68]	Zebrafish	Alk1 knockdown with Antisense morpholino in Zebrafish. This causes a spectrum of vessel alterations that resembles human AVMs.
Chen et al., 2014 [69,70]	Mice	$Alk1^{2f/2f}$ mice. Induction of bAVM phenotype by locally deleting the Alk1 gene expression (Ad-Cre) + Adenovirus VEGF stimulation (AAV-VEGF).
Choi et al., 2014[1,2]	Mice	$Eng^{2f/2f}$ mice / SM22a-Cre mice. Basal ganglia injection of AAV-VEGF. Induction of bAVM
Zhu et al., 2017 [9,16,17]	Mice	$Eng^{2f/2f}$ mice. Inhibition of bAVM angiogenesis by inducing FLT-1 receptor with adenovirus and blocking VEGF effect.
Crist et al., 2018 [31,34,37–39]	Mice	Knockout Smad4f/f;Cdh5-CreERT2 - Smad4-iECKO. To characterize the Smad4 function in the postnatal vasculature.
Zhu et al., 2018 [21,22]	Mice	$Alk1^{2f/2f}$ mice, with induced bAVM using AAV-VEGF and Ad-Cre. Thalidomide and Lenalidomide as an anti-angiogenesis therapy.
Cheng et al., 2020 [46,71–73]	Mice	$Alk1^{2f/2f}$ mice, induced bAVM using Ad-Cre and AAV-VEGF. To test the association of increase VEGF expression with increase AVM hemorrhagic risk
Giarretta et al., 2020 [72,74]	Mice	Efnb2/LacZ heterozygous mice. Sonic hedgehog (SHH) induces arteriovenous malformation when injected in the brain.

where they connect the common carotid artery to external jugular vein, disconnecting it from the subclavian vein. By this way they create a cervical venous like nidus [26,27,29], that we classified as carotid-jugular plexus fistula. The model showed that molecular changes due to flow were induced in endothelial cells at the "nidus" [24,25], making it a unique model for testing radiation therapy effects and secondary obliteration, looking for cellular changes in irradiated cells or the effect of coadjutant prothrombotic agents. [69,70].

Radiation therapy has also been evaluated using different *in vivo* models like the swine RM [75,76], but also *in vitro* models as 3D casts [65] and computer simulations with CFD or mathematical models [66–68].

4.2. Anatomy / education

A last group of bAVM models have been developed for anatomical understanding and education. Three-dimension casts have been used for these purposes, using the evolution of new materials, 3D printing technology and image acquisition. Cast models can be used for surgical planning, medical or patient education and research [69,70].

5. Discussion

Brain AVMs are complex vascular lesions [1,2]. Despite all the advances in imaging diagnosis, treatments and genetics there are still several areas that have great space for uncertainty and unresolved questions. The search for a single model that could emulate all of the features of this disease started several decades ago, but, until now, there is no unique, nor perfect model for bAVMs. Instead of a sole model that could solve all the questions, there has been a progressive development of several models directed to emulate specific characteristics or therapeutic targets of this disease with their advantages and disadvantages (Table 4).

5.1. Title: bAVM Models. Advantages and Disadvantages.

With this scoping review we have detected a change over decades reflected in the published bAVM's models. Because there are no spontaneous AVMs in animal models, all of them require some degree of human manipulation. Early studies were centered in the indirect hemodynamic effects of bAVM, mainly with the use of carotid jugular fistula model [9,16,17]. This was replaced over time with the Rete Mirabile model in swine which allowed the endovascular manipulation, material testing and embolization simulation of the "nidus" [31,34,37–39]. Although their relevance in bAVM knowledge, the main drawback of these models is that they are not located in the brain, so real simulation of the AVM environment, its surroundings and risk of rupture - bleeding is not possible. The search for a real intracerebral AV shunt with a proper nidus has been challenging. Some surgical models with intracerebral shunts were created but they have not been popular or replicated in later publications [21,22]. The possibility to generate a real AVM nidus in the brain has only been possible with transgenic models. Transgenic technology using HHT disease as a genetic AVM model is based on an adenovirus that knocks-down specific genes and develops angiogenesis locally, which leads to the induction of AVM-like lesion in deep brain gray matter, with abnormal vessels, AV shunt and draining veins [46,71–73]. Transgenic models have been the main topic of publication in this field in the last decade, and probably will continue to dominate in the next years as they have been able to reveal several clues of AVM genetic and epigenetic origin/drivers and possible targetted medical therapies[72,74].

In vitro models have been of great use and help for understanding the behavior and hemodynamics of bAVMs. Through computer simulation, created models have transformed an AVM into an electrical circuit, allowing the testing of different hemodynamic situations and the risk of rupture [26,27,29]. Moreover, CFD has been able to use patient's derived data to recreate the flow and test several parameters inside the AVM [24,25]. The main advantage of these models is that they don't need complex human manipulation, use of animals or animal laboratory facilities as the *in vivo* models. Nevertheless, CFD simulation has the drawback that, to create a reliable model, a deep understanding of the real angioarchitecture of the nidus is needed. Current high-resolution imaging techniques still are unable to clearly depict what type of anomalous vascular connections and flow induced biological processes occur inside the nidus, or what really is the so-called nidus. Probably, computer models and more recent 3D printed cast models will continue to evolve and grow in complexity and accessibility. 3D cast models have been good for training and material testing in other vascular diseases as

Table 4
The nine different models with their main characteristics, uses, advantages and disadvantages.

Model	Characteristics	Use	Advantages	Disadvantages
Carotid-Jugular Fistula	In Vivo. Mice, Cats, Rats	Hemodynamic effects of AVMs, Normal Pressure Breakthrough	Allows the testing of hemodynamic effects of AVM in the brain.	No nidus, no intracranial AV shunt, indirect effects model. Requires surgical skills for creating the fistula.
Rete Mirabile	In Vivo. Swine, Sheep	Endovascular embolization, hemodynamic changes, radiotherapy, new embolic materials testing.	Good vessel size to test endovascular materials. Natural vascular structure in selected animals.	Not a real AV shunt. It's an arterio-arterial connection, which requires manipulation to become an AV shunt. No surrounding brain. Not able to assess rupture or hemorrhagic risk. Requires surgical skills for creating the fistula. Cost.
Transgenic	In Vivo. Mice, rats, zebrafish,	Angiogenesis study, AVM development, genetic understanding.	AVM like vascular lesions in the brain. Rupture risk evaluation. Test anti-angiogenic, genetic or novel therapies.	Technical requirements. High technology labs. Cost.
Carotid Jugular Plexus Fistula	In Vivo. Mice	Radiotherapy	Nidus like structure in animal neck. Possibility of testing biological changes in vessels after radiotherapy.	No real AVM nidus. No surrounding brain.Surgical skills for creating the fistula.
Cornea	In Vivo. Rat	Angiogenesis	Possibility to test angiogenesis	No surrounding brain, no AV shunt. No nidus.
AV Shunt Bypass	In Vivo. Dogs	Hemodynamic effects	Direct intracranial effects of AV shunt.	Difficult to create and replicate. Requires high surgical technical skills. No real nidus.
Computer model	In vitro. CFD, Mathematical models	Hemodynamic, Radiotherapy	No laboratory animals needed. High reproducibility.	Difficulties in recreate real vascular AVM architecture.
3D Cast	In vitro. 3D Printed models.	Hemodynamic, radiotherapy, anatomy	Easy to create	Hard to emulate real AVM angioarchitecture.
Biological Graft	In vitro, Chicken wings	Anatomy	Biological 3D model, with nidus like formation. Flow testing.	Simplified AVM model, not real nidus.

aneurysms or stroke, but the complexity of bAVMs angio architecture represents a major technical challenge to create a more reliable replica of the vascular arrangement of the nidus [69,70].

Human Placenta has been described in the last years as an interesting model for endovascular use. Although it has not been oriented to emulate a bAVM, it has showed that some endovascular embolic materials or embolization techniques can be tested using the placenta arterial vessels, which resembles the diameter and bifurcation anatomy of the human brain vasculature [75,76]. It may be that placenta models, together with some modifications, could serve in the future as an interesting *ex vivo* model for studying different treatment of this disease.

5.2. Future directions

As we have reviewed the actual knowledge of bAVM models, we only can expect major developments for the future. Probably one of the main objectives would be to translate transgenic technology and techniques that have been developed in small animals to large animals, like swines. This would allow implementation of research protocols that could evaluate the effects of bAVM over the surrounding brain tissue, in a more similar biological environment like human patients. There are no doubts that transgenic research will continue its progress and will bring new findings and genetic clues of AVM origin and novel therapies that will increase the possibilities of achieving a definite cure for this disease.

Advances in 3D printing and casting techniques should continue their development in order to create realistic models that could reproduce the AVM vascular angioarchitecture and small lumina. High resolution images may depict the complexity of the relationship between arteries and veins in these malformations. Together with cast technology, a real 3D vascular model could be created for hemodynamic evaluations, technique training and material testing.

Finally, we cannot forget that although experimental models are the base of exploring new frontiers in cerebrovascular diseases including AVM management, clinical trials are the final step in testing any therapeutic innovation and options for patients. The combination of basic science, experimental models and clinical knowledge will lead to better treatment for this disease.

6. Conclusions

Several models have been used for research and study of bAVM. Each one of the research questions has its own suitable models, with no unique or ideal one that could account for all the complexity of an AVM. We expect a continuous development of different and more accurate models that could lead to optimize the treatment strategies and increase the cure rate of this disease.

Declaration of Competing Interest

The authors declare that they have no known competing financial interests or personal relationships that could have appeared to influence the work reported in this paper.

Acknowledgement

None.

Funding

This research did not receive any specific grant from funding agencies in the public, commercial, or not-for-profit sectors.

References

[1] R.A. Solomon, E.S. Connolly, Arteriovenous malformations of the brain, N. Engl. J. Med. 376 (19) (2017) 1859–1866, https://doi.org/10.1056/NEJMra1607407.
[2] R.M. Friedlander, Arteriovenous malformations of the brain, N. Engl. J. Med. 356 (26) (2007) 2704–2712, https://doi.org/10.1056/NEJMcp067192.
[3] R. Al-Shahi, J.S.Y. Fang, S.C. Lewis, C.P. Warlow, Prevalence of adults with brain arteriovenous malformations: A community based study in Scotland using capture-recapture analysis, J. Neurol. Neurosurg. Psychiatry 73 (5) (2002) 547–551, https://doi.org/10.1136/jnnp.73.5.547.
[4] J. van Beijnum, H.B. van der Worp, D.R. Buis, et al., Treatment of Brain Arteriovenous Malformations A Systematic Review and Meta-analysis, JAMA 306 (18) (2011) 2011–2019, https://doi.org/10.1098/rspb.2013.0428.
[5] L. da Costa, M.C. Wallace, K.G. ter Brugge, C. O'Kelly, R.A. Willinsky, M. Tymianski, The natural history and predictive features of hemorrhage from brain arteriovenous malformations, Stroke 40 (1) (2009) 100–105, https://doi.org/10.1161/STROKEAHA.108.524678.
[6] J. Mohr, M.K. Parides, C. Stapf, et al., Medical management with or without interventional therapy for unruptured brain arteriovenous malformations (ARUBA): a multicentre, non-blinded, randomised trial, Lancet 15 (9917) (2014) 614–621, https://doi.org/10.5040/9781501329159-594.
[7] K.M. Cockroft, K.E. Chang, E.B. Lehman, R.E. Harbaugh, AVM Management Equipoise Survey: Physician opinions regarding the management of brain arteriovenous malformations, J. NeuroIntervent. Surg. 6 (10) (2014) 748–753, https://doi.org/10.1136/neurintsurg-2013-011030.
[8] A.M. Herrmann, S. Meckel, M.J. Gounis, et al., Large animals in neurointerventional research: A systematic review on models, techniques and their application in endovascular procedures for stroke, aneurysms and vascular malformations, J. Cereb. Blood Flow Metab. 39 (3) (2019) 375–394, https://doi.org/10.1177/0271678X19827446.
[9] R.F. Spetzler, C.B. Wilson, P. Weinstein, M. Mehdorn, J. Townsend, D. Telles, Normal Perfusion Pressure Breakthrough Theory, Clin. Neurosurg. 25 (1978) 651–672, https://doi.org/10.1016/B978-0-12-804075-1.00004-3.
[10] I. Hacking, Scoping studies: advancing the methodology, Implement. Sci. 5 (69) (2010), https://doi.org/10.1017/cbo9780511814563.003.
[11] M.D.J. Peters, C.M. Godfrey, H. Khalil, P. McInerney, D. Parker, C.B. Soares, Guidance for conducting systematic scoping reviews, Int. J. Evid.-Based Healthcare. 13 (3) (2015) 141–146, https://doi.org/10.1097/XEB.0000000000000050.
[12] H. Arksey, L. O'Malley, Scoping studies: Towards a methodological framework, Int. J. Soc. Res. Methodol. Theory Pract. 8 (1) (2005) 19–32, https://doi.org/10.1080/1364557032000119616.
[13] A.C. Tricco, E. Lillie, W. Zarin, et al., PRISMA extension for scoping reviews (PRISMA-ScR): Checklist and explanation, Ann. Intern. Med. 169 (7) (2018) 467–473, https://doi.org/10.7326/M18-0850.
[14] H. Khalil, M. Peters, C.M. Godfrey, P. Mcinerney, C.B. Soares, D. Parker, An Evidence-Based Approach to Scoping Reviews, Worldv. Evid.-Based Nursing. 13 (2) (2016) 118–123, https://doi.org/10.1111/wvn.12144.
[15] A. Liberati, D.G. Altman, J. Tetzlaff, et al., The PRISMA statement for reporting systematic reviews and meta-analyses of studies that evaluate health care interventions: explanation and elaboration, J. Clin. Epidemiol. 62 (10) (2009) e1–e34, https://doi.org/10.1016/j.jclinepi.2009.06.006.
[16] M.K. Morgan, R.E. Anderson, Jr TMS. The effects of hyperventilation on cerebral blood flow in the rat with an open and closed carotid-jugular fistula, Neurosurgery. 25 (4) 1989, 606-611.
[17] J. Hai, M. Ding, Z. Guo, B. Wang, A new rat model of chronic cerebral hypoperfusion associated with arteriovenous malformations, J. Neurosurg. 97 (5) (2002) 1198–1202, https://doi.org/10.3171/jns.2002.97.5.1198.
[18] M.K. Morgan, R.E. Anderson, T.M. Sundt, A model of the pathophysiology of cerebral arteriovenous malformations by a carotid-jugular fistula in the rat, Brain Res. 496 (1–2) (1989) 241–250, https://doi.org/10.1016/0006-8993(89)91071-8.
[19] R. Yassari, T. Sayama, B.S. Jahromi, et al., Angiographic, hemodynamic and histological characterization of an arteriovenous fistula in rats, Acta Neurochir. 146 (5) (2004) 495–504, https://doi.org/10.1007/s00701-004-0248-x.
[20] L.H.S. Sekhon, M.K. Morgan, I. Spence, Normal perfusion pressure breakthrough: The role of capillaries, J. Neurosurg. 86 (3) (1997) 519–524, https://doi.org/10.3171/jns.1997.86.3.0519.
[21] T.A. Pietilä, J.M. Zabramski, A. Thèllier-Janko, et al., Animal model for cerebral arteriovenous malformation, Acta Neurochir. 142 (11) (2000) 1231–1240, https://doi.org/10.1007/s007010070019.
[22] S. Numazawa, T. Sasaki, S. Sato, Y. Watanabe, Z. Watanabe, N. Kodama, Experimental model of intracranial arteriovenous shunting in the acute stage, Neurol Med Chir (Tokyo). 45 (7) (2005) 384, https://doi.org/10.2176/nmc.45.384.
[23] T. Massoud, M. Jain, S213 Strategic decisions when embolizing mixed plexiform and fistulous brain arteriovenous malformations: A stochastic network ensemble biomathematical AVM model reveals higher nidus rupture risk after occluding the fistula first, Neuroradiologyadiology. 60 (1) (2018) 344.
[24] P. Orlowski, P. Summers, J.A. Noble, J. Byrne, Y. Ventikos, Computational modelling for the embolization of brain arteriovenous malformations, Med. Eng. Phys. 34 (7) (2012) 873–881, https://doi.org/10.1016/j.medengphy.2011.09.028.
[25] P. Orlowski, F. Al-Senani, P. Summers, J. Byrne, J.A. Noble, Y. Ventikos, Towards treatment planning for the embolization of arteriovenous malformations of the brain: Intranidal hemodynamics modeling, IEEE Trans. Biomed. Eng. 58 (7) (2011) 1994–2001, https://doi.org/10.1109/TBME.2011.2119317.
[26] G.J. Hademenos, T.F. Massoud, An electrical network model of intracranial arteriovenous malformations: Analysis of variations in hemodynamic and biophysical parameters, Neurol. Res. 18 (6) (1996) 575–589, https://doi.org/10.1080/01616412.1996.11740474.
[27] G. Guglielmi, Analysis of the Hemodynamic Characteristics of Brain Arterivenous Malformations Using Electrical Models: Baseline Settings, Surgical Extirpation

Endovascular Embolization, And Surgical Bypass, Neurosurgery 63 (1) (2008) 1–11, https://doi.org/10.1227/01.NEU.0000315286.77538.57.
[28] P. Kailasnath, J.C. Chaloupka, Mathematical modeling of AVM physiology using compartmental network analysis: Theoretical considerations and preliminary in vivo validation using a previously developed animal model, Neurol. Res. 18 (4) (1996) 361–366, https://doi.org/10.1080/01616412.1996.11740437.
[29] Y.K. Kumar, S.B. Mehta, M. Ramachandra, Numerical modeling of vessel geometry to measure hemodynamics parameters non-invasively in cerebral arteriovenous malformation, Bio-Med. Mater. Eng. 27 (6) (2016) 613–631, https://doi.org/10.3233/BME-161613.
[30] G. Viale, The rete mirabile of the cranial base: A millenary legend, Neurosurgery. 58 (6) (2006) 1198–1207, https://doi.org/10.1227/01.NEU.0000216118.31290.65.
[31] D.H. Lee, C.H. Wriedt, J.C.E. Kaufmann, D.M. Pelz, A.J. Fox, F. Vinuela, Evaluation of three embolic agents in pig rete, Am. J. Neuroradiol. 10 (4) (1989) 773–776.
[32] J.C. Chaloupka, F. Vinuela, J. Robert, G.R. Duckwiler, An in vivo arteriovenous malformation model in swine: Preliminary feasibility and natural history study, Am. J. Neuroradiol. 15 (5) (1994) 945–950.
[33] T.F. Massoud, C. Ji, F. Vinuela, et al., An experimental arteriovenous malformation model in swine: Anatomic basis and construction technique, Am. J. Neuroradiol. 15 (8) (1994) 1537–1545.
[34] T.A. Becker, M.C. Preul, W.D. Bichard, D.R. Kipke, C.G. McDougall, Calcium alginate gel as a biocompatible material for endovascular arteriovenous malformation embolization: Six-month results in an animal model, Neurosurgery. 56 (4) (2005) 793–800, https://doi.org/10.1227/01.NEU.0000156494.94675.BB.
[35] D.F. Vollherbst, R. Otto, A. von Deimling, et al., Evaluation of a novel liquid embolic agent (precipitating hydrophobic injectable liquid (PHIL)) in an animal endovascular embolization model, J. NeuroIntervent. Surg. 10 (3) (2018) 268–273, https://doi.org/10.1136/neurintsurg-2017-013144.
[36] W. Li, S. Liang, W. Zhang, X. Zhao, H. Zhang, X. Lv, Liquid embolic agent Fe3O4-EVOH for endovascular arteriovenous malformation embolisation: Preliminary evaluation in an in vivo swine rete mirabile model, Neuroradiol. J. 33 (4) (2020) 306–310, https://doi.org/10.1177/1971400920917130.
[37] Y. Murayama, F. Viñuela, A. Ulhoa, et al., Nonadhesive liquid embolic agent for cerebral arteriovenous malformations: Preliminary histopathological studies in swine rete mirabile, Neurosurgery. 43 (5) (1998) 1164–1172, https://doi.org/10.1097/00006123-199811000-00081.
[38] T.F. Massoud, Transvenous retrograde nidus sclerotherapy under controlled hypotension (TRENSH): Hemodynamic analysis and concept validation in a pig arteriovenous malformation model, Neurosurgery. 73 (2) (2013) 332–342, https://doi.org/10.1227/01.neu.0000430765.80102.77.
[39] T.F. Massoud, Temporary cvp elevation enhances avm retropermeation during simulated endovascular trensh—transvenous retrograde nidus sclerotherapy under controlled hypotension hemodynamic feasibility in a pig model, Neuroradiology 60 (2018).
[40] R. Jahan, T.D. Solberg, D. Lee, et al., An Arteriovenous Malfromation Model For Steriotactic Radiosurgery Research, Neurosurgery. 61 (1) (2007) 152–159, https://doi.org/10.1227/01.NEU.0000255506.58719.F8.
[41] J. McDonald, P. Bayrak-Toydemir, R.E. Pyeritz, Hereditary hemorrhagic telangiectasia: An overview of diagnosis, management, and pathogenesis, Genet. Med. 13 (7) (2011) 607–616, https://doi.org/10.1097/GIM.0b013e3182136d32.
[42] S. Tual-Chalot, S.P. Oh, H.M. Arthur, Mouse models of hereditary hemorrhagic telangiectasia: Recent advances and future challenges, Front. Genet. (2015;5(FEB): 1–13.), https://doi.org/10.3389/fgene.2015.00025.
[43] J. Satomi, R.J. Mount, M. Toporsian, et al., Cerebral vascular abnormalities in a murine model of hereditary hemorrhagic telangiectasia, Stroke 34 (3) (2003) 783–789, https://doi.org/10.1161/01.STR.0000056170.47815.37.
[44] E.J. Choi, W. Chen, K. Jun, H.M. Arthur, W.L. Young, H. Su, Novel brain arteriovenous malformation mouse models for type 1 hereditary hemorrhagic telangiectasia, PLoS ONE 9 (2) (2014), https://doi.org/10.1371/journal.pone.0088511.
[45] E.J. Choi, E.J. Walker, F. Shen, et al., Minimal homozygous endothelial deletion of eng with VEGF stimulation is sufficient to cause cerebrovascular dysplasia in the adult mouse, Cerebrovasc. Dis. 33 (6) (2012) 540–547, https://doi.org/10.1159/000337762.
[46] E.J. Walker, H. Su, F. Shen, et al., Arteriovenous malformation in the adult mouse brain resembling the human disease, Ann. Neurol. 69 (6) (2011) 954–962, https://doi.org/10.1002/ana.22348.
[47] J. Tu, Y. Li, Z. Hu, Notch1 and 4 signaling responds to an increasing vascular wall shear stress in a rat model of arteriovenous malformations, Biomed Res. Int. 2014 (2014) 10–12, https://doi.org/10.1155/2014/368082.
[48] P.A. Murphy, T.N. Kim, G. Lu, A.W. Bollen, C.B. Schaffer, R.A. Wang, Notch4 normalization reduces blood vessel size in arteriovenous malformations, Sci. Transl. Med. 4 (117) (2012) 1–12, https://doi.org/10.1126/scitranslmed.3002670.
[49] P.A. Murphy, T.N. Kim, L. Huang, et al., Constitutively active Notch4 receptor elicits brain arteriovenous malformations through enlargement of capillary-like vessels, PNAS 111 (50) (2014) 18007–18012, https://doi.org/10.1073/pnas.1415316111.
[50] C. Papagiannaki, F. Clarençon, S. Ponsonnard, et al., Development of an angiogenesis animal model featuring brain arteriovenous malformation histological characteristics, Journal of NeuroInterventional Surgery. 9 (2) (2017) 204–210, https://doi.org/10.1136/neurintsurg-2015-012173.
[51] D. Konya, Ö. Yildirim, Ö. Kurtkaya, et al., Testing the angiogenic potential of cerebrovascular malformations by use of a rat cornea model: Usefulness and novel assessment of changes over time, Neurosurgery. 56 (6) (2005) 1339–1345, https://doi.org/10.1227/01.NEU.0000159886.08629.B7.
[52] K. Kiliç, D. Konya, Ö. Kurtkaya, A. Sav, M.N. Pamir, T. Kiliç, Inhibition of angiogenesis induced by cerebral arteriovenous malformations using Gamma Knife irradiation, J. Neurosurg. 106 (3) (2007) 463–469, https://doi.org/10.3171/jns.2007.106.3.463.
[53] A. Akakin, A. Ozkan, E. Akgun, et al., Endovascular treatment increases but gamma knife radiosurgery recreases angiogenic activity of arteriovenous malformations: An in vivo experimental study using a rat cornea model, Neurosurgery. 66 (1) (2010) 121–129, https://doi.org/10.1227/01.NEU.0000363154.88768.34.
[54] P. Corti, S. Young, C.Y. Chen, et al., Interaction between alk1 and blood flow in the development of arteriovenous malformations, Development. 138 (8) (2011) 1573–1582, https://doi.org/10.1242/dev.060467.
[55] B.P. Walcott, BMP signaling modulation attenuates cerebral arteriovenous malformation formation in a vertebrate model, J. Cereb. Blood Flow Metab. 34 (10) (2014) 1688–1694, https://doi.org/10.1038/jcbfm.2014.134.
[56] E.R. Rochon, P.G. Menon, B.L. Roman, Alk1 controls arterial endothelial cell migration in lumenized vessels, Development (Cambridge). 143 (14) (2016) 2593–2602, https://doi.org/10.1242/dev.135392.
[57] K. Wang, S. Zhao, B. Liu, et al., Perturbations of BMP/TGF-β and VEGF/VEGFR signalling pathways in non-syndromic sporadic brain arteriovenous malformations (BAVM), J. Med. Genet. 55 (10) (2018) 675–684, https://doi.org/10.1136/jmedgenet-2017-105224.
[58] M.T. Lawton, C.L. Stewart, A.A. Wulfstat, et al., The transgenic arteriovenous fistula in the rat: An experimental model of gene therapy for brain arteriovenous malformations, Neurosurgery. 54 (6) (2004) 1463–1471, https://doi.org/10.1227/01.NEU.0000125004.89129.B9.
[59] A. Karunanyaka, J. Tu, A. Watling, K.P. Storer, A. Windsor, M.A. Stoodley, Endothelial molecular changes in a rodent model of arteriovenous malformation: Laboratory investigation, J. Neurosurg. 109 (6) (2008) 1165–1172, https://doi.org/10.3171/JNS.2008.109.12.1165.
[60] K.P. Storer, J. Tu, M.A. Stoodley, R.I. Smee, Expression of endothelial adhesion molecules after radiosurgery in an animal model of arteriovenous malformation, Neurosurgery. 67 (4) (2010) 976–983, https://doi.org/10.1227/NEU.0b013e3181ee36bc.
[61] N. Raoufi-Rad, Z. Zhao, J. McHattan, et al., Irradiation induces molecular changes in endothelial cells of a rat AVM model, Mol. Imag. Biol. 15 (1) (2013).
[62] J. Tu, Y. Li, Z. Hu, Z. Chen, Radiosurgery inhibition of the Notch signaling pathway in a rat model of arteriovenous malformations: Laboratory investigation, J. Neurosurg. 120 (6) (2014) 1385–1396, https://doi.org/10.3171/2013.12.JNS131595.
[63] A.J. Gauden, L.S. McRobb, V.S. Lee, et al., Occlusion of Animal Model Arteriovenous Malformations Using Vascular Targeting, Transl. Stroke Res. 11 (4) (2020) 689–699, https://doi.org/10.1007/s12975-019-00759-y.
[64] A.A.F. de Salles, T.D. Solberg, P. Mischel, et al., Arteriovenous malformation animal model for radiosurgery: The rete mirabile, Am. J. Neuroradiol. 17 (8) (1996) 1451–1458.
[65] F. Bing, R. Doucet, F. Lacroix, et al., Liquid embolization material reduces the delivered radiation dose: Clinical myth or reality? Am. J. Neuroradiol. 33 (2) (2012) 320–322, https://doi.org/10.3174/ajnr.A2943.
[66] T.F. Massoud, G.J. Hademenos, A.A.F. de Salles, T.D. Solberg, Experimental radiosurgery simulations using a theoretical model of cerebral arteriovenous malformations, Stroke 31 (10) (2000) 2466–2477, https://doi.org/10.1161/01.STR.31.10.2466.
[67] B. Andisheh, M.A. Bitaraf, P. Mavroidis, A. Brahme, B.K. Lind, Vascular structure and binomial statistics for response modeling in radiosurgery of cerebral arteriovenous malformations, Phys. Med. Biol. 55 (7) (2010) 2057–2067, https://doi.org/10.1088/0031-9155/55/7/017.
[68] L. Eng, J. Fabrikant, R. Levy, M. Phillips, K. Frankel, E. Alpen, An experimental compartmental flow model for assessing the hemodynamic response of intracranial arteriovenous malformations to stereotactic radiosurgery, Neurosurgery. 28 (2) (1991) 251–259.
[69] M. Dong, G. Chen, J. Li, et al., Three-dimensional brain arteriovenous malformation models for clinical use and resident training, Medicine (United States) 97 (3) (2018), https://doi.org/10.1097/MD.0000000000009516.
[70] X. Ye, L. Wang, K. Li, et al., A three-dimensional color-printed system allowing complete modeling of arteriovenous malformations for surgical simulations, J. Clin. Neurosci. 77 (2020) 134–141, https://doi.org/10.1016/j.jocn.2020.04.123.
[71] W. Zhu, H. Su, Somatic ALK1 gene mutations mediated by an adenoviral vector expressing CRISPR/CAS9 induces arteriovenous malformation in the brain angiogenic region of adult mice, Angiogenesis 21 (111–167) (2018).
[72] W. Zhu, W. Chen, D. Zou, et al., Thalidomide reduces hemorrhage of brain arteriovenous malformations in a mouse model, Stroke 49 (5) (2018) 1232–1240, https://doi.org/10.1161/STROKEAHA.117.020356.
[73] P. Cheng, L. Ma, S. Shaligram, et al., Effect of elevation of vascular endothelial growth factor level on exacerbation of hemorrhage in mouse brain arteriovenous malformation, J. Neurosurg. 132 (5) (2020) 1566–1573, https://doi.org/10.3171/2019.1.JNS183112.
[74] E.J. Walker, H. Su, F. Shen, V. Degos, K. Jun, W.L. Young, Bevacizumab attenuates VEGF-induced angiogenesis and vascular malformations in the adult mouse brain,

Stroke 43 (7) (2012) 1925–1930, https://doi.org/10.1161/STROKEAHA.111.647982.
[75] H. Okada, J. Chung, D.M. Heiferman, D.K. Lopes, Assessment of human placenta as an ex-vivo vascular model for testing of liquid embolic agent injections with adjunctive techniques, J. NeuroIntervent. Surg. 10 (9) (2018) 892–895, https://doi.org/10.1136/neurintsurg-2017-013474.
[76] J.C.K. Kwok, W. Huang, W.C. Leung, et al., Human placenta as an ex vivo vascular model for neurointerventional research, J. NeuroIntervent. Surg. 6 (5) (2014) 394–399, https://doi.org/10.1136/neurintsurg-2013-010813.

II.4. Main Results and comments of Paper 1.

Several models have been used for studying brain AVMs, ranging from in vitro to in vivo models. There is no "perfect" model that could resemble all human brain AVM characteristics and we found many models for which questions or problems could be assessed [54–59], and we defined nine types of BAVM models with a main division of in vivo or in vitro (Table 3).

	Model Type		
In Vivo	Transgenic = 52 (29.4%)	Rete mirabile = 46 (26%)	Carotid-Jugular Fistula = 21 (11.9%)
	Carotid-Jugular Plexus Fistula = 19 (10.7%)	AV Shunt Bypass = 3 (1.7%)	Cornea model = 3 (1.7%)
In Vitro	Computational = 23 (13%)	3D Cast = 9 (5.1%)	Biological Graft = 1 (0.6%)

Table 3. Main BAVM models.
Main division of in vivo or in vitro, and the specific models with their publication's total number and frequency (%).

We also found that models could be used for one or more purposes (Table 4)

Subject / Characteristic	**Model**
Genetics, Angiogenesis	Mouse (deletion / gene implant), Zebrafish
Radiosurgery treatment	Rat, Carotid Jugular model
Endovascular treatment, Embolization materials	Swine rete mirabile

AVM Flow, hemodynamics	Computer / Mathematical / Electric
Anatomy, teaching	3D printed models

Table 4. AVM models and their use.

Summary table of BAVM models and their use. From Brain arteriovenous malformations: A scoping review of experimental models. Rivera et al, 2021[60].

This scoping review provided a clear overview of the evolution of BAVM models over the past decades, along with the changing trends in publication topics. The review began with the use of models to study hemodynamic effects in mice. This was followed by the exploration of rete mirabile models in swine. In recent times, there has been a substantial surge in interest and advancements in transgenic mouse models, with the objective to understand the genetic basis of BAVM origin and potential therapeutic targets [60].

Endovascular models have been limited, due to the absence of this brain disease in animals that could resemble a human size BAVM. Nevertheless, the swine rete mirabile has become the preferred model for simulating BAVMs for endovascular techniques / materials, due to their dimension and because, with some anatomical modifications, it could simulate arterial to venous flow (shunt) through a "nidus" like structure[61,62]. The carotid rete mirabile of the pig is a network of microvessels, average diameter 154 μm situated at the termination of each ascending pharyngeal artery (APA) as they penetrate the skull base. Each RM is connected across the midline to the contralateral rete through a cluster of midlines inter-retial micro vessels of similar caliber. The entire vascular structure formed by bilateral RM and their midline connections occupies the cavernous sinus. It has morphological similarities to a human cerebral plexiform AVM nidus but lacks its hallmark of arteriovenous shunting, thus, this has been solved with surgical creation of an anastomosis between the common carotid artery and

ipsilateral jugular vein, creating an arterial and a "venous side" of this RM network[62]. Other authors have modified and simplified this surgical route creating a "venous side" using a balloon guiding catheter and opening the flow of one side to the exterior[51].

In vitro models were a very small group in the scoping review. They have been divided in computational simulations of BAVM hemodynamics or physical models that could be used to represent anatomically a BAVM for endovascular testing and training. Models have been simple and 3D printing was not described for endovascular purposes at the moment of the review.

This scoping study gave us the hint to explore in vitro models as a way of developing a new BAVM model for endovascular use. Although the swine RM has been used for endovascular purposes, and by our group in the animal lab at Limoges France, it faces some limitations as maintenance cost, need for special animal facilities and laboratories, limitation for moving animals outside these locations, and the requirement of some complex anatomical preparations, such as surgical anastomosis to recreate an AV shunt.

The article in perspective:

There isn't a single ideal model for Brain Arteriovenous Malformations (BAVM), as various questions and challenges demand diverse approaches to tailor a model to specific requirements. These models can be broadly categorized into two groups: those employing living species (in vivo) and those utilizing artificial systems (in vitro).

BAVM models development and interest have been changing in the last decades. Recently, significant attention has been directed towards transgenic models, primarily involving rodents, to replicate BAVMs for genetic research and future treatments. This paper marks the inaugural comprehensive review encompassing all existing BAVM models.

II.5. Questions regarding in vitro models.

With an in vitro BAVM model project in mind for TVE, we have had to face several questions:

1. Which have been the in vitro models for BAVM embolization procedures?
2. Can be 3D printing used to create a BAVM model?
3. Is it possible to create an in vitro BAVM model for endovascular transvenous embolization using 3D printing?

III.1. In vitro vascular models.

In vitro comes from the Latin word “glass” and describes medical procedures, tests, and experiments that researchers perform outside of a living organism. In vitro models have been successfully used for endovascular purposes in brain aneurysms. Phantoms of this vascular disease have been created with silicon models and more recently using 3D printing technology. In vitro aneurysm models are created with hollow channels and elastic materials that allows catheter and microcatheter navigation inside them, and moreover, the use and deployment of devices such as coils, stents or intrasaccular materials for treating the aneurysms. Aneurysm models are typically constructed by gathering data from patients, followed by several digital processes to produce the final physical product [63]. Additive manufacture (AM) which is the process of creating objects summing layer by layer as 3D printing, is very suitable for reproducing complex architectures as vascular anatomies and high customization needs[63]. In vitro aneurysm models are widely used and play an important role in medical training, demonstrations, teaching, testing new materials and rehearsal of real cases [64–68].

III.1.1. In vitro models for Brain arteriovenous malformations.

A different situation has been seen for BAVM. Although in vitro models for BAVM are not new, because of their complex angioarchitecture and smaller vessels diameter, it has been very challenging to create realistic models as it has been done for brain aneurysms. In the late 1970s, Kerber et al. introduced two simple BAVM models within a flow circuit. In one model, they used an animal vessel as the BAVM, while in the other, a blood filter served as the nidus [53,69]. In 1981, Debruin et al. tested their calibrated-leak balloon device for embolizations using a

simple transparent plastic tube connected to a circulating plasma system under free fall pressure[70]. Probably one of the first attempts to create a more complex model of BAVM nidus came from Bartynski et al. in which they used scouring pad as a mesh within a sac, connected with tubes and called it “sandwich bag”. With this model, they were able to test Isobutyl 2-cianocrylate (IBC-2) embolizations in a flow circuit (Figure 8) [71].

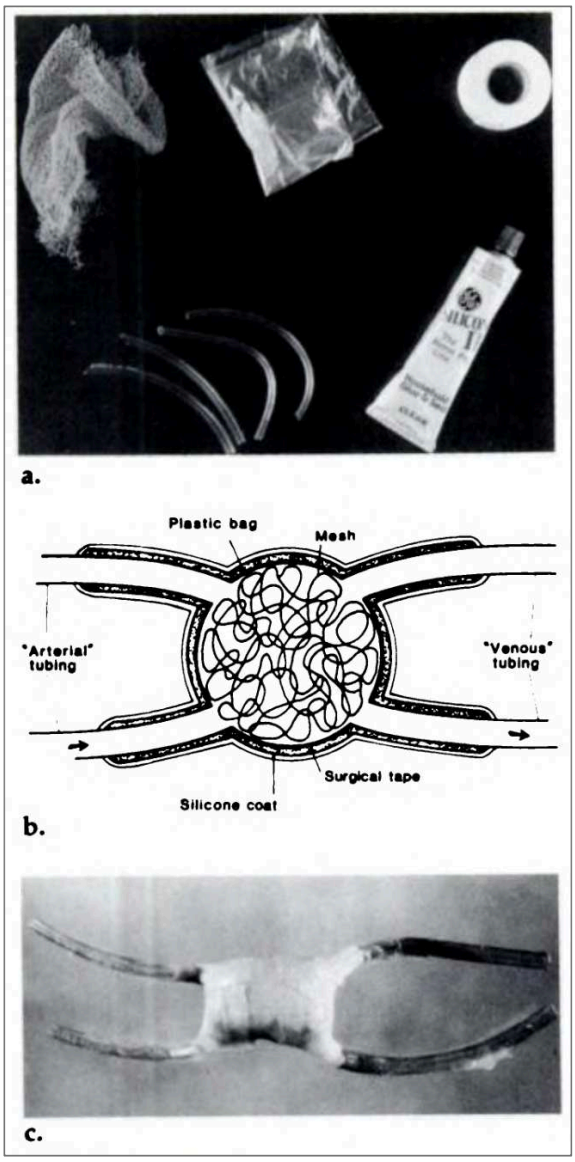

Figure 8. Bartynski et al[71] in vitro model.
AVM model a) Components of model are surgical tape, sandwich bag, plastic mesh, silicon sealant, and plastic tubing. b) Cross-sectional diagram of model. c) Photograph of completed model covered in watertight silicone sealant.

Later, Park and colleagues employed a glass tube filled with springs, connected to a flow pump circuit, to replicate a BAVM nidus. This setup was used for testing the newly developed polyvinyl acetate (PVA) material[72]. In 2003 an artificial nidus was created by Inagawa, using small beads inside a syringe or tube. This model was used in 2016 by Ishikawa et al to perform several embolization tests [73,74]. Recent embolization material's devolvement has led to the use of new in vitro models, as the silicon honeycomb-like nidus created by Vollherbst et al. in 2017. The model was used to test and compare Onyx 18 and PHIL 25 injections using different pause techniques[75] to determine differences between them (Figure 9).

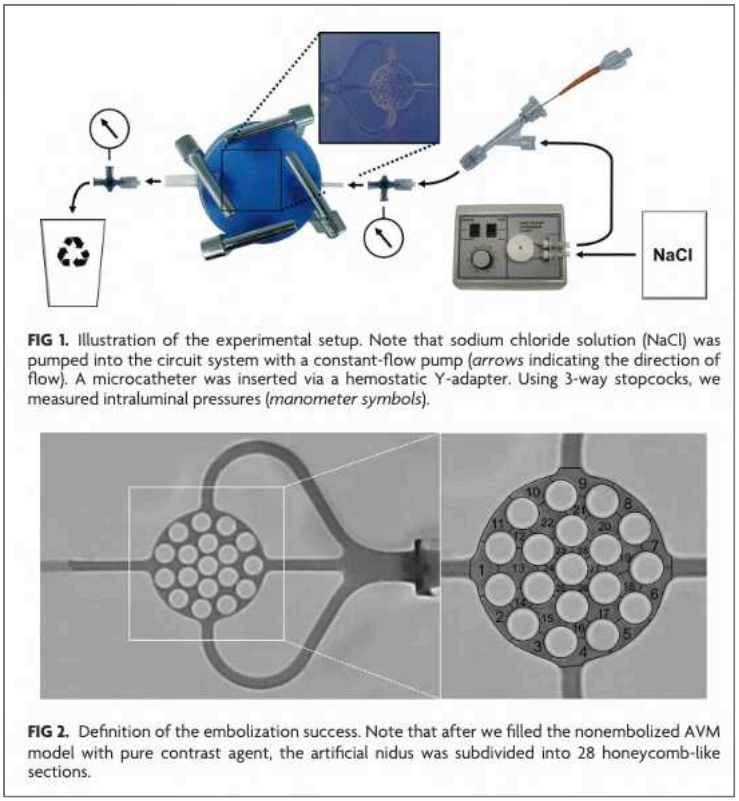

FIG 1. Illustration of the experimental setup. Note that sodium chloride solution (NaCl) was pumped into the circuit system with a constant-flow pump (*arrows* indicating the direction of flow). A microcatheter was inserted via a hemostatic Y-adapter. Using 3-way stopcocks, we measured intraluminal pressures (*manometer symbols*).

FIG 2. Definition of the embolization success. Note that after we filled the nonembolized AVM model with pure contrast agent, the artificial nidus was subdivided into 28 honeycomb-like sections.

Figure 9. From Vollherbst et al[75] in vitro model.

The most realistic in vitro BAVM model has been created recently by the group of Kaneko et al. In 2020 they were the first to report and create a model using real patient data and 3D

printing. They used a similar technique as has been used for brain aneurysms: They printed a solid cast of the BAVM anatomy and then covered it with silicon. The inner solid cast was lately dissolved resulting in a hollow structure of small vessels suitable to test EVOH injections[76] (Figure 10).

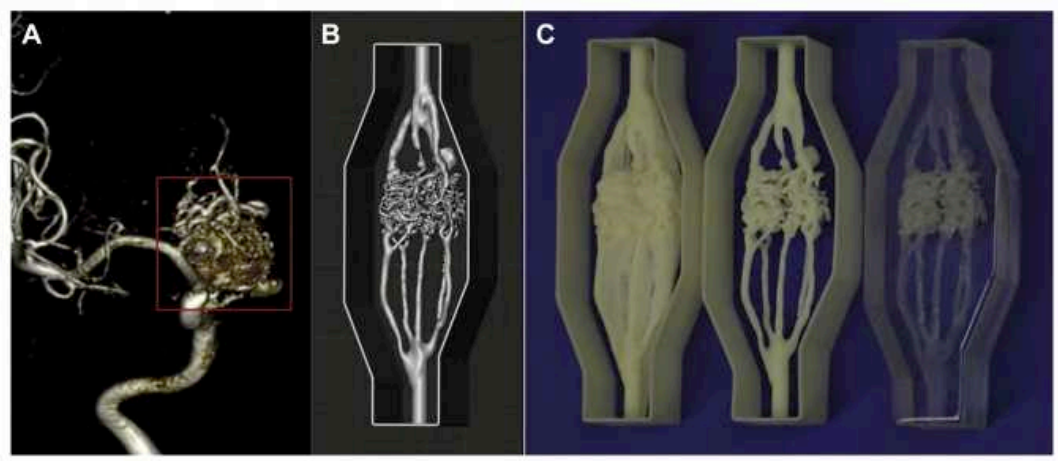

Figure 1. Manufacturing process of hollow arteriovenous malformation (AVM) models. (**A**) Digital imaging and communication in medicine data are obtained by rotational angiography. The AVM nidus is extracted (*red rectangle*) and converted to an stl file. (**B**) The stl file is loaded on the MeshMixer. Artificial feeders and drainers are added. (**C**) *Left*: The acrylonitrile, butadiene, and styrene solid mold with supports. The space between small nidal vessels is filled with the supporting material. *Middle*: The inner vascular mold after the supports are removed by washing. *Right*: Hollow silicone model after inner plastic mold is dissolved by acetone.

Figure 10. From Kaneko et al[77] in vitro model.

Three-dimensional printing looks like a very interesting way for creating a new BAVM model. We decided to review and search the main 3D printing techniques that could be suitable for our work.

III.2. Three-dimensional printing models.

III.2.1. Definition.

Three-dimensional printing is an additive manufacturing technique that constructs 3D objects from a CAD model. It can be done in a variety of processes in which material is deposited, joined, or solidified under computer control, with the material being added together (such as plastics, liquids or powder grains being fused), typically layer by layer.

III.2.2. Fused Deposition Modelling.

Before the experience by Kaneko et al. the use of 3D printing in BAVM was only the creation of solid cast models, mainly for educational, demonstration purposes or radiosurgery planning[78–80]. These models used a 3D printing technique called Fused Deposition Modelling (FDM) in which heated plastic filaments are heated and melted to create different forms adding the material layer by layer (Figure 11 and 12).

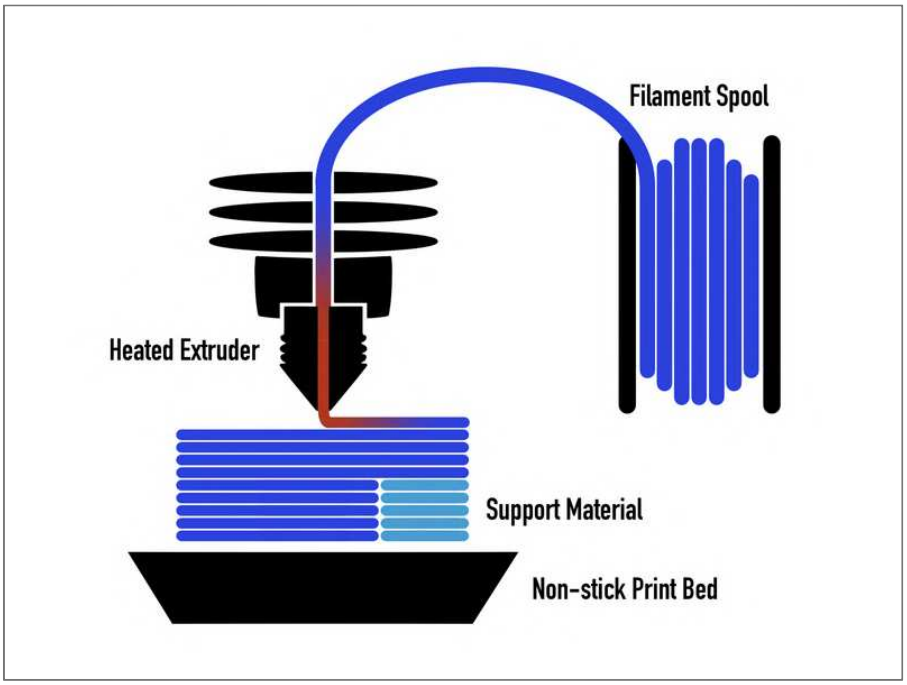

Figure 11. The FDM printing process.

Image Source:

https://dozuki.umd.edu/Wiki/Introduction_to_Fused_Deposition_Modeling_%28FDM%29

Figure 12. An FDM printer.

Image Source: https://bit.ly/3RNxHWX

Products produced with this technique usually lack high resolution and FDM result sometimes in notorious staircase effect. On the other hand, because of its resolution it's not possible to create small diameter hollow channels. The first 3D model of a patient's BAVM was reported by Thawani et all in 2016. In their experience they were able to recreate a solid FDM model of a BAVM and used it to train surgeons and increase the anatomical understanding of the disease before surgery[80].

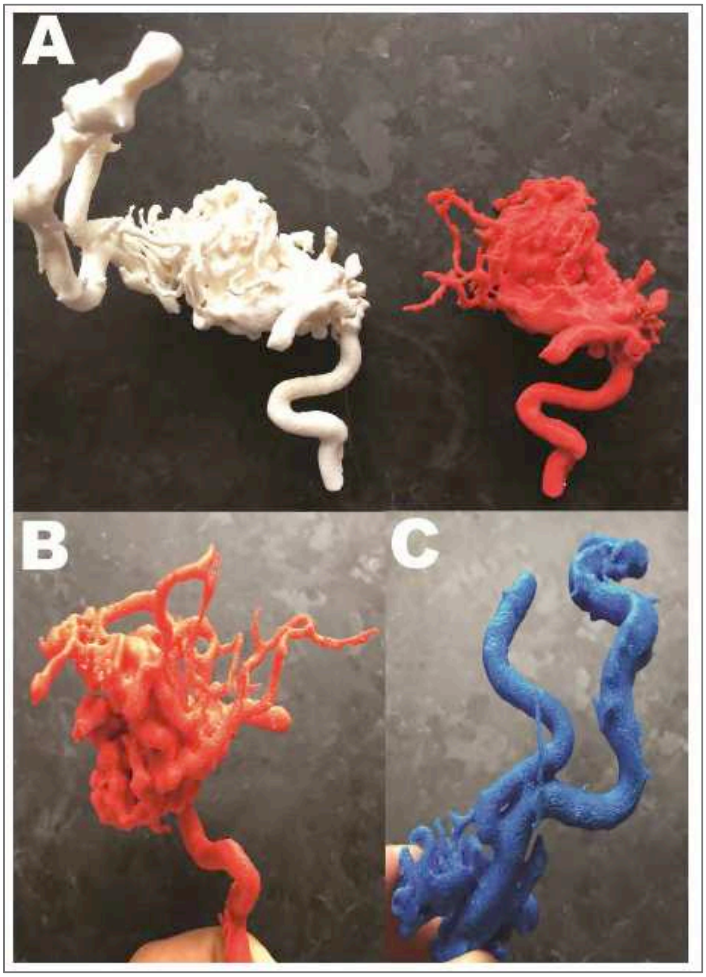

Figure 13. From Thawani et al. A 3D printed BAVM model using FDM[80]

Because of the limitations that present FDM to create hollow channels, a solution used for aneurysms has been to print a solid inner vessel mold and then cover it with silicone. The inner printed solid cast is then dissolved to leave the silicon and flexible hollow structure with channels. Silicone has elastic characteristics that are very suitable for vascular models, and it has been widely used for this purpose[81]. The same process was used by Kaneko et al. in their 3D printed BAVM model: a solid inner 3D printed FDM covered in silicon that was latter dissolved[76].

III.2.2.1. Stereolithography.

Stereolithography (SLA) is a 3D printing technique that uses photopolymers as liquid resins that are solidified (cured) layer by layer with the pass of a high-definition ultraviolet (UV) light source. It is also an additive technique, and the classical configuration has the liquid material contained in a bath which is progressively polymerized with UV light in layers[82] (Figure 14).

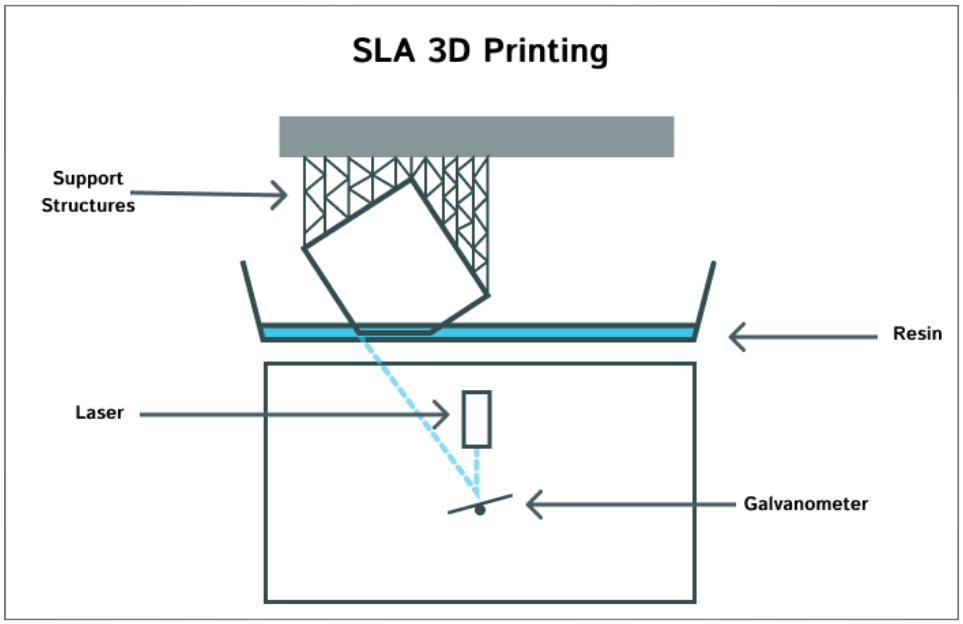

Figure 14. The SLA 3D printing process using a bath of resin and a UV light source that cures the resin layer by layer.

The advantages of SLA printing is that it allows fast prototyping from CAD (Computer-Aided Design) and watertight products with minimum or no staircase effect contrary to what is observed with other 3D printing techniques. Moreover, it can produce sub millimetric high resolution structures with intricate details.

The technique has been used in vascular diseases, to create hollow aneurysm models for surgery or endovascular training using real patients' data exported in DICOM (Digital Imaging and Communications in Medicine) from diagnostic machines as DSA, CTA or MRA [65,83,84]. These

SLA models have provided realistic training environments for physicians, hands-on education, material development and testing, teaching, and case rehearsals[65].

Although this technology has been used for brain aneurysms simulations, it has not been used for BAVM models. Brain AVMs have complicated architectures, with unclear anatomical definition of the nidus and small intricated vessels with diameters that could be under 300 µm[85], in comparison to brain aneurysms that are usually over 1 mm with parent vessels ranging from 2-5mm at the circle of Willis.

The challenge was to determine how to use SLA or other 3D printing technique to create a BAVM model with hollow channels.

III.3. Micro / Millifluidics.

Micro / Millifluidics is the science of precise laboratory control and manipulation of fluids that are geometrically constrained to a small scale, with network of channels and usually within a chip or cartridge. The dimension of channels is on the micro or milli-scale. The term millifluidics is used for channel diameters of greater than 1mm. Less than 1mm are termed submillifluidics (0.5-1mm), large microfluidics (100-500µm) or true microfluidics if under 100µm[86]. This technology allows researchers and engineers to manipulate liquids and fluids used in chemical synthesis, drug development, diagnosis, biotechnology, or material science. Micro / millifluidic devices typically include hollow channels, valves, and pumps designed to manipulate and direct the flow of fluids on a millimeter scale. These devices can be used to create miniaturized laboratories or "lab-on-a-chip" systems, allowing for high-throughput experimentation, reduced sample and reagent consumption, and rapid analysis[82].

Micro / millifluidics have used complex and expensive techniques to create the containers and chips, mainly using photolithography, soft lithography, and milling technique. Thus, in the last years they have incorporated SLA to their creation process. These have changed the design possibilities, with fast iterations, and a significant cost reduction. The process normally started with the 3D design in CAD, exported in STL (Standard Triangle Language) and then to 3D printer[87–89]. The possibility of creating such small hollow channels, package in a cartridge, took our attention and we saw the possibility of using the same technology for designing and creating a novel in vitro BAVM model using this technique.

IV.1. 3D printer selection.

The first step of this process was the selection of the 3D printer. Looking in the market we choose the Formlabs Form 3B (Formlabs, Somerville MA, USA) SLA printer because of its high-definition characteristics, biocompatible materials, but also because it has been promoted and used for printing micro / millifluidic chips (Fig 15).

Figure 15. A millifluidic Chip printed with Formlabs 3D printer.
Image Source: www.formlabs.com

This printer uses a new technology called low force stereolithography (LFS) in which a 250mW laser, cure (solidify) a photopolymer (resin) contained in a liquid bath. It can print with a resolution from 25µm to 300µm per slide (Figure 16).

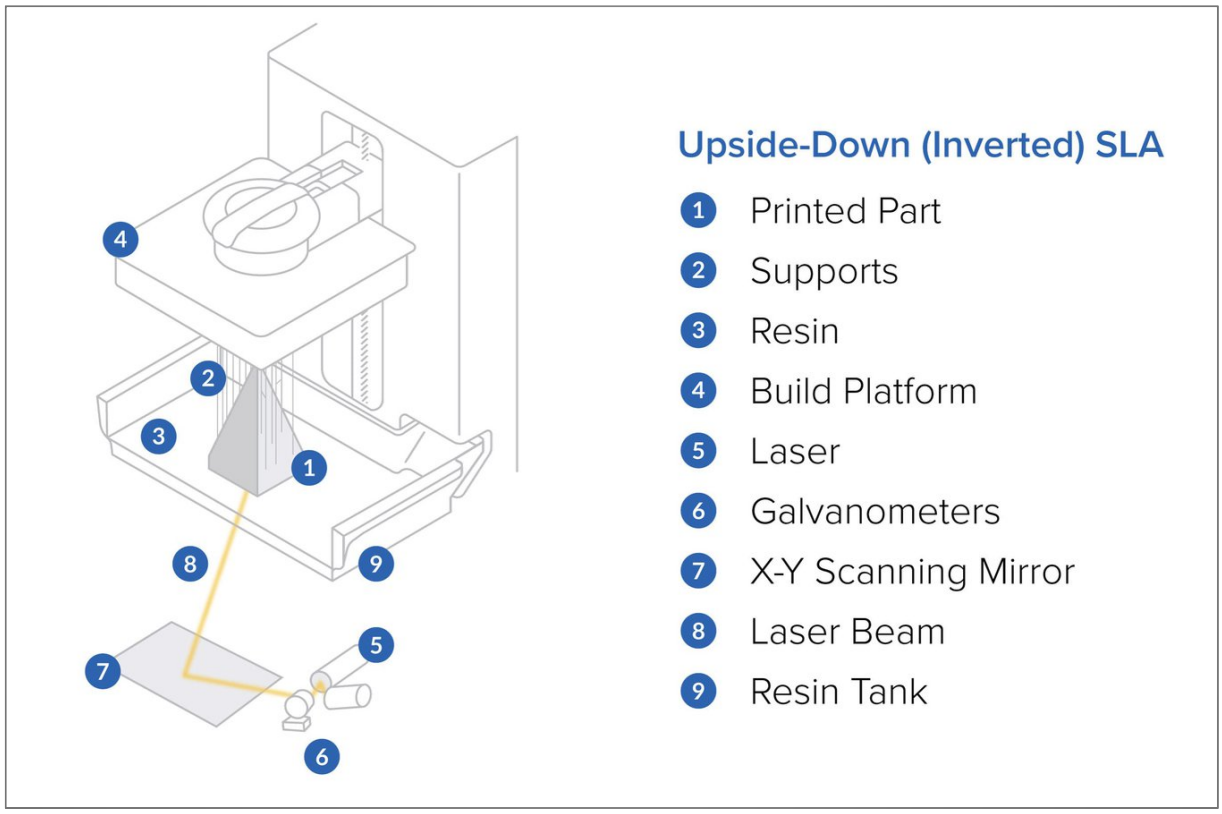

Figure 16. The Formlabs 3D printer.
This type of SLA printer it's called "Inverted SLA" and uses Low Force Stereolithography (LFS).
Image Source: www.formlabs.com

IV.1.1. Resin material.

For printing our in vitro models, we decided to use a transparent material called Clear V4® (Formlabs, Somerville MA, USA). This would allow a clear vision of the interior, and in our case of the embolization process. Clear V4 is a transparent resin that can be polished up to near optical transparency, allowing showcasing internal features and elements.

IV.2. Chip Design

Our first step in the design of a new in vitro BAVM model was to define and create a structure with hollow channels. The model was designed using CAD software (Fusion 360, Autodesk California USA). We started with a simple configuration that contained hollow tubes and external connectors in two different parallel circuits (Figure 17). CAD design was exported in STL language to the 3D printer. We called our first model Chip_1.

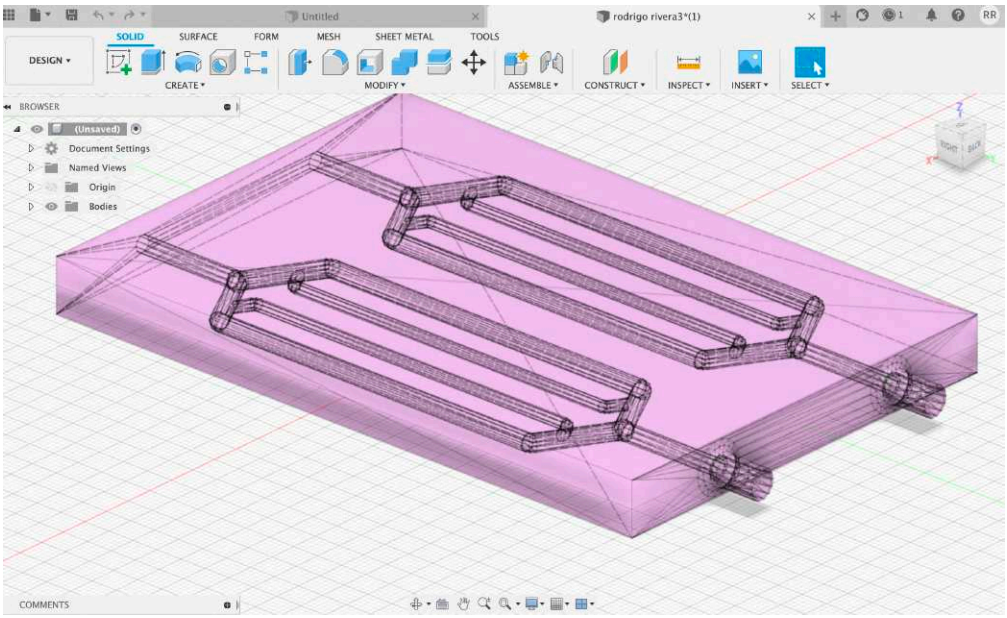

Figure 17. CAD design image from Fusion 360 software of Model Chip_1.

SLA file was then prepared for 3D printing using PreForm software (Formlabs, Somerville MA, USA) (Figure 18). This software allows:

- Planning of the printing process.
- Checking of the geometry.

- Defining the position within the printing platform.
- Determining the number of models to print.
- Creating supports for printing.
- Selecting printer and printer resolution.
- Defining printing material (resin type).

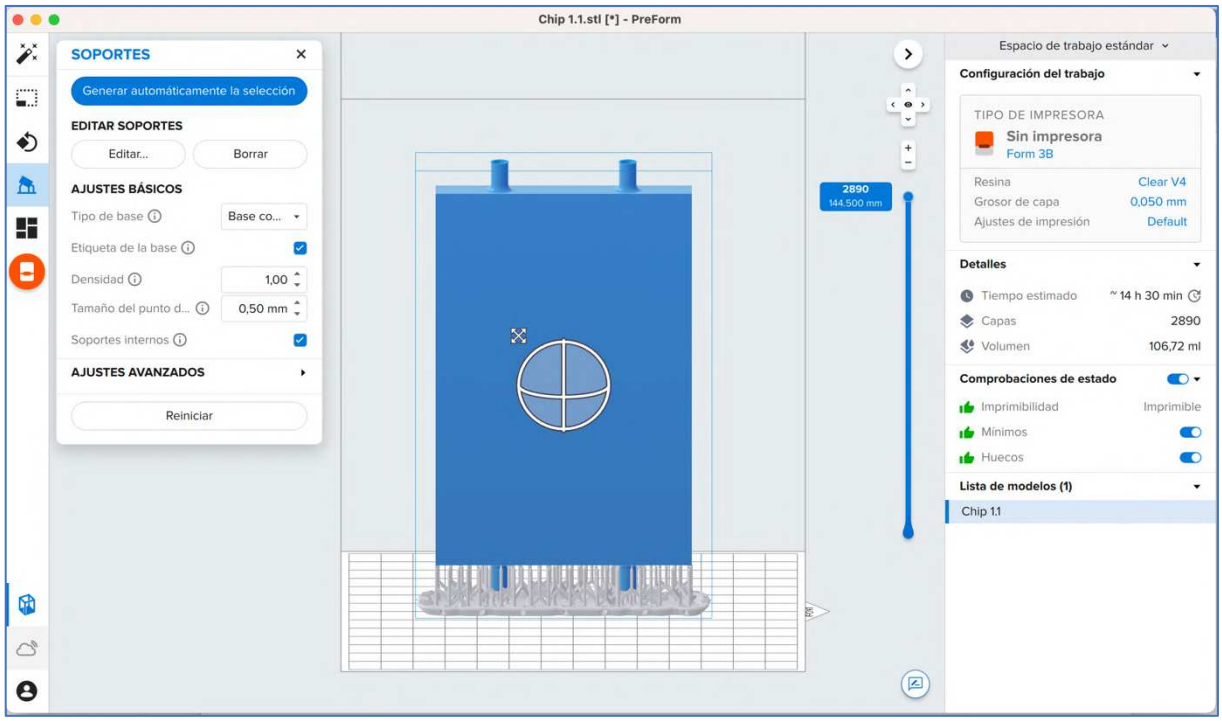

Figure 18. Formlabs PreForm Software with model Chip_1.

We printed the CAD using Formlabs Clear V4 Resin in the Formlabs 3B printer (Figure 19). After printing, the model was washed in isopropyl alcohol (IPA) bath for several minutes. After cleaning the outer and inner residual resin material, the model was exposed to more UV light to complete the curing process and to obtain the maximal physical characteristics. This final curing was done using an UV light chamber.

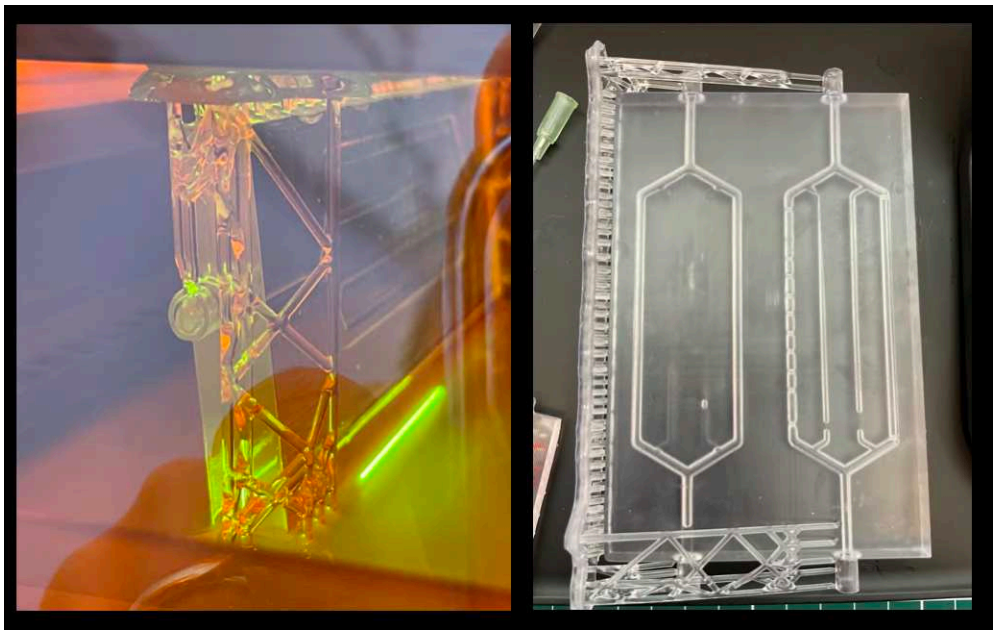

Figure 19. The printing process of Chip_1.
A) The model at the printer. The laser is visible in the lower part, curing the piece layer by layer. B) Final model outside the printer. Inner channels were not opened because we could not adequately clean the residual resin.

Because of the transparency of the material, it allowed the clear visualization of the inner channels. Some internal channels were not opened due to difficulties in the cleaning of uncured resin with IPA (Figure 19).

We tested Chip_1 model under X-rays using an angiograph machine, Philips Azurion 7 biplane (Philips Healthcare, Amsterdam Netherlands) (Figure 20).

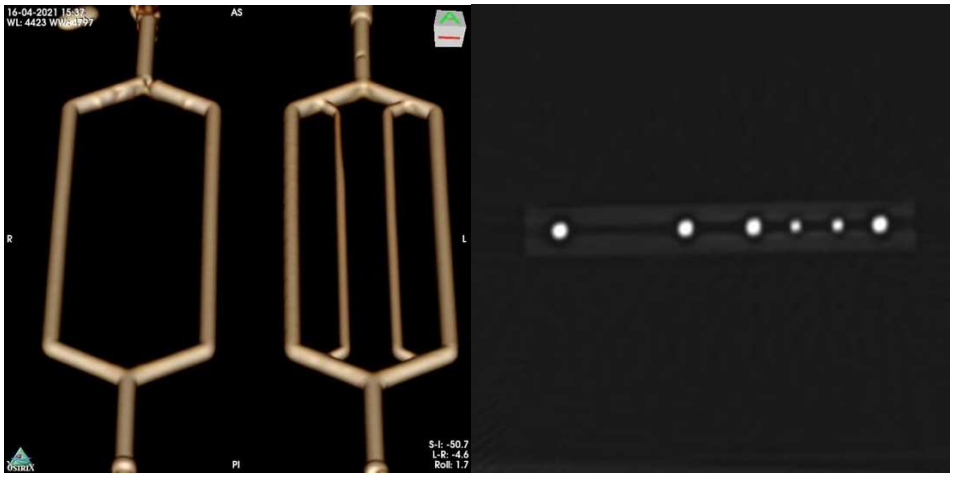

Figure 20. Angiographic study of Chip_1.

A) 3D volume rendering reconstructionof Chip_1. B) Sectional cut of the model with MIP (Maximum Intensity Projection). The inner tube diameters were 3mm.

We perform 2D digital subtraction Angiography using Visipaque® Iodixadol iodine contrast (GE HealthCare, Chicago IL, USA) and rotational 3D images with VR and MIP reconstructions. Images were reconstructed using a Philips workstation.

IV.2.1. Model Chip_2

Our next model evolution aimed for better external connections and softer curves at inner tubes. We incorporated luer lock connectors to improve perfusions and injections (Figure 21).

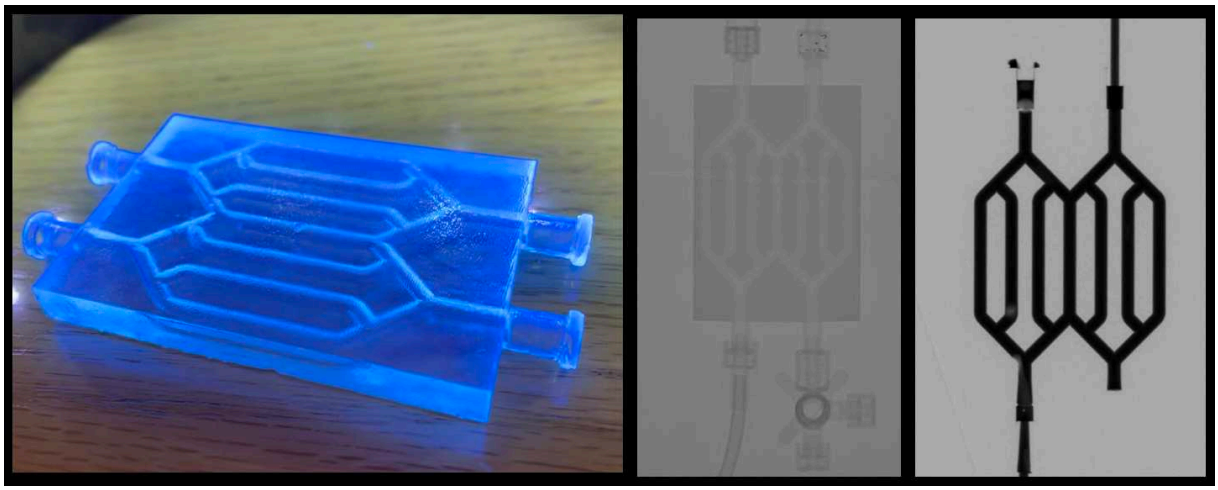

Figure 21. Model Chip_2.

A) The model just out of the printing process. B) Chip_2 under X-rays, connected to several tubes. C) Contrast-enhanced image under X-rays.

IV.2.2. Model Chip_3

For Chip_3 we jumped to a more functional design for endovascular use. A single channel model with some dilatations and a simple nidus like section. In this model we incorporated a one-sided input and output. We also decreased the inner diameter tubes to 2mm with an adequate visual opening (Figure 22).

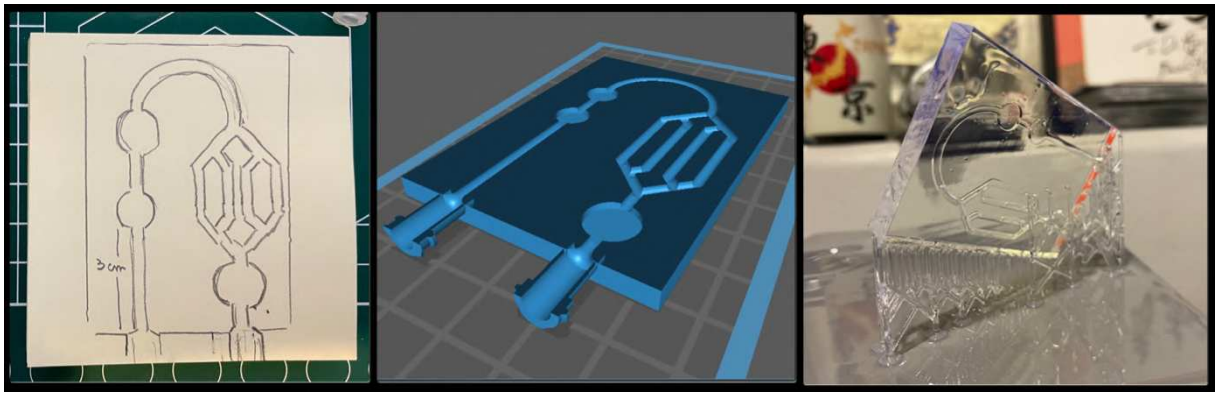

Figure 22. Model Chip_3.

A) Paper draft of the design of Chip_3. B) CAD design image. C) The model at the printing platform.

IV.2.3. Model Chip_4

This model was an evolution of Model Chip_3 with softer inner curves and more spherical shape of the dilatations (Figure 23). We developed a new design technique for creating these more natural geometries and softer edges.

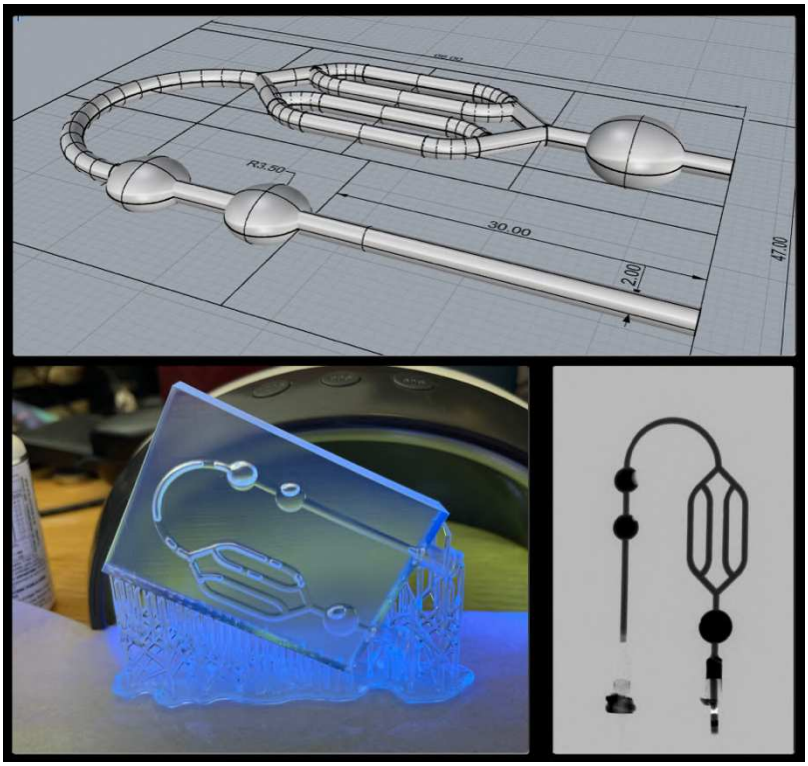

Figure 23. Chip_4.
A) CAD design with more naturel curves and geometry. B) At printing platform. C) X-Ray test using 2D DSA and contrast media.

Evaluation with DSA showed excellent permeability of 2mm channels with good filling of the dilatations and the “nidus”.

IV.3. Channel diameter testing.

Using model Chip_4 we tried to go under 2mm channel diameter. We used the same printer configurations, Clear V4 Resin and 100µm resolution slides. We printed 3 different versions with channels diameters of 1mm, 1.5mm and 2mm (Figure 24).

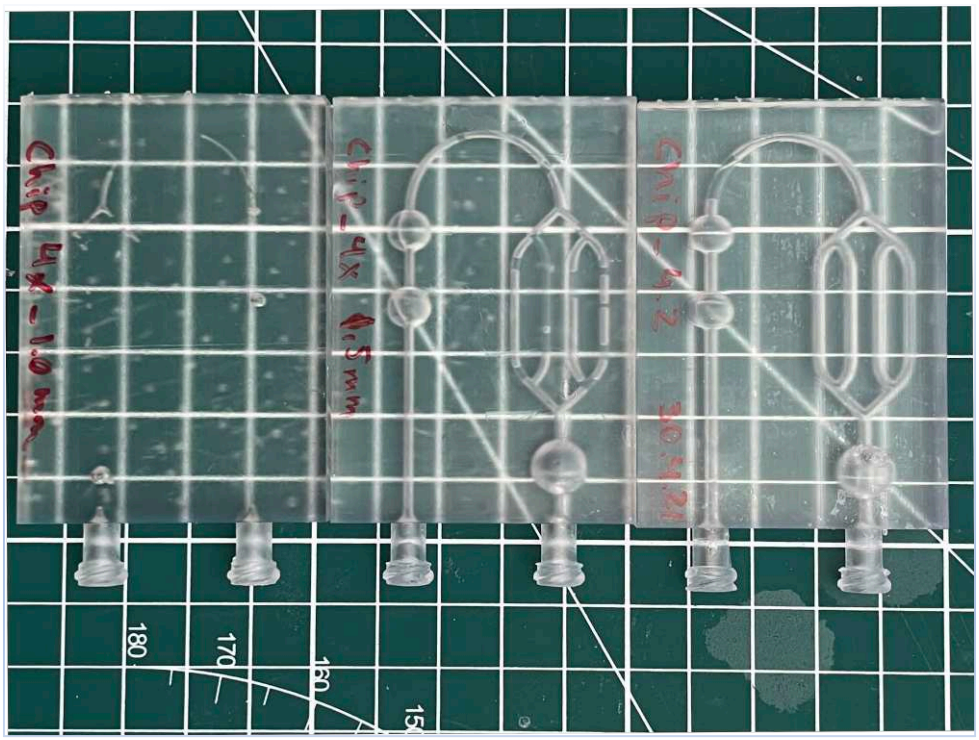

Figure 24. Chip_4 inner channel test.

From left to right, 1mm diameter model, 1.5mm model and 2mm model. Channels at 1mm were not able to open and cleaned. Models with 1.5 and 2mm channels were well printed and channels opened.

Good permeability was reached in the 1.5 and 2mm channel models. We were not able to open 1mm channels in this model. The residual resin inside the model was not possible to be cleaned.

IV.3.1. Open channel diameter tests.

In this experiment we designed several models with open channels and different diameters to test the capacity of the printer to create and define these structures.

For this purpose, we designed a half model Chip_4, cut in half and exposed open inner tubes, using different diameters: 0.25mm, 0.5mm, 1mm, 1.5mm and 2mm. We printed using 25µm per slide resolution (the higher resolution of Formlabs 3B printer). All models were adequately printed, and channels had a correct definition at visual inspection and macro photography (Figure 25). This confirmed us that the problem of printing lower diameter channels in the models was not the printer resolution, thus it was the ability of cleaning the residual liquid resin inside channels.

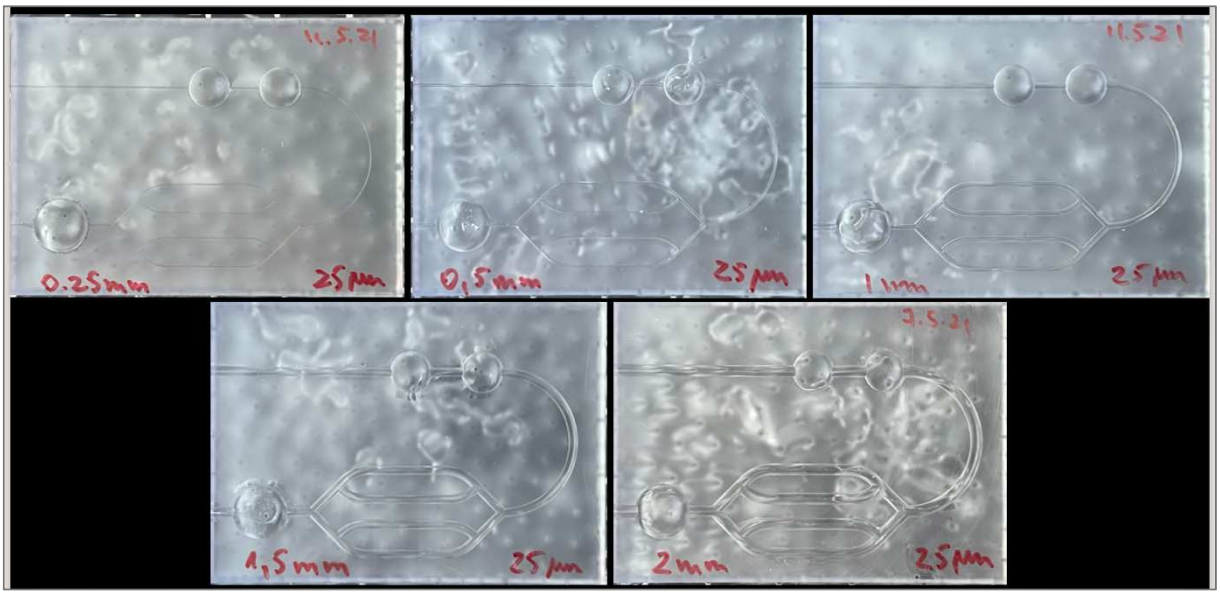

Figure 25. Printed half models for diameter testing.

IV.4. Dimethyl Sulfoxide (DMSO) Test

DMSO is the solvent contained within the liquid embolic agents that are used for BAVM embolizations, as EVOH or PHEMA. DMSO is highly corrosive and usualy affects several polymers and plastics. We tested the reaction of direct application of DMSO to the surface of the model for 15 minutes and internal injections to our resin model. We observed that after this time, there were no superficial changes and no corrosion to luer lock hub or inner channels (Figure 26).

Figure 26. DMSO test on Chip_4 and Chip_3.
A) Surface test with a drop of DMSO. After 15min no changes were seen in the model. B) Inner test injection of DMSO. No corrosion was seen at luer lock connector or inner channels.

IV.5. Liquid Embolic Agent test on the model.

We performed the first anterograde (arterial) embolization test on our model under X-rays at the Angio Suite of the Instituto de Neurocirugia Dr. Asenjo, Santiago Chile, using a Siemens Artis Zee biplane (Siemens Healthineers, GmbH, Germany).

Materials:

- Model Chip_4.1

- EVOH LEA: Squid 18 (Balt, Montmorency France)
- Microcatheter: Sonic 1.5F 25 (Balt, Montmorency France).
- Sodium Chloride (NaCl 0.9%) at room temperature.

Under continuous NaCl 0.9% infusion of the model with hydrostatic pressure, we navigated with Sonic 1.5F microcatheter inside the model. We then injected Squid 18 through the microcatheter. We were able to advance forward the material, reach the "nidus" and fill all dilatations. Visibility under DSA was excellent. The material injection felt realistic, it advanced in the regular fashion with a plug and push technique[90], which means that LEA after reaching distal resistance during injection it flows backwards as reflux. This reflux allows the precipitation around the microcatheter creating a plug that will allow further forward advance of the material by overcoming the distal pressure resistance (Figure 27).

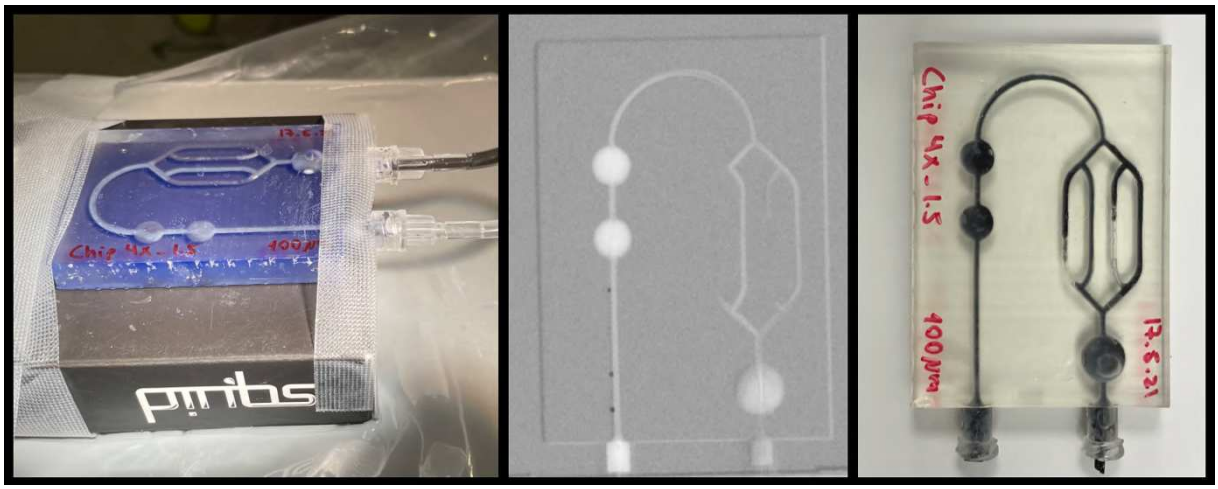

Figure 27. Squid 18 embolization test using Chip_4.1.

A) The model at the angiograph table fixed with tapes over a Squid box. B) Road Map X-rays vision of the model and the Sonic 1.5F in position. C) Macroscopic vision of the model afger embolization with Squid 18. The black coloration is due to tantalum of Squid 18.

After this test we determined that:

- EVOH embolization in the model was feasible.
- EVOH precipitates and behaves like real BAVM embolizations.
- Procedure could be measured and recorded.

IV.6. Towards a more realistic BAVM model design

After the pilot phase of model Chip_1 to 4 we decided to create a structure that could resemble more to a BAVM (Figure 28). The model was named MAV_1 and the components were:

- Channels of 1.5mm (less diameter).
- An entrance for the “arterial” side.
- A “nidus” made of 3 different channels connected to the “vein”.
- A vein pouch with output.
- A “normal” channel that bypasses the “AVM”.

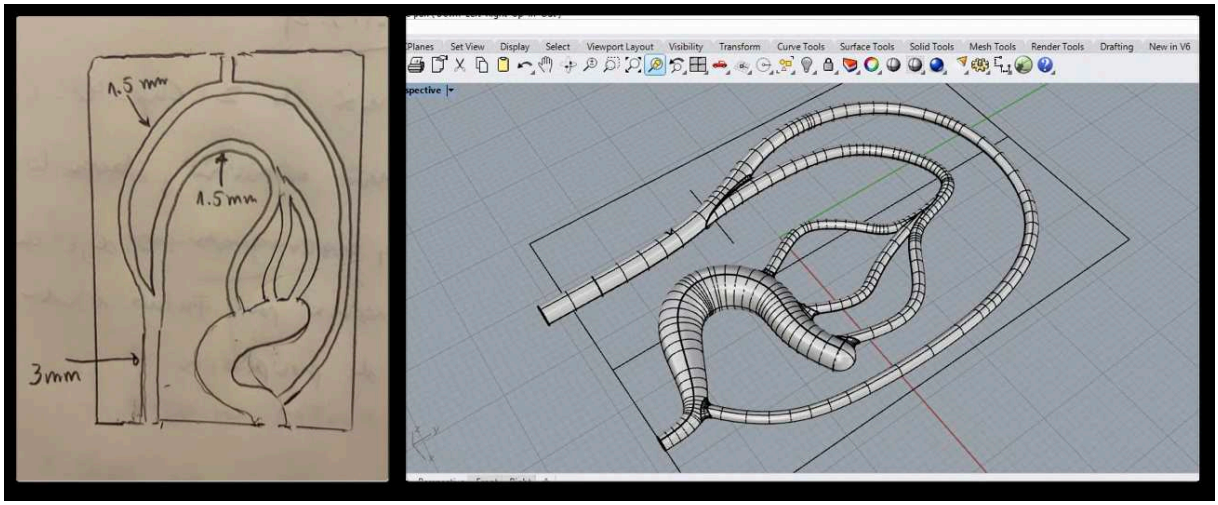

Figure 28. MAV_1 model design.

A) The design draft of model MAV_1, channel diameters and their components. B) CAD design image of the model.

The model was printed using the Formlabs Form 3B and Clear V4 resin. Channels were totally open at visual inspection and confirmed with the DSA + 3D rotational studies at the angio suite (Figure 29).

Figure 29. MAV_1 model printing and testing.

A) At final process of 3D printing, still with supports. B) X-ray contrasted 3D rotational image. All channels are well opened.

IV.6.1. Model MAV_2 and 3

These versions represented a change in the design process. To create more biologic like structures we used a different CAD software and process with Rhinoceros 3D (Robert McNeel & Associates, USA). It resembles model MAV_1 but with softer curves and more natural

aspect. Model MAV_3 included some dilatations as aneurysms inside the “AVM” circuit (Figure 30).

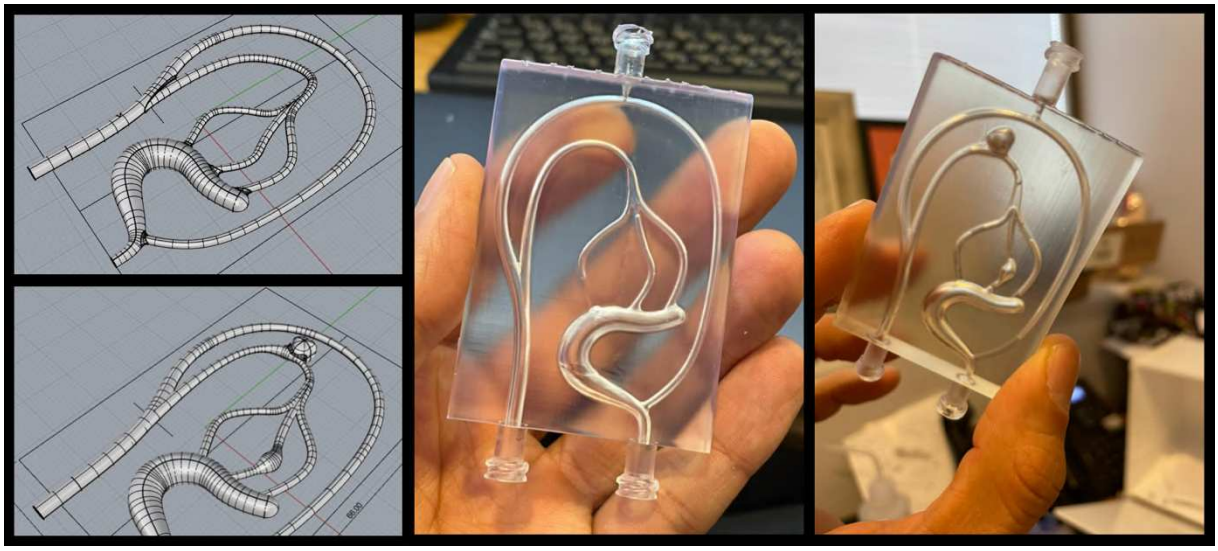

Figure 30. MAV_2 and 3 models.
A) CAD of model MAV_2 and MAV_3. B) MAV_2 after printing. An upper luer lock connector was included to facilitate external channel resin cleaning. C) Printed MAV_3 model. Fusiform like dilatations were created in the circuit.

IV.6.2. Looking for more complex AVM designs.

Our next evolution of models came with design Model MAV_4. In this version, we used model MAV_3 as base and added more vessels to the nidus, but at the same time we also elaborated a volume of the nidus in other axis. Additionally, we changed the case design to reduce extra use of resin in the container (Figure 31).

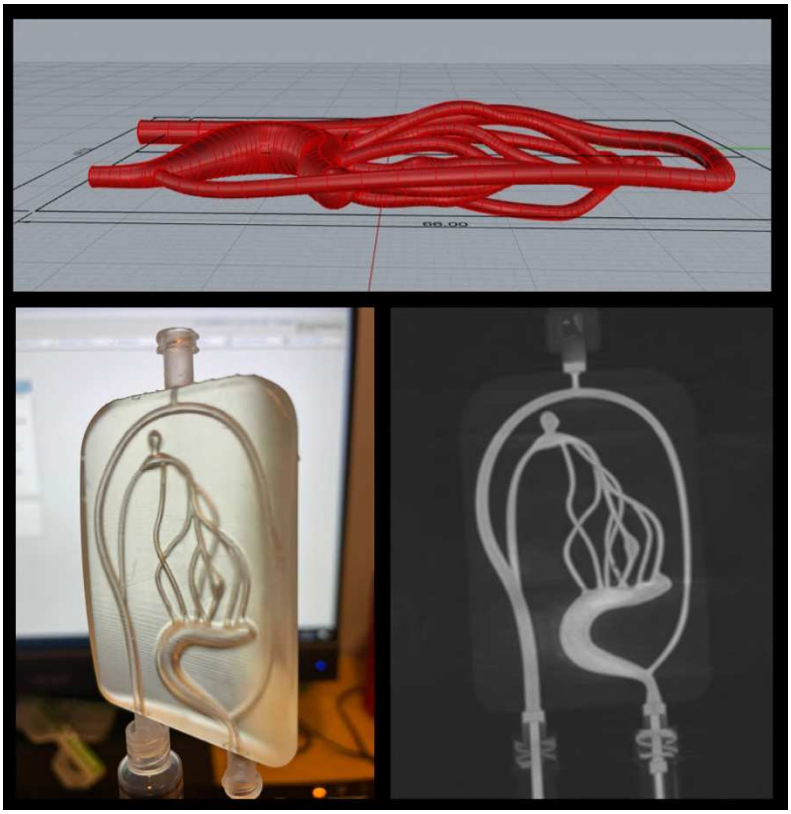

Figure 31. MAV_4 model.
A) CAD model of MAV_4. Now there is a volume in other axis. Not all the model is fixed to one plane. B) printed model within its container. C) X-ray vision of the model using road map.

IV.6.3. The evolution of the models

After several iterations we were able to create a more realistic BAVM model, with better nidus, and channels (Figure 32).

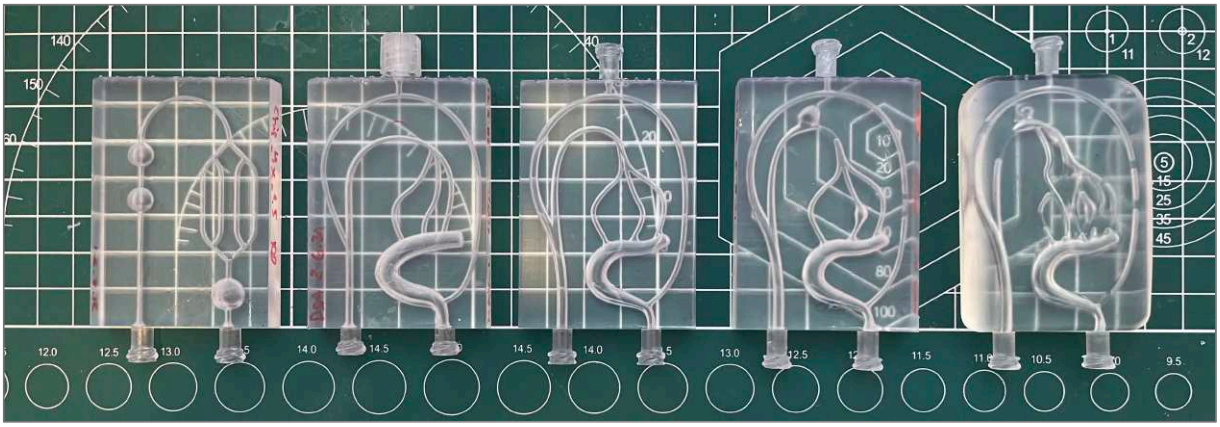

Figure 32. The model evolution.

From left to right: Chip_4, MAV_1, MAV_2, MAV_3 and MAV_4.

IV.7. Liquid Embolic Agent embolization Test 2

Based on the new design, we tested EVOH embolization. For this session we prepared the following setting:

- Model MAV_4 model.
- LEA: PHIL 25 (Microvention Aliso Viejo, CA USA)
- Apollo 1.5F 30 microcatheter (Medtronic, Parkway MN USA).
- Expedion microguidewire (Medtronic, Parkway MN USA).
- Philips Azurion 7 biplane.
- Sodium Chloride (NaCl 0.9%) flush of the model at room temperature.

Embolization was done using the plug and push technique. Initial dead space injection of DMSO followed by LEA injection of PHIL 25. Reflux was controlled up to the proximal bifurcation. A realistic and good filling of the nidus was achieved and occlusion of the vein (Figure 33).

Figure 33. MAV_4 embolization with PHIL 25.

A) Angio Suite setting, with a tripod and camera to record the procedure. B) X-ray vision of the model with precipitating PHIL 25. C) Two MAV_4 models. On the right the one that has been embolized with PHIL 25. PHIL 25 is macroscopically white, because it has no tantalum and it is visible at x-rays with a bonded iodine molecule.

IV.8. Continuous BAVM model design evolution.

Next models represented a continuous of improvements at nidus complexity and inner diameter reduction (Table 5).

Model	New characteristics	Material	Test / Use
MAV_5	More channels in the nidus. "Normal" circuit connected directly to the vein, to create a wash effect on the AVM drainage.	Clear V4 Resin	DSA / 3D

	Minimum diameter of tubes = 1mm		
MAV_6	Added tortuosity to vessels at nidus	Clear V4 Resin	DSA / 3D
MAV_7	Modified version of MAV_5, with changes in nidal tubes for a better resin wash and channel permeabilization	Clear V4 Resin	DSA / 3D
MAV_8	Elimination of external bypass channel, as used in MAV_7. Simpler and smaller external cage, to reduce Resin use.	Clear V4 Resin	DSA / 3D CFD LEA test embolizations
MAV_9	Restore of external bypass circuit with a modification using a small parallel circuit as “the brain”.	Clear V4 Resin	DSA / 3D CFD LEA test embolizations

Table 5. Evolution and characteristics from model MAV_5 to MAV_9.

IV.9. Liquid Embolic Agent embolization test 3.

We used model MAV_8 for the third LEA test embolization session. In this opportunity materials were:

- Model MAV_8
- Sodium Chloride (NaCl 0.9%) flush at normal temperature
- Contrast: Visipaque 270 (GE Healtcare, Chicago IL USA)

- Microcatheter: Sonic 1.2F 25mm (Balt Montmorency, France)
- Guidewire: Hybrid 0.007” (Balt Montmorency, France).
- LEA: Squid 18 (Balt Montmorency, France).
- Pump: Sys Cooking mini pump. 390ml/min with continuous flow.
- Pressure sensor (TruWave, Edwards Lifesciences Services GmbH, Germany).
- Angiograph: Philips Azurion 7 biplane.

In this test we were able to use a simple pump, with continuous flow (390ml/min) and measured the input pressure to the model (middle arterial pressure of 80mmHg).

We embolized from an anterograde fashion from the arterial side, filling the nidus up to the vein using the plug and push technique (Figure 34).

After this test, we decided to modified MAV_8 with a bypass circuit as seen on MAV_7 and a mini resistance circuit as a normal “brain” for a better flow to the model, but also for continuous flush.

Figure 34. Embolization test 3. MAV_8.
A) Angio Suite setting of the model on the table. B) Model after Squid 18 embolization. An almost complete filling of the nidus and vein.

IV.10. Computational Flow Dynamic Studies (CFD).

Computational Flow Dynamics is a branch of fluid mechanics that uses numerical analysis and data structures to analyze and solve problems that involve fluid flows.

The purpose of using CFD in our models was to analyze the fluid behavior and flow patterns inside the channels.

For this purpose, CAD data was processed with ANSYS Fluent software (Canonsburg, PA, USA) transforming the image in multiple triangles (10 million elements) that were analyzed (Figure 35). We assumed a non-Newtonian fluid (Carreau's model), rigid walls and constant inflow velocity to calculate various variables, such as pressure, velocity, and wall shear stress (WSS) in the model (Figure 35 and 36).

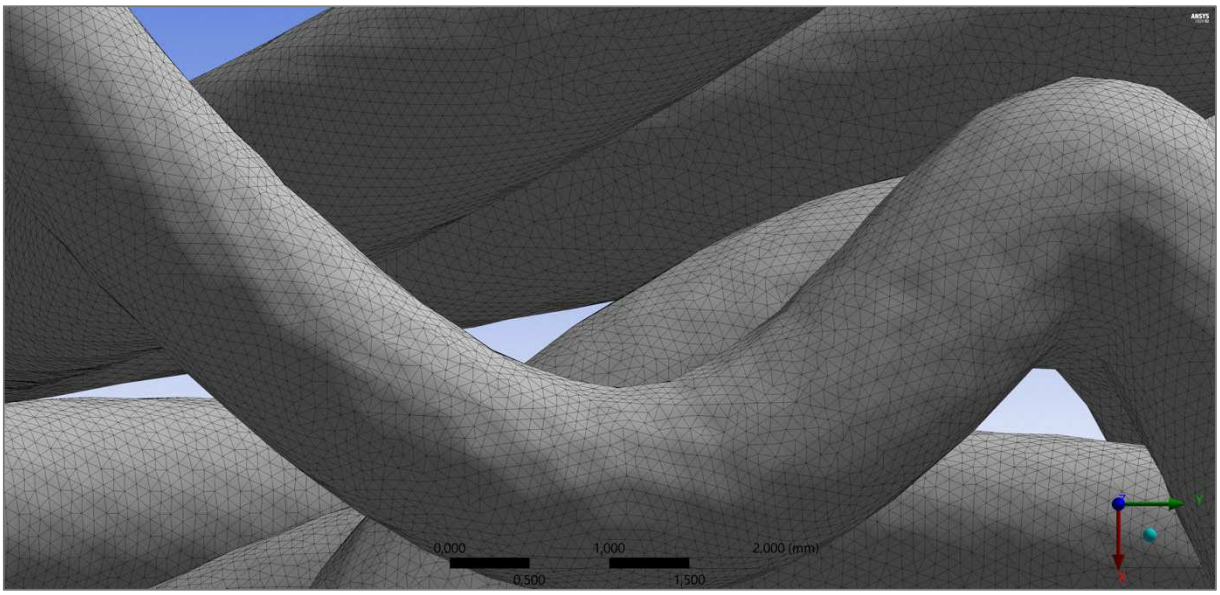

Figure 35. A zoom image of the triangle image transformation using the model data.
Each of these triangle areas are a zone for CFD analysis.

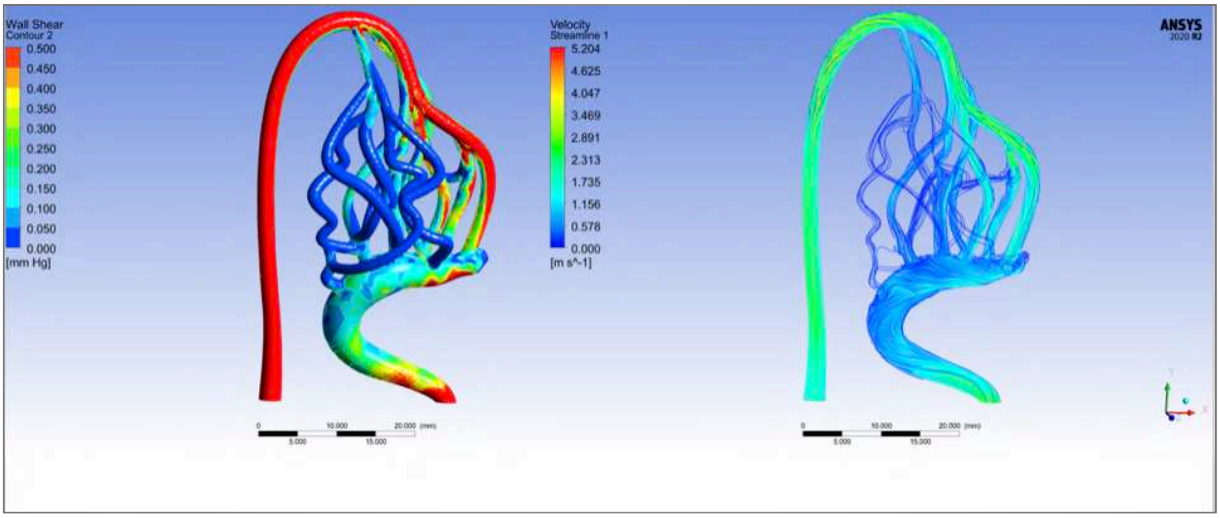

Figure 36. CFD images from Ansys software.

A) Wall Shear Stress (WSS) data from the model. High WSS can be seen at the entrance and the reduced in part of the nidus. B) Velocity streamlines of the model. Higher velocities were seen at the arterial side with a reduction in nidus and vein.

Wall Shear Stress and velocity lines were asymmetrically distributed within the model and the nidus. High WSS and velocities were seen as expected in the arterial inflow. Moreover, the nidus showed a heterogenic decrease in WSS and velocities.

The CFD study allowed us to confirm the feasibility of these analysis in the model. Simulation of the flow could be correlated with filling patterns during embolization and could help to modify or create specific models with different flow conditions.

IV.11. Pulsatile Flow Pump

We incorporated the use of a new pulsatile pump: FlowTek 125 (United Biologics, Santa Ana, CA, USA). This new pump allowed us to create a new setting for the tests and LEA embolization project. The FlowTek 125 is a pulsatile pump that generates cycles from 30 to 125 beats per minute (bpm), and flow rates between 0.7-5.1L/min (Figure 37).

Figure 37. FlowTek 125 Pump (United Biologics Santa Ana CA USA).
Image is showing the water container + pump.

IV.12. Flow determination in the model

Because the pulsatile pump has modifiable beats per minute (bpm) and Flow percentages (%) we were interested in determining the real flow in the BAVM model using different setting.

For this purpose, we used model MAV_8 connected to the Flow Tek 125 pump. We created a closed circuit with sodium chloride (NaCl 0.9%) running through the BAVM model. We measured the total NaCl volume that passed through the model, using a graded test tube during 10 seconds under different parameters of pulse and flow % and then extrapolated to 60 seconds (Table 6).

Pulse	25%	50%	75%	100%
70 bpm	60 ml/min	156 ml/min	192 ml/min	348 ml/min
90 bpm	60 ml/min	168 ml/min	324 ml/min	432 ml/min

Table 6. Flow determination (ml/min) under different pump conditions.
We tested two bpm conditions and four different flow percentages.

Chapter V. Endovascular Embolizations using a novel BAVM in vitro model.

V.1. Context and problem.

As we ended our first phase of design and creation of an in vitro BAVM model we faced the purpose of testing its utility in an experimental environment. We proposed to test the model with arterial side embolizations, the most conventional endovascular route. In this approach, nidus is filled and closed injecting LEA from the arteries. A bigger chance of closing and curing the BAVM is achieved by filling more nidus. If there is curative intention of the BAVM by endovascular route the vein must also be filled with LEA at the end of procedure, with already controlled proximal inflow.

This test phase was the first LEA embolization simulation on an in vitro BAVM model created with SLA 3D printing.

V.2. Presentation of article 2.

Endovascular Treatment Simulations using a novel in vitro brain arteriovenous malformation model based on three-dimensional printing millifluidic technology.

In this paper our objective was to describe and evaluate a novel in vitro BAVM model for endovascular treatments using 3D printing with millifluidic technology.

In the article we described the process of creating the model using SLA 3D printing. We then choose two different ways for validating the model: A structural and a functional validation process. For structural validation we compared measures from the CAD and the printed models. We measured channel diameters and compared if there was a correlation between the design and the printed version. Moreover, we performed a DMSO test in the model and CFD

evaluations. For functional analysis, we performed LEA embolizations in 10 models by different operators, with two different techniques. We also performed a Likert Scale questionnaire for qualitative evaluation on the user's experience of using this model.

V.3. PDF of article 2 on Interventional Neuroradiology.

Original Research Article

INR INTERVENTIONAL NEURORADIOLOGY

Interventional Neuroradiology
1–8

DOI: 10.1177/15910199231184605
journals.sagepub.com/home/ine
Sage

Endovascular treatment simulations using a novel *in vitro* brain arteriovenous malformation model based on three-dimensional printing millifluidic technology

Rivera Rodrigo[1,2], Cespedes Alvaro[3], Cruz Juan Pablo[1], Rivera Gladys Carlota[4], Valencia Alvaro[4], Rouchaud Aymeric[2,5] and Mounayer Charbel[2,5]

Abstract

Background: Brain arteriovenous malformations (bAVM) are complex vascular diseases. Several models have been used to simulate endovascular treatments; thus *in vitro* models have not been widely employed because it has been difficult to recreate realistic phantoms of this disease.

Objective: To describe the development and evaluate the preliminary experience of a novel bAVM *in vitro* model for endovascular embolization using millifluidic three-dimensional (3D) printing technology.

Methods: We designed a bAVM phantom starting from simple to more complex designs, composed of a nidus, feeding arteries and draining vein. We recreate the design by using millifluidic technology with stereolithography 3D printing. Structural and functional tests were performed using angiographic images and computer flow dynamics. Treatment simulations with ethylene vinyl alcohol were tested using two different microcatheter position techniques. A Likert-scale questionnaire was applied to perform a qualitative evaluation of the model.

Results: We developed a realistic model of a bAVM with hollow channels. The structural evaluation showed a high precision of the 3D printing process. Embolization tests with the liquid agent gave similar sensations and material behaviour as *in vivo* cases. There were no significant differences between microcatheter position techniques, thus we observed a trend for better nidus filling with a deeper in-nidus position technique.

Conclusions: We were able to create and test a novel bAVM *in vitro* model with stereolithography 3D printing in resin. It showed a high capacity for simulating endovascular embolization characteristics, with an excellent user experience. It could be potentially used for training and testing of bAVM embolizations.

Keywords

Arteriovenous malformation, surgical model, therapeutic embolization, simulation training, 3D printing

Received 29 March 2023; revised June 8, 2023; accepted 9 June 2023

Introduction

Brain arteriovenous malformations (bAVM) are complex vascular lesions consisting of abnormal connections between arteries and veins through a tangle of vessels called 'nidus'.[1,2] Various strategies for treating bAVMs exist, with endovascular treatment being a fundamental tool for managing this disease, as co-adjuvant or stand-alone therapy, especially with the development of new tools and access strategies.[3–8]

There is an increasing need for endovascular training and simulations in bAVMs, to test materials, techniques and prepare for more complex endovascular approaches.[9] Several experimental models have been used for endovascular simulation on bAVM over the years. Although the swine rete mirabile (RM) has become the preferred model due to its anatomical characteristics and size, using animals is expensive, requires some surgical interventions, specific animal facilities and care.[9–13] As an

[1]Neuroradiology Department, Instituto de Neurocirugia Dr Asenjo, Santiago, Chile
[2]CNRS XLIM UMLR 7252, Université de Limoges, Limoges, France
[3]Department of Design and Manufacturing, Universidad Santa Maria, Viña del Mar, Chile
[4]Department of Mechanical Engineering, Universidad de Chile, Santiago, Chile
[5]Neuroradiology Department, CHU, Limoges, France

Corresponding author:
Rodrigo Rivera, Neuroradiology Department, Instituto de Neurocirugia, Jose Manuel Infante 553, PO Box 7500691, Providencia, Santiago, Chile.
Email: rodrigorivera@me.com

alternative, *in vitro* models have been developed for endovascular simulation over the years with varying grades of complexity depending on different materials.[14–21] However, creating a realistic vessel and nidus anatomy with hollow channels has been challenging due to the intricate structure of this vascular disease.

Millifluidic is the science of precise Lab control and manipulation of fluids that are geometrically constrained to a small-scale container, typically with networks of channels lower than 1mm in diameter. This technology has been using three-dimensional (3D) printing as a cost-effective way to create chips or cartridges, replacing more expensive industrial manufacturing techniques such as lithography.[22,23] The goal of this study was to describe the development and evaluate the preliminary experience of a novel bAVM *in vitro* model for endovascular embolization using millifluidic 3D printing technology.

Material and methods

We started developing brain AVM-like phantoms using computer-aided design (CAD) software (Fusion 360, Autodesk California USA and Rhinoceros 3D, Robert McNeel & Associates, USA) by iteration from simple models up to more complex 3D structures with a nidus, feeding arteries and draining vein within a transparent volume cartridge that we termed 'AVM Chip'. We got to this simplified configuration based on the authors (CM, RR and AR) experience in bAVM geometry. The model dimension resembles a small bAVM with a nidus of about 3cm maximum diameter. For AVM tubing designs, we used NURBS (Non-Uniform Rational B-Spline) methodology, which is based on parametric polynomial curves with Bézier control points. This method allows the formation of an endoskeleton through a sweep of isogeometric hexahedral control meshes. These meshes are compatible with hemodynamic analysis and 3D rapid prototyping processes, which enable greater accuracy and efficiency in the design and simulation of the model.[24] The final CAD data was then exported using standard triangle language to 3D printing, based on millifluidic technology using a stereolithography (SLA) Form 3B 3D printer and transparent resin (Clear V4) (FormLabs, Somerville, MA, USA) (Figure 1).

The evaluation process for the AVM Chip involved two separate stages:

Structural evaluation: We used digital subtraction angiography (DSA) and 3D reconstructions on a Philips Azurion 7 Biplane (Philips Healthcare, Amsterdam, the Netherlands) to test channel permeability and diameters in three AVM Chip models. We measured and compared six channel diameter points between the CAD model and the 3D-printed versions. Moreover, we tested the printed model resistance to dimethyl sulfoxide (DMSO) (the solvent used for liquid embolic agents [LEAs] in bAVM endovascular treatment). For this purpose, we applied 1ml of DMSO to the resin surface of the model and to the Luer Lock connector. We search for any erosion, melting or disruption of the exposed material after 30 min of being in contact with the solvent. A computer fluid dynamic (CFD) study was done to evaluate the flow patterns and characteristics of the model. The CAD data was processed with ANSYS Fluent software (Canonsburg, PA, USA) transforming the image into multiple triangles (10 million elements) that were analyzed. We assumed a non-Newtonian fluid (Carreau's model), rigid walls and constant inflow velocity to calculate various variables, such as pressure, velocity and wall shear stress (WSS) in the model.

Functional evaluation: We created a closed flow circuit using the AVM Chip connected to a pulsatile pump with a flow rate of 168 ml/min and 90 cycles per minute as the Heart Rate (FlowTek 125, United Biologics, Santa Ana, CA, USA). The system was perfused with Sodium Chloride (NaCl) 0.9% saline at room temperature (21° C). Simulations of AVM transarterial embolizations were subsequently performed in ten models by seven different interventional neuroradiologists from the involved centers (with at least 7-year experience each), using a Siemens Icono Biplane (Siemens Healthineers, GmbH, Germany) and Philips Azurion Biplane (Philips Healthcare, Amsterdam Netherlands). For the afferent arterial microcatheterization, we employed a Sonic 1.2F 25mm microcatheter and Hybrid 0.008″ microguidewire (Balt, Montmorency, France). Two distinct microcatheter positions and techniques were tested: (1) Deep within the nidus and close to the draining vein and (2) Proximal to the nidus in an arterial position (Figure 2).

The microcatheter was flushed with DMSO, and Squid 18 ethylene vinyl alcohol LEA (Balt, Montmorency, France) was injected under fluoroscopy. Depending on the position of the microcatheter, a different technique was used; for position 1, the objective was to have an early filling of the vein and then retrogradely the nidus; for position 2, the objective was to fill with LEA from nidus to vein. Injections were paused for 30 s if: LEA reflux overpassing the proximal marker of the microcatheter, early vein filling on position 2 or vein filling reaching 'normal' vein when using position 1. We determined the total injected LEA volume, total time of the procedure, total filled nidus volume and its percentage, capacity of forming a proximal plug, capacity of secondary advances after plug and the ability of LEA to advance in different points after pauses. Nidus LEA volume filling was calculated using 3D rotational images with a 4 s protocol (Siemens Healthineers, GmbH, Germany). Images were segmented with 3D Slicer (Open Source), Autodesk Meshmixer (San Rafael, CA USA) and PreForm (FormLabs, Somerville MA, USA) software. The AVM Chip occlusion percentages (nidus + vein) in technique 1 and technique 2 were obtained by comparing them with the volume from CAD images.

A qualitative analysis was applied using a Likert scale[25] by seven interventional neuroradiologists that performed the embolization sessions, answering the following questionnaire: (1) Does the microcatheter behave like in real patients using the 3D model? (2) Does the LEA injection feel realistic in the 3D model? (3) Do you

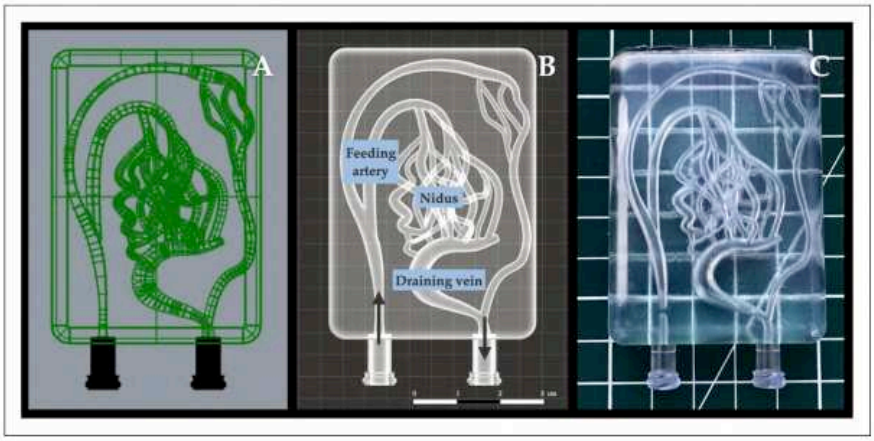

Figure 1. The design process of an AVM chip. (A) CAD tubing design using NURBS methodology; (B) Volume rendering of CAD in STL version (Meshmixer Autodesk, San Rafael CA USA), with AVM usual structures of feeding artery, nidus and draining vein; design is ready for 3D printing; (C) SLA 3D-printed version of the model using transparent resin (Clear V4 Resin, Formlabs Somerville MA, USA). CAD: computer-aided design; NURBS: non-uniform rational B-Spline; STL: standard triangle language; SLA: stereolithography.

think that the 3D model is useful to test LEA embolization? (4) Is the AVM Chip model suitable for embolization training and learning? Likert scale was composed of five grades: strongly agree, agree, neither agree nor disagree, disagree and strongly disagree. Statistical significance was determined ($p < 0.05$) by comparing groups with Mann–Whitney test using SPSS 29. This research was approved by the local Institutional Review Board.

Results

Structural validation

There was a high correlation value between channel measurements of the CAD design and the 3D rotational images of 3 different printed models (Table 1).

When measuring the model resistance to DMSO we found after 30 min on the exposed surfaces or connectors, which the resin material showed no changes, erosions or malfunctions. Luer Locks remained fully operational for performing injection tests.

The CFD evaluation showed that the velocity followed a laminar pattern with higher values in the inner part of the channels, decreasing towards the exterior. An important decrease in velocity was observed in the medial part of the nidus, which continued towards the venous pouch. The WSS was low in almost all parts of the nidus with slightly lower values in its medial portion, as velocity patterns (Figure 3).

Functional evaluation

Treatment simulations were completed in all 10 AVM Chip models. When comparing embolization technique 1 with embolization technique 2, we found no significant differences in total procedure time, total LEA volume, AVM Chip nidal occlusion in ml and occlusion percentage (Table 2) (Figure 4). Thus, there was a non-significant trend to a higher nidal volume occlusion when using technique 1 vs technique 2 (0.95 vs 0.84 ml and 73.6% vs 65.1%), and shorter total procedure time. Users were able to create a plug in all models, secondary advance after plug and different re-direction of LEA advance after pauses.

The results of the Likert-scale evaluation showed that users agreed and strongly agreed with all questions, indicating that catheterization and embolization on the AVM Chip felt like real cases and that the model could serve as an effective testing and educational tool (Table 3).

Discussion

Brain arteriovenous malformations are a complex vascular disease difficult to understand and to treat effectively. Over the last decade, there have been dramatic advancements in endovascular techniques and materials, leading to better clinical and angiographic outcomes.[5,7,8,26,27] However, due to the complexity of the disease, highly experienced endovascular operators are required and, therefore, there is an increasing need for training and simulations to ensure that a high standard of care is reached and maintained.[9]

Creating endovascular models for bAVMs has been challenging due to several reasons, including the absence of natural bAVMs in animals, intricate vascular anatomy, poor definition of the nidus with current imaging technology and difficulties in the segmentation process for creating artificial hollow channels. The RM in swine has been commonly used as its structure naturally resembles a nidus, and although it lacks an arteriovenous (AV) shunt, surgical preparations allow for the creation of an AV communication for endovascular embolizations.

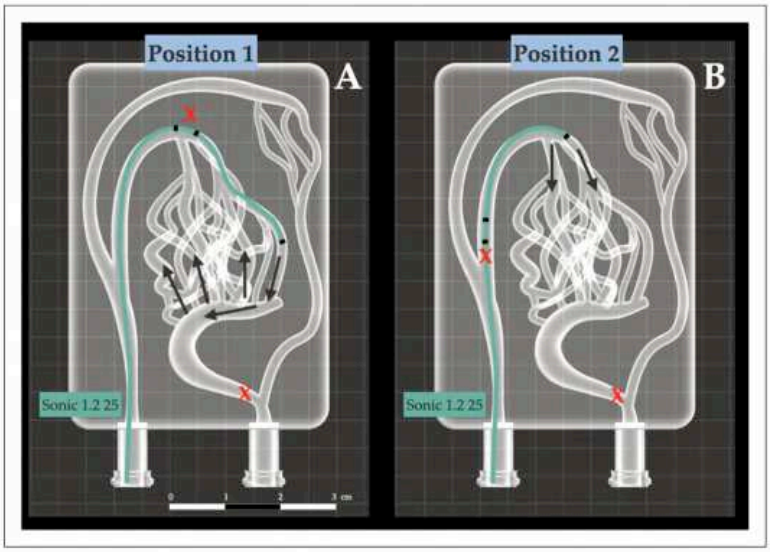

Figure 2. Microcatheter position for techniques 1 and 2. Two different techniques were used for testing the AVM Chip embolization depending on the microcatheter position. Position 1: Sonic 1.2F Sonic was situated near the draining vein and technique include embolization from vein to nidus. In position 2: Sonic 1.2F microcatheter was positioned more proximal and the LEA is advanced from nidus to vein. LEA: liquid embolic agent.

Table 1. Structural measure correlations between CAD and 3D-printed models.

Measure	CAD	Model 1	Model 2	Model 3	VARs	SD
1	1,6	1,57	1,54	1,57	0,0006	0,0244949
2	1,58	1,57	1,54	1,6	0,000625	0025
3	3,17	3,37	3,2	3,2	0,0083	0,0911043
4	1,75	1,73	1,74	1,73	0,00009167	0,0095743
5	2,17	2,33	2,27	2,2	0,00515833	0,0718215
6	1,49	1,33	1,27	1,53	0,01556667	0,1247664
	Correlation	Corr_CAD_M1	Corr_CAD_M2	Corr_CAD_M2		
		0,9960618	0,9922891	0,9990989		

Six different points were measured in three models and compared with the CAD design. Measures in mm. Correlations between the CAD model and each of the 3D-printed AVM Chip models. Corr_CAD_M1: Correlation between CAD and Model 1. Corr_CAD_M2: Correlation between CAD and Model 2. Corr_CAD_M3: Correlation between CAD and Model 3. CAD: computer-aided design.

The main drawback of this model is its cost, as dedicated animal care and facilities are needed, and surgical preparations are technically challenging.[10–13,28–30] *In vitro*, models have been successfully used in other vascular anomalies like brain aneurysms,[31–35] and these models can currently be created using silicon or 3D printing with individual patient data for training and rehearsal before real-case treatment. This fundamental and key step in planning a treatment is still not available for bAVMs, one of the reasons being that small hollows channels and anatomy reproducibility are much more difficult to achieve with bAVMs.[21] *In vitro* models for bAVM simulation are not new and have been used since the early 80s including simple tubing, venous grafts, glass/rubber tubes with beads, springs or balls, sac with mesh pads, open pore cellulose sponges inside an elastomer structure, silicon honeycomb-like structures, and recently, a 3D-printed silicon model.[14–18,21,36,37]

Our *in vitro* model for AVM embolization differs from previously published models as it uses a novel 3D printing technique called SLA, which up to our knowledge has not been reported for this purpose. SLA uses liquid resins that are solidified (or cured) layer by layer with the pass of a laser. The advantage of this technique is that it allows the production of watertight products with minimum or imperceptible stair-stepping effect, which can occur with deposit 3D printing techniques, and can also produce high-resolution structures with intricate details.

Microfluidics has been using SLA for several years and has become a revolutionary technique for creating chips or

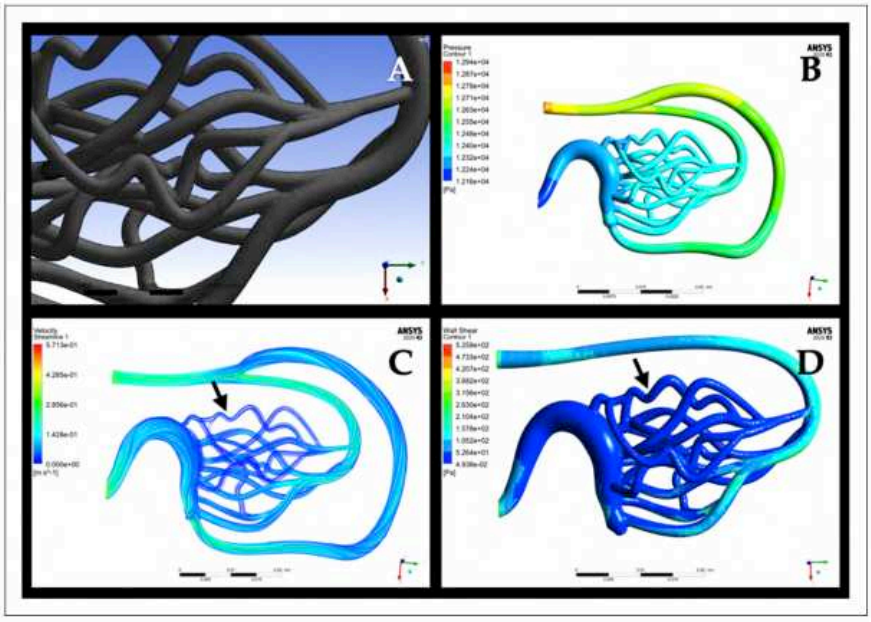

Figure 3. CFD study in the AVM chip. (A) Multiple triangle elements define the geometry for CFD analysis. (B) Pressure pattern in the model. Pressure is high at the entrance, and it decreases through the model up to the vein. (C and D) Velocity flow lines and WSS. The medial part of the nidus (black arrows) showed slightly slower velocity and WSS than the rest of the model. CFD: computer fluid dynamics; WSS: wall shear stress.

Table 2. Results between technique 1 vs technique 2.

	Technique 1	Technique 2	Significance
Total procedure time (h:min:seg)	0:14:37	0:19:15	NS
Total LEA Volume (ml)	1.6	1.5	NS
AVM nidal occlusion (ml)	0.95	0.84	NS
AVM nidal occlusion (%)	73.6	65.1	NS

Results of embolization technique 1 vs technique 2. Statistical analysis was done using Mann–Whitney test (significance $p < 0.05$). Numerical results are expressed in median. NS: non-significant.

cartridges for lab use, with a significant reduction in cost compared to previous, more expensive manufacturing processes.[22,23] This method involves the printing of small hollow channels for fluid lab testing. We used this technology for our model to manufacture AVM-like anatomies with millimetric hollow channels. After several iterations, we were able to design a suitable model combining the use of CAD, NURBS and 3D printing with SLA, which we called AVM Chip. We found an excellent degree of accuracy when comparing the CAD vs the 3D-printed version in the structural validation phase, and the AVM Chip proved to be resistant to DMSO, which is a very corrosive product for plastic materials.

Computer fluid dynamic simulations showed interesting results reflecting some of the findings during AVM Chip embolization. Slow velocity and low WSS were seen in simulations at the medial zone of the model nidus (Figure 3), the same zone that was constantly less filled with LEA during the different embolization tests (Figure 4). A possible explanation could be that LEA tends to be directed more to high velocity as found in CFD simulations due to anatomic characteristics of the model, with less penetration to slower nidal portions. Although CFD was calculated without a microcatheter inside the model, it could explain that anatomically speaking, slow areas could have had less tendency to be filled by the LEA.

In this study, we also tested two different microcatheter positions and embolization techniques. We found no significant differences between the two techniques ($p > 0.05$) in all studied parameters, although there was a trend favouring technique 1, with a slightly better AVM Chip embolization percentage, less material and less embolization procedure time (Table 2). Maybe larger number of cases may be needed to show a statistical difference. Nonetheless, users found interesting to be able to test and practice the LEA behaviour in different situations, and they considered that microcatheter position was a very remarkable teaching point during sessions, as in both techniques, the LEA behaved similarly as *in vivo* in the formation of a plug, advance after plug formation and redirection of the material after various pauses.

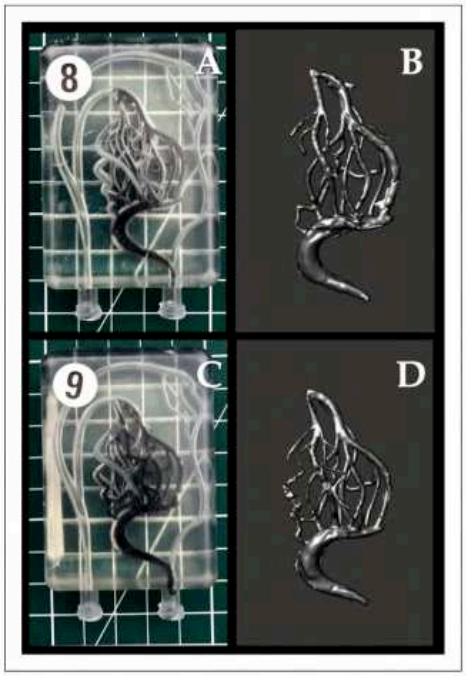

Figure 4. AVM CHIP embolization with EVOH. AVM Chip Models 8 and 9 were embolized with EVOH using different techniques. Model 8 (A) with technique 2 and Model 9 (C) with technique 1. On the side (B and D), a volume rendering segmentation of the EVOH material of the corresponding model, was obtained with angiographic 3D rotational images and generated with Meshmixer (Autodesk, San Rafael, CA, USA). EVOH: ethylene vinyl alcohol.

Table 3. Results of Likert-scale questionnaire.

	Strongly agree	Agree	Nor agree nor disagree	Disagree	Strongly disagree
Question 1	25%	62.5%	0	12.5%	0
Question 2	62.5%	25%	12.5%	0	0
Question 3	75%	25%	0	0	0
Question 4	87.5%	12.5%	0	0	0

Results of Likert-scale questionnaire. Question 1) Does the microcatheter behave like in real patients using the 3D model? Question 2) Does the LEA injection feel realistic in the 3D model? Question 3) Do you think that the 3D model is useful to test LEA embolization? Question 4) Is the AVM Chip model suitable for embolization training and learning? LEA: liquid embolic agent.

The user appreciation of embolization tests in the models was in general very positive. More than 87.5% of users agreed or highly agreed about the utility of the model in LEA embolization. The only parameter in which a less favourable assessment was seen was the microcatheter navigation feeling within the model channels (12.5%). The microcatheter presented high friction in some of the tests, which could be related to the inner surface rugosity of the resin material of the model. We aim to keep working on achieving less friction in future models with different printing techniques for less rugosity and the use of liquids that ameliorate the friction effect. There was a 100% agreement between operators, that our model is suitable for testing and teaching, being one of the main goals for which it was designed.

One of the main difficulties of recreating and *in vitro*, bAVM is the complex structure. DSA with 3D rotational capacities show details of the disease, but the segmentation process is complex and often not accurate due to the millimetric or sub-millimetric vessel diameter that is involved in the nidus. Artificial intelligence (AI) has been explored as a tool to perform automatized bAVM segmentation with encouraging results.[38]

Although our model is not built from data obtained from a real bAVM, we recreated a simplified model that could resemble an AVM anatomy. Using different techniques such as NURBS, we were able to produce a model that allows LEA embolization with a high resemblance to *in vivo* procedures. We are focusing on achieving segmentation and 3D printing of real bAVMs with patient's specific data with sub-millimetric channels for the near future. This process would allow endovascular testing and rehearsal of treatments before patient embolization.

Our work has several limitations. As previously mentioned, we used a simulated simplified AVM-like anatomy and not real patient data. The model walls are rigid, different from elastic, soft and mobile vessels seen in real bAVM and could not react to materials as vasospasm seen in some AVM embolizations. Our model does not have sub-millimetric channels and this is because the process of creating hollow channel and cleaning the inner lumen of uncured resin is complex. Near future work is on the course on this direction for creating sub-millimetric channels of real AVM-specific cases. Moreover, the model channels were mainly untortuous allowing easier microcatheter navigation, which usually do not happen in real-life cases. On the other hand, our model could not simulate or induce a nidus rupture, being one of the main risks during bAVM endovascular treatment. We did not determine the internal model porosity or resistance to microcatheter friction, and we used ambient temperature NaCl for testing at 21°C, which could affect microcatheter navigation or material behaviour. Lastly, the overall number of tested models was low.

We create a functional 3D printing *in vitro* model for LEA embolization testing and simulation. We believe that 3D-printed based models will represent the next generation in bAVM simulation, ushering in a new level of sophistication and innovation to training, development and teaching in the field of AVM management.

In conclusion, we were able to build and test a novel bAVM *in vitro* model, built by using SLA 3D printing

in resin. It showed a high capacity for simulating LEA embolization characteristics and user experience approval. The model could be potentially used for training and testing bAVM embolizations.

Acknowledgements

The authors would like to thank Balt France (Montmorency France) for donating all the material that were used during the embolizations tests of the AVM Chip Models (Squid 18, Sonic 1.2F25 microcatheters and Hybrid 0,007″ micro guidewires). The authors would like to thank physicians that were involved in embolization tests and answering the Likert-scale questionnaire: Professor Laurent Spelle MD. Neuri, Bicetre Hospital, Paris France. Suzana Saleme MD, Neuroradiology Department, CHU Limoges, France. Henrique Alfonso MD, Neuroradiology Department, CHU Limoges, France. Daniel Echeverria MD, Neuroradiology Department, Instituto de Neurocirugia Dr Asenjo, Santiago, Chile.

Authors contributions

RR contributed to the design, conception, embolization tests, analysis of data and management of the research. CM and AR contributed to the design of the study, analysis of data, configuration of the model and the embolization tests. AC performed all the designs and CAD of the models and analysis of data. AV and CR contributed to performing the CFD analysis of the models. JPC contributed to the design, analysis of data, English revision and embolization tests. All authors contributed to the analysis of the data and the drafting and/or editing of the manuscript. All authors approved the final manuscript.

Ethical approval

This research was approved by the local Institutional Review Board.

Declaration of conflicting interests

The author(s) declared no potential conflicts of interest with respect to the research, authorship, and/or publication of this article.

Funding

The author(s) received no financial support for the research, authorship, and/or publication of this article.

ORCID iDs

Rivera Rodrigo https://orcid.org/0000-0001-8991-0972
Cruz Juan Pablo https://orcid.org/0000-0002-7524-7273
Rouchaud Aymeric https://orcid.org/0000-0003-0902-3375

References

1. Solomon RA and Connolly ES. Arteriovenous malformations of the brain. *N Engl J Med* 2017; 376: 1859–1866.
2. Friedlander RM. Arteriovenous malformations of the brain. *N Engl J Med* 2007; 356: 2704–2712.
3. Beijnum Jv, Worp Hvd, Buis DR, et al. Treatment of brain arteriovenous malformations: a systematic review and meta-analysis. *JAMA* 2011; 306: 2011–2019.
4. Mohr J, Parides MK, Stapf C, et al. Medical management with or without interventional therapy for unruptured brain arteriovenous malformations (ARUBA): a multicentre, non-blinded, randomised trial. *Lancet* 2014; 15: 614–621.
5. Mendes GAC, Kalani MYS, Iosif C, et al. Transvenous curative embolization of cerebral arteriovenous malformations: a prospective cohort study. *Clin Neurosurg* 2018; 83: 957–964.
6. Saatci I, Geyik S, Yavuz K, et al. Endovascular treatment of brain arteriovenous malformations with prolonged intranidal onyx injection technique: long-term results in 350 consecutive patients with completed endovascular treatment course - clinical article. *J Neurosurg* 2011; 115: 78–88.
7. Koyanagi M, Mosimann PJ, Nordmeyer H, et al. The transvenous retrograde pressure cooker technique for the curative embolization of high-grade brain arteriovenous malformations. *J Neurointerv Surg* 2021; 13: 637–641.
8. Chapot R, Stracke P, Velasco A, et al. The pressure cooker technique for the treatment of brain AVMs. *J Neuroradiol* 2014; 41: 87–91.
9. Vollherbst DF, Hantz M, Schmitt N, et al. Experimental investigation of transvenous embolization of arteriovenous malformations using different in vivo models. *J Neurointerv Surg* 2022: 1–6.
10. Massoud TF, Ji C, Viñuela F, et al. Laboratory simulations and training in endovascular embolotherapy with a swine arteriovenous malformation model. *Am J Neuroradiol* 1996; 17: 271–279.
11. Massoud TF, Ji C, Vinuela F, et al. An experimental arteriovenous malformation model in swine: anatomic basis and construction technique. *Am J Neuroradiol* 1994; 15: 1537–1545.
12. Massoud TF. Transvenous retrograde nidus sclerotherapy under controlled hypotension (TRENSH): hemodynamic analysis and concept validation in a pig arteriovenous malformation model. *Neurosurgery* 2013; 73: 332–342.
13. Chaloupka JC, Vinuela F, Robert J, et al. An in vivo arteriovenous malformation model in swine: preliminary feasibility and natural history study. *Am J Neuroradiol* 1994; 15: 945–950.
14. Kerber CW and Flaherty LW. A teaching and research simulator for therapeutic embolization. *Am J Neuroradiol* 1980; 1: 167–169.
15. Kerber CW, Bank WO and Cromwell LD. Calibrated leak balloon microcatheter: a device for arterial exploration and occlusive therapy. *Am J Roentgenol* 1979; 132: 207–212.
16. Bartynski WS, O'Reilly GV and Forrest MD. High-flow-rate arteriovenous malformation model for simulated therapeutic embolization. *Radiology* 1988; 167: 419–421.
17. Inagawa S, Isoda H, Kougo H, et al. In-vitro simulation of NBCA embolization for arteriovenous malformation. *Interv Neuroradiol* 2003; 9: 351–358.
18. Park S, Yoon H, Suh DC, et al. An arteriovenous malformation model for testing liquid embolic materials. *Am J Neuroradiol* 1997; 18: 1892–1896.
19. Kerber CW, Hecht ST and Knox K. Arteriovenous malformation model for training and research. *Am J Neuroradiol* 1997; 18: 1229–1232.
20. Vollherbst DF, Otto R, von Deimling A, et al. Evaluation of a novel liquid embolic agent (precipitating hydrophobic injectable liquid (PHIL)) in an animal endovascular embolization model. *J Neurointerv Surg* 2018; 10: 268–273.
21. Kaneko N, Ullman H, Ali F, et al. In vitro modeling of human brain arteriovenous malformation for endovascular

simulation and flow analysis. *World Neurosurg* 2020; 141: e873–e879.
22. Lee JM, Zhang M and Yeong WY. Characterization and evaluation of 3D printed microfluidic chip for cell processing. *Microfluid Nanofluidics* 2016; 20: 1–15.
23. Weisgrab G, Ovsianikov A and Costa PF. Functional 3D Printing for Microfluidic Chips. *Adv Mater Technol* 2019; 4: 1900275.
24. Zhang Y, Bazilevs Y, Goswami S, et al. Patient-specific vascular NURBS modeling for isogeometric analysis of blood flow. *Comput Methods Appl Mech Eng* 2007; 196: 2943–2959.
25. Joshi A, Kale S, Chandel S, et al. Likert Scale: explored and explained. *Br J Appl Sci Technol* 2015; 7: 396–403.
26. Saatci I, Geyik S, Yavuz K, et al. Endovascular treatment of brain arteriovenous malformations with prolonged intranidal Onyx injection technique: long-term results in 350 consecutive patients with completed endovascular treatment course - clinical article. *J Neurosurg* 2011; 115: 78–88.
27. Mounayer C, Hammami N, Piotin M, et al. Nidal embolization of brain arteriovenous malformations using onyx in 94 patients. *Am J Neuroradiol* 2007; 28: 518–523.
28. De Salles AAF, Solberg TD, Mischel P, et al. Arteriovenous malformation animal model for radiosurgery: the rete mirabile. *Am J Neuroradiol* 1996; 17: 1451–1458.
29. Murayama Y, Massoud TF and Viñuela F. Transvenous hemodynamic assessment of experimental arteriovenous malformations. Doppler guidewire monitoring of embolotherapy in a swine model. *Stroke* 1996; 27: 1365–1372.
30. Massoud TF and Hademenos GJ. Transvenous retrograde nidus sclerotherapy under controlled hypotension (TRENSH): a newly proposed treatment for brain arteriovenous malformations - concepts and rationale. *Neurosurgery* 1999; 45: 351–365.
31. Paramasivam S, Baltsavias G, Psatha E, et al. Silicone models as basic training and research aid in endovascular neurointervention - A single-center experience and review of the literature. *Neurosurg Rev* 2014; 37: 331–337.
32. Nawka MT, Spallek J, Kuhl J, et al. Evaluation of a modular in vitro neurovascular procedure simulation for intracranial aneurysm embolization. *J Neurointerv Surg* 2020; 12: 214–219.
33. Marciuc EA, Dobrovat BI, Popescu RM, et al. 3D printed models—a useful tool in endovascular treatment of intracranial aneurysms. *Brain Sci* 2021; 11: 598.
34. Pravdivtseva MS, Peschke E, Lindner T, et al. 3D-printed, patient-specific intracranial aneurysm models: from clinical data to flow experiments with endovascular devices. *Med Phys* 2021; 48: 1469–1484.
35. Yamaki VN, Cancelliere NM, Nicholson P, et al. Biomodex patient-specific brain aneurysm models: the value of simulation for first in-human experiences using new devices and robotics. *J Neurointerv Surg* 2021; 13: 272–277.
36. Ishikawa M, Horikawa M, Yamagami T, et al. Embolization of arteriovenous malformations: effect of flow control and composition of n-butyl-2 cyanoacrylate and iodized oil mixtures with and without ethanol in an in vitro model. *Radiology* 2016; 279: 910–916.
37. Vollherbst DF, Sommer CM, Ulfert C, et al. Liquid embolic agents for endovascular embolization: evaluation of an established (Onyx) and a novel (PHIL) embolic agent in an in vitro AVM model. *Am J Neuroradiol* 2017; 38: 1377–1382.
38. Chenoune Y, Tankyevych O, Li F, et al. Three-dimensional segmentation and symbolic representation of cerebral vessels on 3DRA images of arteriovenous malformations. *Comput Biol Med* 2019; 115: 103489.

V.4. Main Results and comments of article 2.

In this paper we demonstrated the feasibility of a novel technique for creating a new in vitro BAVM model. We were able to perform the test in 3 different environments and operators: Dupuytren CHU at Limoges France, Bicetre Hospital Paris France, and Instituto de Neurocirugia Dr. Asenjo, Santiago Chile (Figure 38).

Figure 38. Functional testing were performed in three different environments.

A) and B) Dupuytren CHU at Limoges France. C) Angio Suite at Bicetre Hospital, Paris France. D) Close up of the model at the angio Suite of Instituto de Neurocirugia Dr. Asenjo in Santiago Chile.

The model was suitable for endovascular embolizations, and structural validations were positive with an adequate correlation between the CAD and the printed models. In functional validations we tested two different techniques, that differed on the microcatheter position and the way we targeted the nidus (Figure 39).

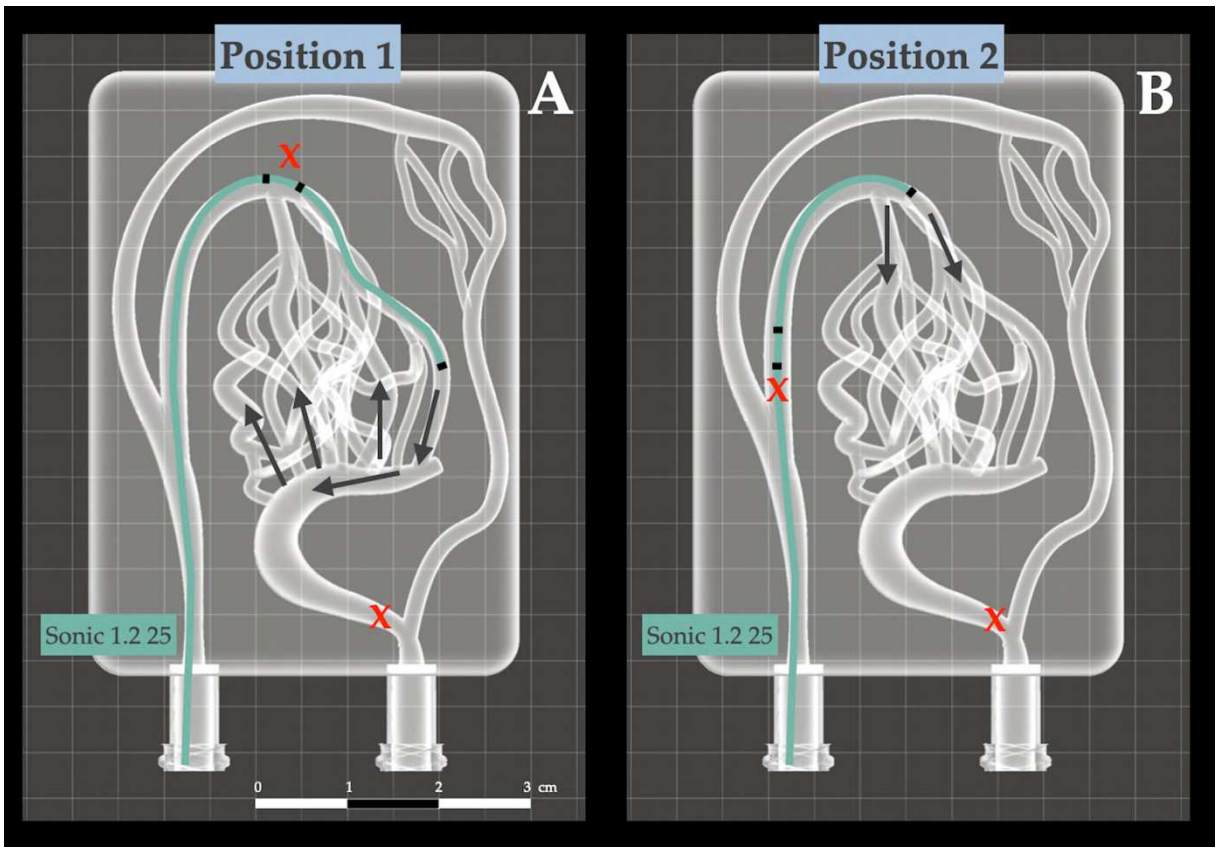

Figure 39. Two different techniques used for AVM embolization.

A) Deep microcatheter position at the nidus. In this position, the plan was to start filling the vein and then retrogradely fill the nidus. B) A proximal to nidus position of the microcatheter. The objective was to start filling the nidus and finally occlude the vein. Red crosses show the limit of reflux into arterial side, or the limit of filling at the venous drainage.

Both groups behaved similarly with no significant differences in variables as total procedure time, total LEA volume and AVM nidal occlusion percentage. Thus, what was more interesting was that all users stated, in the qualitative questionnaire, that LEA embolization behavior was

like real cases. The plug and push technique were always possible and definitely the model resembles a LEA embolization that could serve as model for teaching and learning, as stated in the Likert Scale questionnaire results.

One of the limitations of this model was the artificial configuration of the AVM. We used a proposed design based on authors experiences, with arteries, nidus and vein, thus, this gave us the drive for our next model design, using real patient's data.

The article in perspective:

We created a functional in vitro BAVM model for LEA embolization tests. Moreover, we used an unreported 3D printing technique for this purpose using SLA millifluidic techniques.

The model allowed satisfactory embolizations, and operators confirmed that the BAVM model reproduced with realism an embolization process, and this could be used for teaching, testing and learning.

This model introduces 3D printing as a viable resource for creating in vitro AVM models. It described a specific technique that could be used for future developments in the field, changing the way doctors could be trained and learn.

Chapter VI. In vitro BAVM model based on patient's data.

VI.1. Development of an in vitro model using real patient data.

Next step of our development was to create an in vitro SLA model using real patient's data. For this purpose, we searched for a BAVM that could be captured and transformed to a resin model.

VI.1.1. Acquisition of patient data

A patient with a BAVM was diagnosed using a Siemens Icono Biplane. Images were obtained using 2D DSA and 3D images. The BAVM was located at the left temporo occipital lobe, with a main feeder from the temporo occipital artery of left middle cerebral artery (MCA), a nidus of 1.8cm and a single superficial draining vein to the transverse sinus (Figure 40). Type 1 of Spetzler Martin classification.

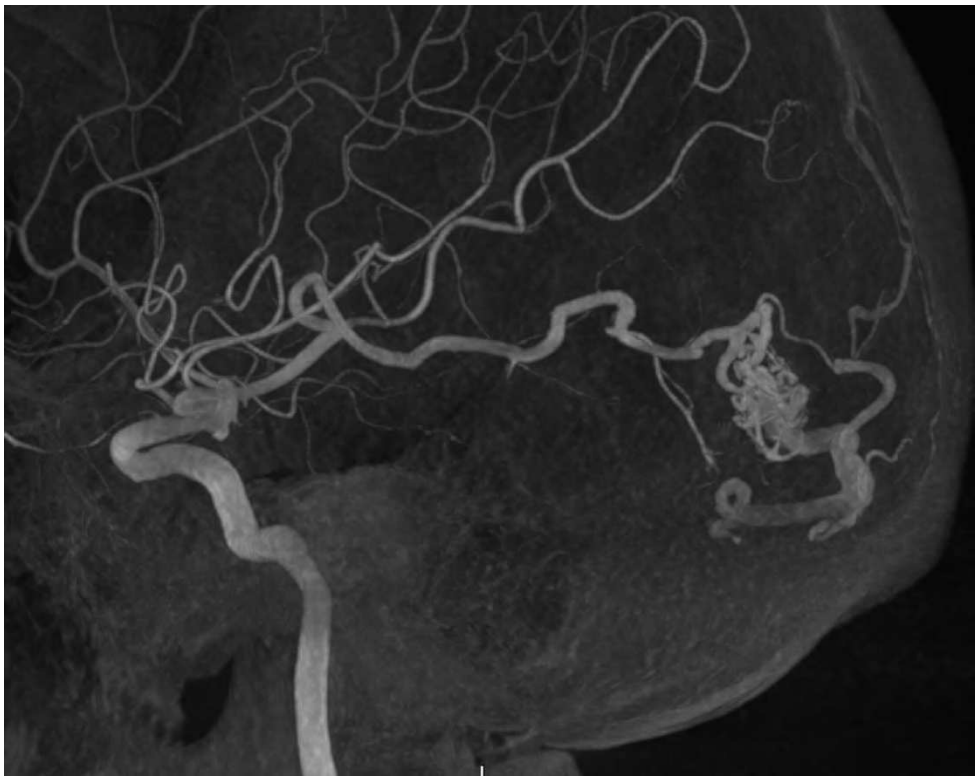

Figure 40. Left temporo occipital BAVM used for segmentation.
3D MIP reconstruction image. The BAVM is filled by a temporal branch of the middle cerebral artery. A small nidus of 1.8cm and a single draining vein.

VI.1.2. Segmentation process.

One of the most challenging steps in reproducing a BAVM is the definition of small vessel at the nidus and the segmentation process. We processed the DICOM file with Slicer (Slicer Platform open source https://www.slicer.org). This software allowed to segmentate the 3D rotational images, define the BAVM, and transform it into SLT language (Figure 41).

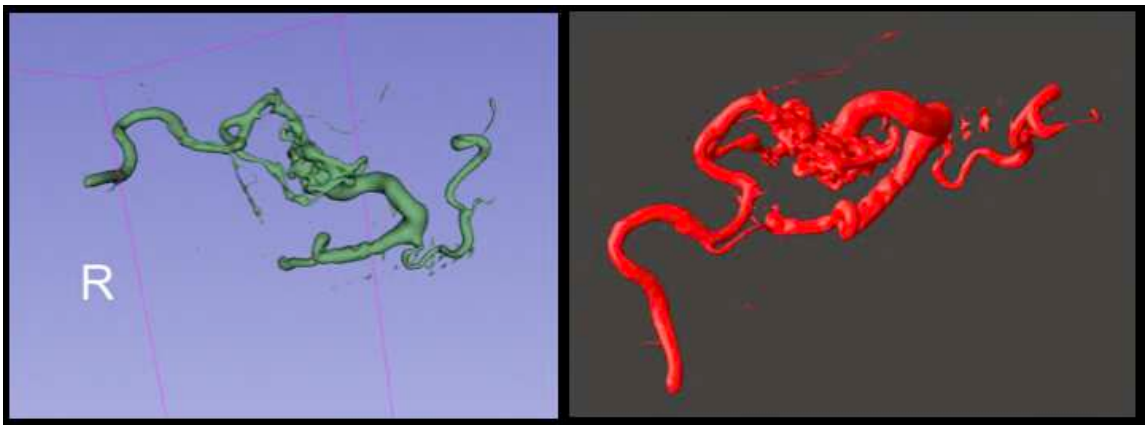

Figure 41. Segmentation process of the BAVM.
A) 3D image after segmentation using Slicer 3D software. B) 3D reconstruction and rendering with Meshmixer® software.

The SLT file was then processed on Fusion 360 (Fusion 360, Autodesk California USA) and Rhinoceros (Robert McNeel & Associates, USA) to create a new chip that we named model MAV_10 (Figure 42). We modified some angulations of the input and output of the BAVM to fit it within a container and create external connectors (Luer Locks). The model was printed using the Formlabs Form 3B and Clear V4 resin and tested in the Azurion 7 angiograph with contrast media. DSA and 3D rotational images were acquired.

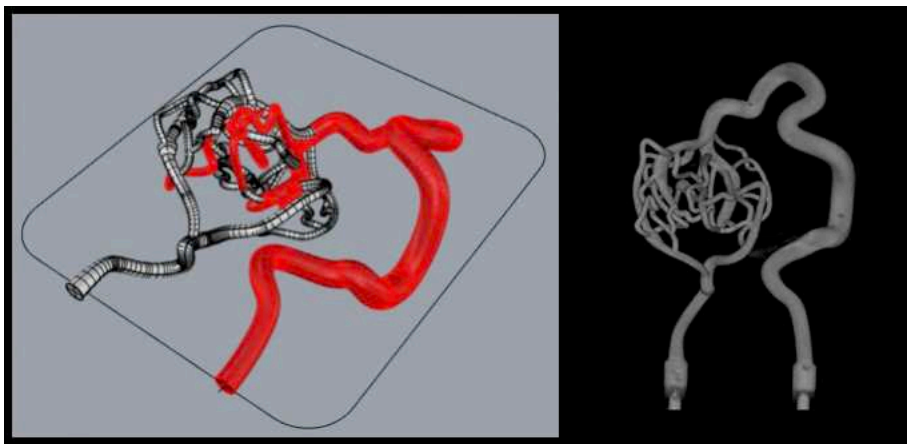

Figure 42. Model MAV_10.
A) CAD image of the design. B) An X-ray 3DRA reconstruction after using contrast media.

VI.1.3. Flow and Pressure measurements in model MAV_10

We used a closed circuit using the FlowTek 125 pump and sodium chloride (NaCl 0.9%) at ambient temperature. We tested two conditions of pulse (70 and 90 beats per minute) and four flow % conditions at the pump (25-50-75-100%). We tested for 10 seconds the volume (in ml) that passed through the model using a labeled test tube. We extrapolated this data to 60 seconds to obtain the flow rate in ml/min (Table 7). A pressure sensor in the arterial input was configured using a 3-way connector (Figure 43) for testing different MAP values during different flow conditions (Table 8).

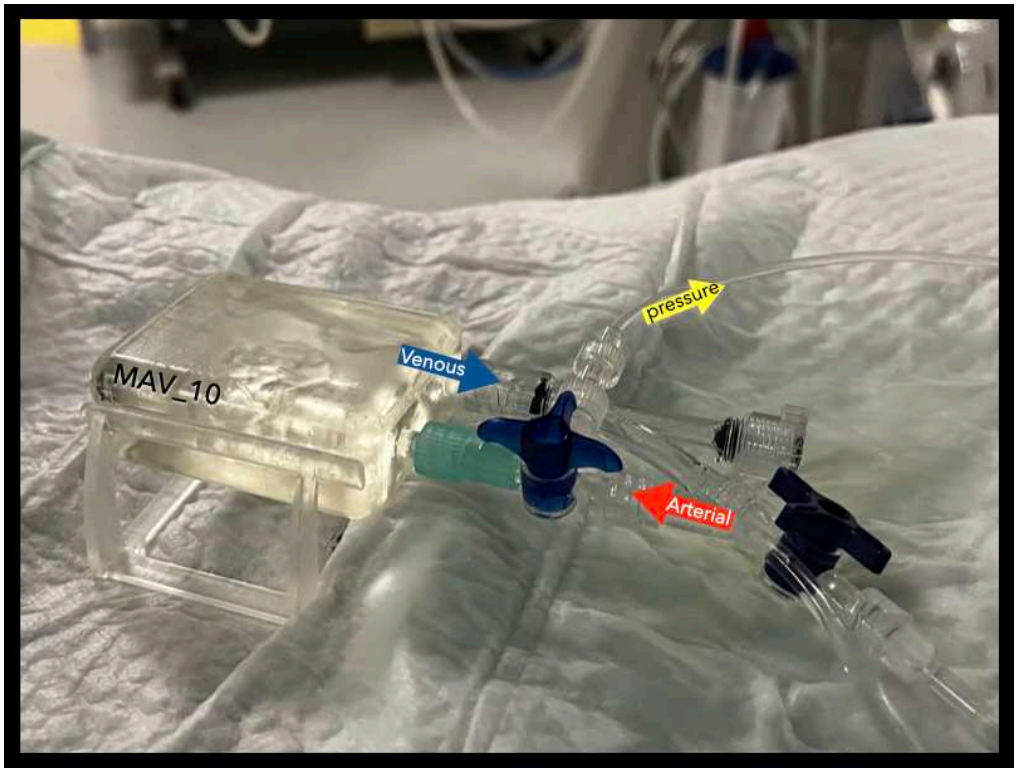

Figure 43. Setting of Model MAV_10 in the angio suite table.
We measured flow and pressure at different pump conditions.

Pulse (bpm)	25%	50%	75%	100%
70	30 ml/min	60 ml/min	120 ml/min	168 ml/min
90	36 ml/min	144 ml/min	222 ml/min	300 ml/min

Table 7. Calculated flow at different pump conditions.
We tested two pulses 70 and 90 bpm and we changed the percentage of the given flow measuring the output with a labeled test tube.

	40%	45%	50%	55%	60%	65%
MAP mmHg	45	61	82	100	121	141

Table 8. Calculated MAP at different pump conditions.

We changed the percentage of given flow by the pump. With a constant pulse MAP increased as flow increases.

MAP = Mean Arterial Pressure. All measures were done with a pulse of 90 bpm.

Chapter VII. In Vitro BAVM model for Transvenous Embolization

VII.1. Context and Problem

Transvenous Embolization has become a novel endovascular treatment for selected BAVM, changing the paradigm that the venous occlusion or closure should be avoided unless there is already total exclusion of the nidus or control of arterial flow. This novel endovascular technique implies a demanding knowledge of the venous system, microcatheter navigation and endovascular skills. Training and testing for this route have become an important need for preparing medical doctors for performing safer and successful procedures.

As we started this thesis and after searching for the problem, we were able to define that there were no models for TVE, and because of their characteristics, in vitro models using 3D printing could be an interesting way of adding new knowledge to the field. Recently, and during the developing of this thesis, the first TVE model was described and published by Vollherbst et al. This was an in vivo model based on the swine rete mirabile. Authors were able to modify the RM in two ways: a classical one by surgically creating an arteriovenous shunt from carotid to jugular vein; or an easier one by connecting a catheter at the venous side to the exterior to generate the AV gradient[51]. Continuing our initial objectives, we started designing different models up to a more realistic version of an in vitro BAVM that could be used for TVE simulations. We believe that in vitro models could have several advantages as lower price, easy setup, transportability, customization, reproducibility, and standardization. Moreover, they have advantages over animal models that need special facilities, expensive cares, could not be moved easily to other facilities, nor be used in human dedicated angiosuites, and require surgical modifications for their functionality as an AV shunt.

VII.2. Presentation of Article 3.

In this article we focused on answering the main objective and question of our research. We described the process of model design, and we tested the model performing several TVE with LEA. This is the first known description of a 3D printed model using SLA for TVE.

VII.3. Article 3. Submitted to Journal of NeuroInterventional Surgery (JNIS).

Brain Arteriovenous Malformation In Vitro Model for Transvenous Embolization Using Three-Dimensional Printing and Real Patient Data.

RIVERA, Rodrigo[1,2]; CESPEDES, Alvaro[3]; CRUZ ,Juan Pablo[1]; ROUCHAUD, Aymeric[2,4]; MOUNAYER Charbel[2,4].

[1] Neuroradiology Department, Instituto de Neurocirugia Dr. Asenjo, Santiago, Chile.
[2] CNRS XLIM UMLR 7252, Université de Limoges, France
[3] Department of Design and Manufacturing, Universidad Santa Maria, Viña del Mar, Chile
[4] Neuroradiology Department, CHU Limoges, France

Total number of tables: 1
Total number of figures: 3
Word count:

Keywords: Arteriovenous Malformation, Surgical model, Therapeutic Embolization, Simulation Training, 3D printing, Transvenous Embolization.

Abstract.

Background. Transvenous embolization (TVE) has emerged as a novel technique for treating some selected brain arteriovenous malformations (BAVM) with high reported occlusion rates. However, it requires anatomical and technical skills to be successful and to ensure patient safety. Training and testing are therefore essential for preparing clinicians to perform these procedures. Our aim was to develop and tested a novel patient specific BAVM in vitro model for TVE using three-dimensional (3D) printing technology.

Methods. We developed a BAVM in vitro model based on real patient data using stereolithography resin 3D printing. We created a closed pulsed circuit with flow passing from arterial to vein side and tested the effect of mean arterial pressure on retrograde nidal filling with contrast injections. Transvenous embolization simulations were performed using an ethylene vinyl alcohol liquid embolic agent injected through microcatheters, with or without coils at the vein.

Results. Retrograde contrast advance to nidus was directly related to lower mean arterial pressure. TVE tests with liquid embolic agent reproduced the usual embolization plug and push technique. We found no differences between the two TVE group conditions, and venous coils didn't increase nidus penetration or reduce injection time in the model.

Conclusions. We were able to develop and test a functional in vitro BAVM model for TVE using 3D printing, emulating its conditions and characteristics. Better contrast penetration was achieved with less mean arterial pressure and no embolization advantage was found by adding coils to the vein in this model.

Keywords: Arteriovenous Malformation, Surgical model, Therapeutic Embolization, Simulation Training, 3D printing, Transvenous Embolization.

What is already known on this topic:

Training and testing for transvenous embolization treatment in brain arteriovenous malformations (BAVMs) have become increasingly critical. Models have proven invaluable in some cerebrovascular diseases; however, there is currently no described in vitro BAVM model specifically designed for training in this endovascular technique.

What this study adds:

We developed and tested a new functional TVE in vitro BAVM model, based on patient data, using stereolithography 3D printing. This is the first described in vitro model for this purpose and could be used for training, research and rehearsal of endovascular treatments.

How this study might affect research, practice or policy:

This in vitro model could become a practical, reproducible and lower cost system to train doctors in this complex TVE technique. It could be transported and be available in any angio suite of the world. Moreover, it could be used in the development and testing of new endovascular tools.

Introduction.

Endovascular embolization is a well-accepted treatment strategy for Brain Arteriovenous Malformations (BAVM), either as a standalone therapy or as part of multimodal management together with microsurgery or radiosurgery[1].

The classical and more used endovascular treatment has been the transarterial approach using microcatheters to inject liquid embolic agents (LEA) to fill the nidus and exclude it partially or completely from the circulation[1–4].

Since the early stages of BAVM treatment, it has been a dogma to avoid occluding the vein until complete arterial or nidal control is achieved. An abrupt or unintended venous occlusion could result in an increase on intranidal pressure leading to a potentially secondary catastrophic bleeding[3,5]. Despite these considerations, some theoretical conceptualizations, animal experiments and clinical series showed that transvenous embolization (TVE) for BAVM was feasible as a potential route for endovascular treatment[6,7]. More recent series have shown TVE to be a game changer strategy for curative endovascular treatment of selected cases, demonstrating much higher occlusion rates than the classical arterial route[8,9].

The venous approach is technically demanding requiring a thorough anatomical knowledge and highly developed endovascular skills. Endovascular training, material testing and simulations for this access strategy have become an important need for achieving technical success and ensuring patient safety in the last years. Recently, Vollherbst et al, presented the first TVE in vivo model using a swine rete mirabile[10]. No other transvenous animal or in vitro model has been described so far, although these lasts have been widely used for other BAVM endovascular treatment simulations[11–18].

The purpose of this study was to present the development and test of a novel in vitro BAVM in vitro model for TVE using stereolithography (SLA) three-dimensional (3D) printing and real patient data.

Material and Methods

This research was approved by the local Institutional Review Board. An in vitro BAVM model was designed based on real patient data. We selected a left temporal BAVM, under 3 cm of diameter with single superficial venous drainage (Grade I according to Spetzler Martin classification)[19]. A three-dimensional rotational acquisition (3DRA) was performed using a Siemens Icono biplane angiography system (Siemens Healthineers, GmbH, Germany). The BAVM vessels information was exported in DICOM (Digital Imaging and Communications in Medicine) format, and a segmentation process was done using 3D Slicer (Slicer Platform open source https://www.slicer.org). The BAVM structure with the nidus was defined and transformed to STL (Standard Triangle Language). We created a container or "chip" where the BAVM model was fitted using Computer-Aided Design (CAD) software (Fusion 360, Autodesk California USA and Rhinoceros 3D, Robert McNeel & Associates, USA). A size threshold of 150 μm was applied as the acquisition modalities could not appropriately define nidal structures under this size, and therefore we removed from final model after the segmentation process. We added an external bypass channel that represented "normal" flow and luer lock connectors to the arterial input and venous output of the model.

CAD final model was exported on STL for 3D printing process. We used a commercial Form 3B printer (FormLabs, Somerville MA, USA) with transparent resin (Clear V4) to create the model using stereolithography (Figure 1).

We created a closed circuit setting of tubes and connectors with a pulsatile pump (FlowTek 125, united Biologics, Santa Ana CA USA), that we used for all tests. The pump could modify the pulse and flow percentage, and circulation was always from arterial to venous side.

Transvenous approach (TVA) injection test. We aimed to determine the ideal pressure regimen of the system to allow counter flow advance through the transvenous approach. The pulsatile pump was programmed with 60 cycles per minute, and ten different flow percentages were tested: 70-65-60-55-50-45-40-35-30-25%. The circuit used Sodium Chloride (NaCl) 0.9% at 36°C. Pressure was measured using a transducer (TruWave, Edwards Lifesciences Services GmbH, Germany) in a 3-way connector at the entrance of the

arterial part of the model and registered as mean arterial pressure (MAP). We placed an Excelsior 1018 microcatheter (Stryker Neurovascular, Fremont CA, USA) at the venous collector and iodinated contrast was manually injected (Visipaque 270, GE Chicago IL, USA) under biplane fluoroscopy using a Philips Azurion 7 biplane (Philips Healthcare, Amsterdam Netherlands. We graded the contrast filling pattern by dividing the model in four different sections and assigning a score from 0 to 3 (0 no nidus filling and 3 representing maximum retrograde contrast advance). Filling grade was compared with different MAP values using Pearson correlation test, significance was defined as $p \leq 0.05$.

Transvenous embolization test. We aimed to recreate the conditions of TVE using LEA in two different settings and evaluated the impact of venous coiling on nidal occlusion rate, total embolization time and number of stops after reflux. For this purpose, we used the BAVM model connected to the pulsatile pump. Normal saline at 36°C was used to fill the system. All embolizations were done with a pulse of 60 cycles per minute and 30% flow rate, which resulted in a MAP of 21mmHg and systolic pressure of 74mmHg. Under these settings, the flow at the model was 42ml/min. Under biplane fluoroscopy we performed retrograde LEA embolizations with Ethylene Vinyl Alcohol (EVOH) copolymer (Squid 18, Balt Montmorency France). Two experienced (+10 years) interventional neuroradiologists performed the embolizations. We embolized 12 models separated in two groups:

- **Group 1.** This group consisted in 6 models. A 1.5F microcatheter (Apollo 1.5 30mm, Medtronic, Minneapolis MN USA) was navigated and positioned at the origin of main vein over a 0,008" micro guidewire (Hybrid, Balt Montmorency, France). Death space of the microcatheter was flushed with Dimethyl Sulfoxide (DMSO). LEA was injected through the microcatheter manually as the usual manner, making 30 seconds pauses when reflux over the microcatheter was seen or when filling arterial feeder up to main arterial side. Procedure was stopped when reflux was greater than the venous drainage, or when no more nidus filling was seen after several injection and pause cycles.
- **Group 2.** This group consisted in 6 models. A 1.5F microcatheter was navigated and positioned in the same position as group 1. A second microcatheter (Vasco 10+, Balt,

Montmorency France) was placed in a proximal position at the venous side, approximately 40 mm back from the first microcatheter tip. One bare platinum coil (Barricade 10x34 Frame complex coil) was deployed at this point using the "porcelain vein technique" as described by Dr. Mounayer[9], in which EVOH is deposited in centripetal and circumferential manner along the vessel wall during reflux reducing progressively the inner diameter without blocking the venous output[9]. The LEA was then injected through the Apollo microcatheter using the technique and injection/pause cycles as group 1.

We measured total injection time, number of pauses and total injected LEA volume in both groups. We also determined the occlusion percentage of the nidus by a 3DRA acquisition without contrast at the end of embolization procedure. LEA at the model was segmented using 3D Slice software and total filling volume was calculated with PreForm Software (FormLabs, Somerville MA, USA). Percentage of nidal occlusion was calculated using the total nidal volume from the CAD model minus the calculated nidal LEA volume with 3DRA. We used the Mann-Whitney U test to evaluate the differences between the two groups. Statistical significance was determined as a $p \leq 0.05$.

Results.

TVA injection test

We found a statistically significant correlation between MAP and contrast media retrograde filling through the AVM model (p=0.001) (Figure 2). With lower MAP values, a greater contrast nidal penetration and higher filling score were found.

Transvenous embolization test.

LEA was injected retrogradely to the model using EVOH in two groups with described techniques. No differences were found between group 1 (no coils on the venous side) and group 2 (bare platinum coil on venous collector) in any of the different measured variables (Table 1).

Embolizations were done using the usual plug and push technique. Transparent resin material allowed a direct and easy visualization of the embolization process. Digital subtraction angiography controls performed at the end of the embolization session showed no nidal contrast filling in all models presented.

Discussion.

Transvenous embolization has been described and increasingly used in the last years demonstrating to be an outstanding approach to achieve BAVM cure in highly selected patients. Large series have showed great nidal occlusion rates and similar safety profile as the usual endovascular trans-arterial approach[9,20]. This evolving technique requires physician's proper training and teaching, development of specific devices and testing of new materials. Various models have been used for decades for these purposes, being the swine rete mirabile the model of choice for endovascular training and testing[21–23]. In vitro models have been less explored to simulate BAVM embolizations due to several limitations: difficulties in defining the real nidal anatomy using the currently available imaging modalities, complicated segmentation processes and the complexity of building small hollow small channels. Several models have been described since the late 70s for endovascular use, using different materials and structures that could resemble an BAVM or nidus, from straight tubes to honeycomb like structures, passing through tubes filled with beads, scouring pads, sponges, blood filters or springs[13–17,24,25]. A search for more realistic features has been done in the last years. Kaneko et al described an in vitro BAVM model with realistic features and hollow channels using 3D printing technique with a combination of solid printing and silicon coverage ready for LEA embolizations after dissolution of inner solid compounds[12]. Our group recently described a different new technology process using SLA 3D printing and millifluidic technique that allows us to create an in vitro BAVM model with small hollow channels that can be used for training and endovascular simulations[18]. These in vitro models have been used to replicate arterial embolization treatments, but no TVE approaches have been performed. As previously stated, the only TVE model described so far in the literature has been a swine rete mirabile in vivo model [10]. In vivo models are of great importance and utility for endovascular training but animal management, care facilities, transportation and cost are a great barrier for their massive use.

In this study, we were able to present a novel in vitro BAVM model for TVE. We were able to reproduce a BVAM anatomy of a real patient and translate it to a 3D printing SLA container. This process is an evolution of our early described SLA model in which we created

a simulated nidus anatomy[18]. This is a first step, and we are aware that many challenges remain to adequately recreate true nidal structures, but the current model opens many possibilities for training, rehearsal, and material testing, as it has been done previously with brain aneurysms [26–29]. Our new in vitro model has smaller hollow channels and more realistic structures and vessels. We expect more advances in the near future, as acquisition imaging techniques and 3D printing technologies continue to improve and will eventually allow the creation of smaller hollow or tubular structures.

Counter flow contrast injection proved to be in direct relation to MAP. Our model allowed us to define different pressure settings, and nidus retrograde filling was larger as systemic pressure was lower, with a statistically significant correlation. This concept was firs described by Massoud et al with their TRENSH (Transvenous Retrograde Nidus Sclerotherapy Under Controlled Hypotension) technique, injecting contrast in a retrograde manner in a swine rete mirabile model. Contrast retrograde penetration was greater with lower MAP pressure values[6]. The same concept has been applied in real TVE cases to create local or systemic hypotension for fast and complete nidal penetration, as proximal arterial balloon inflation, cardiac rapid ventricular pacing or systemic induced hypotension[9,20,30].

TVE in our model behaved similar to real cases. Navigation of the microcatheters was realistic and plausible with some extra friction as expected on in vitro cases[26]. Injection of LEA began with some reflux to the vein after which it began to advance through the nidus in the plug and push fashion. Rapidly a plug was created, and fast and initial filling of the nidus was possible. Secondary reflux began and was controlled as much as possible with 30 seconds stops until our limit reflux was reached. We expected to have different occlusion results between our two experimental groups, with faster and greater nidal penetration in the second group in which we used coils in the vein side. Nevertheless, we found no statistically significant differences. We think that the absence of clot formation within the coils (because the use of NaCl that replaces blood) and the limited number of coils used (one long coil) may explain these results, as these are factors that contribute to a stronger and better vein flow control. Our aim was to standardize the procedure and test the porcelain vein technique, so no other materials as glue were used, as described in venous pressure cooker[20]. Nidal

occlusion percentage was near 60%, although we expected a greater penetration and filling, we saw complete angiographic exclusion at the end of the procedure in all cases.

Our model and experience have several limitations. It is a solid in vitro model so there are no elastic features as real vessels, and model could not simulate procedure related rupture as in vivo BAVM. Friction inside the model felt higher than human vessels, thus still microcatheter navigation was adequately possible. Although we created a model based on a real BAVM, there are still anatomical limitations of the reproducibility and we couldn't replicate some smaller vessels because of actual image resolution, segmentation and hollow vessel printing. Number of tested models was limited, and we didn't test other flow control techniques at the venous side that could contribute in a better nidal occlusion penetration, neither proximal arterial flow control with balloons was used.

Finally, and despite some intrinsic limitations, we believe that our model presented several advantages as the model size, reproducibility, easy transportation and setup in any place or angiographic suite. The model is transparent, and although we didn't actively test this feature, embolization is feasible and controllable without the use of X-rays. The procedure could be well tested under direct vision or enhanced with a camera or video magnification. We were able to create a functional 3D printing in vitro BAVM model for TVE that could be used for training, teaching and testing new techniques and materials. We expect newer features and advances in the future, as this technology evolves.

Acknowledgments.
We would like to thank Balt (Montmorency France) for donating some of the material that were used during the embolizations tests as Squid 18 and Barricade coils.

Conflict of Interest Statement.
The authors declare no conflict of interest in this topic and research.

Authors Contribution
RR contributed to the design, conception, and management of the research. RR and JPC performed the embolization tests. CM and AR contributed to the design of the study and analysis of data. AC performed all the designs and CAD of the models All authors contributed in the analysis of the data, and the drafting and/or editing of the manuscript. All authors approved the final manuscript.

Competing Interests
Authors declare no competing interests regarding this article.

References.

1 Beijnum J van, Worp HB van der, Buis DR, *et al.* Treatment of Brain Arteriovenous Malformations A Systematic Review and Meta-analysis. *JAMA* 2011;**306**:2011–9. doi:10.1098/rspb.2013.0428

2 Saatci I, Geyik S, Yavuz K, *et al.* Endovascular treatment of brain arteriovenous malformations with prolonged intranidal Onyx injection technique: Long-term results in 350 consecutive patients with completed endovascular treatment course - Clinical article. *J Neurosurg* 2011;**115**:78–88. doi:10.3171/2011.2.JNS09830

3 Valavanis A, Pangalu A, Tanaka M. Endovascular treatment of cerebral arteriovenous malformations with emphasis on the curative role of embolisation. *Interventional Neuroradiology* 2005;**11**:37–42.

4 Loh Y, Duckwiler GR. A prospective, multicenter, randomized trial of the Onyx liquid embolic system and N-butyl cyanoacrylate embolization of cerebral arteriovenous malformations: Clinical article. *J Neurosurg* 2010;**113**:733–41. doi:10.3171/2010.3.JNS09370

5 Houdart E, Gobin YP, Casasco A, *et al.* A proposed angiographic classification of intracranial arteriovenous fistulae and malformations. *Neuroradiology* 1993;**35**:381–5.

6 Massoud TF, Hademenos GJ. Transvenous retrograde nidus sclerotherapy under controlled hypotension (TRENSH): A newly proposed treatment for brain arteriovenous malformations - Concepts and rationale. *Neurosurgery* 1999;**45**:351–65. doi:10.1097/00006123-199908000-00031

7 Nguyen TN, Chin LS, Souza R, *et al.* Transvenous embolization of a ruptured cerebral arteriovenous malformation with en-passage arterial supply: Initial case report. *J Neurointerv Surg* 2010;**2**:150–2. doi:10.1136/jnis.2009.001289

8 Chapot R, Stracke P, Velasco A, *et al.* The Pressure Cooker Technique for the treatment of brain AVMs. *Journal of Neuroradiology* 2014;**41**:87–91. doi:10.1016/j.neurad.2013.10.001

9 Mendes GAC, Kalani MYS, Iosif C, *et al.* Transvenous Curative Embolization of Cerebral Arteriovenous Malformations: A Prospective Cohort Study. *Clin Neurosurg* 2018;**83**:957–64. doi:10.1093/neuros/nyx581

10 Vollherbst DF, Hantz M, Schmitt N, *et al.* Experimental investigation of transvenous embolization of arteriovenous malformations using different in vivo models. *J Neurointerv Surg* 2022;:neurintsurg-2022-018894. doi:10.1136/neurintsurg-2022-018894

11 Vollherbst DF, Sommer CM, Ulfert C, *et al.* Liquid embolic agents for endovascular embolization: Evaluation of an established (Onyx) and a novel (PHIL) embolic agent in an in vitro AVM model. *American Journal of Neuroradiology* 2017;**38**:1377–82. doi:10.3174/ajnr.A5203

12 Kaneko N, Ullman H, Ali F, *et al.* In Vitro Modeling of Human Brain Arteriovenous Malformation for Endovascular Simulation and Flow Analysis. *World Neurosurg* 2020;**141**:e873–9. doi:10.1016/j.wneu.2020.06.084

13 Ishikawa M, Horikawa M, Yamagami T, *et al.* Embolization of arteriovenous malformations: Effect of flow control and composition of n-butyl-2 cyanoacrylate

and iodized oil mixtures with and without ethanol in an in vitro model. *Radiology* 2016;**279**:910–6. doi:10.1148/radiol.2015142583

14 Inagawa S, Isoda H, Kougo H, *et al.* In-vitro simulation of NBCA embolization for arteriovenous malformation. *Interventional Neuroradiology* 2003;**9**:351–8. doi:10.1177/159101990300900404

15 Debrun GM, Vinuela F V., Fox AJ, *et al.* Two different calibrated-leak balloons: Experimental work and application in humans. *American Journal of Neuroradiology* 1982;**3**:407–14.

16 Kerber CW, Bank WO, Cromwell LD. Calibrated leak balloon microcatheter: A device for arterial exploration and occlusive therapy. *American Journal of Roentgenology* 1979;**132**:207–12. doi:10.2214/ajr.132.2.207

17 Park S, Yoon H, Suh DC, *et al.* An arteriovenous malformation model for testing liquid embolic materials. *American Journal of Neuroradiology* 1997;**18**:1892–6.

18 Rivera R, Cespedes A, Cruz JP, *et al.* Endovascular treatment simulations using a novel in vitro brain arteriovenous malformation model based on three-dimensional printing millifluidic technology. *Interventional Neuroradiology* Published Online First: 2023. doi:10.1177/15910199231184605

19 Spetzler RF, Martin NA. A proposed grading system for arteriovenous malformations. *J Neurosurg* 1986;**65**:476–83. doi:10.3171/jns.1986.65.4.0476

20 Koyanagi M, Mosimann PJ, Nordmeyer H, *et al.* The transvenous retrograde pressure cooker technique for the curative embolization of high-grade brain arteriovenous malformations. *J Neurointerv Surg* 2021;**13**:637–41. doi:10.1136/neurintsurg-2020-016566

21 Massoud TF, Ji C, Vinuela F, *et al.* An experimental arteriovenous malformation model in swine: Anatomic basis and construction technique. *American Journal of Neuroradiology* 1994;**15**:1537–45.

22 Samaniego EA, Derdeyn CP, Hayakawa M, *et al.* In vivo evaluation of the new PHIL low viscosity in a swine rete mirabile model. *Interventional Neuroradiology* 2018;**24**:706–12. doi:10.1177/1591019918784915

23 Murayama Y, Viñuela F, Ulhoa A, *et al.* Nonadhesive liquid embolic agent for cerebral arteriovenous malformations: Preliminary histopathological studies in swine rete mirabile. *Neurosurgery* 1998;**43**:1164–72. doi:10.1097/00006123-199811000-00081

24 Bartynski WS, O'Reilly G V., Forrest MD. High-flow-rate arteriovenous malformation model for simulated therapeutic embolization. *Radiology* 1988;**167**:419–21. doi:10.1148/radiology.167.2.3357949

25 Kerber CW, Hecht ST, Knox K. Arteriovenous malformation model for training and research. *American Journal of Neuroradiology* 1997;**18**:1229–32.

26 Paramasivam S, Baltsavias G, Psatha E, *et al.* Silicone models as basic training and research aid in endovascular neurointervention - A single-center experience and review of the literature. *Neurosurg Rev* 2014;**37**:331–7. doi:10.1007/s10143-014-0518-x

27 Nawka MT, Spallek J, Kuhl J, *et al.* Evaluation of a modular in vitro neurovascular procedure simulation for intracranial aneurysm embolization. *J Neurointerv Surg* 2020;**12**:214–9. doi:10.1136/neurintsurg-2019-015073

28 Pravdivtseva MS, Peschke E, Lindner T, *et al.* 3D-printed, patient-specific intracranial aneurysm models: From clinical data to flow experiments with endovascular devices. *Med Phys* 2021;**48**:1469–84. doi:10.1002/mp.14714
29 Yamaki VN, Cancelliere NM, Nicholson P, *et al.* Biomodex patient-specific brain aneurysm models: The value of simulation for first in-human experiences using new devices and robotics. *J Neurointerv Surg* 2021;**13**:272–7. doi:10.1136/neurintsurg-2020-015990
30 Waqas M, Dossani RH, Vakharia K, *et al.* Complete flow control using transient concurrent rapid ventricular pacing or intravenous adenosine and afferent arterial balloon occlusion during transvenous embolization of cerebral arteriovenous malformations: Case series. *J Neurointerv Surg* 2021;**13**:324–30. doi:10.1136/neurintsurg-2020-016945

Figure 1. The process from the DICOM image to the model.

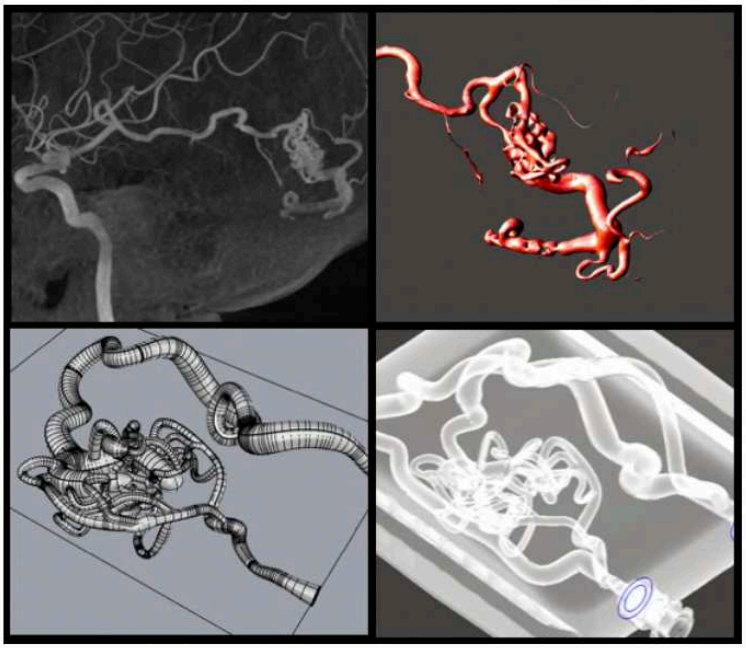

A) MIP 3D reconstruction of the left temporal BAVM. SM 1. B) Segmentation a 3D representation using 3D Slicer and Meshmixer Software. C) CAD representation of the BAVM model design following the main characteristics of the original disease. D) Final in vitro model inside the container, with transparent material and external "normal" channel. DICOM=Digital Imaging and Communications in Medicine. MIP=Maximum Intensity Projection. BAVM=Brain Arteriovenous Malformation. CAD=Computer-Aided Design.

Figure 2. Contrast media retrograde test.

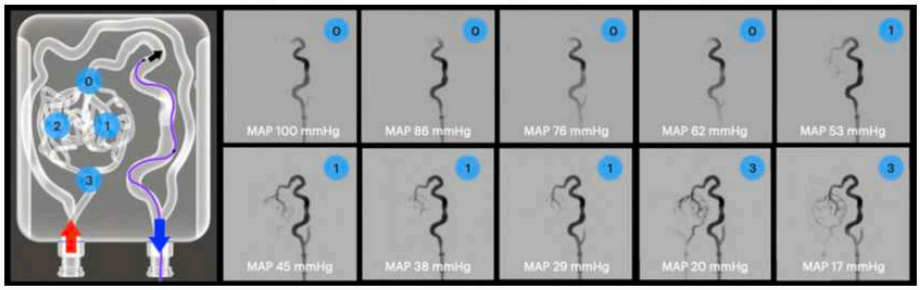

Injections were done using an Echelon 10 microcatheter and iodinated contrast. We tested 10 different input pressures from 10 different flow percentages, and we graded the retrograde advance from 0 to 3. 0=no significant advance; 1= one venous limb complete filling; 2= two venous limbs complete filling; 3=complete venous filling plus proximal arterial filling.

Figure 3. Transvenous embolization tests.

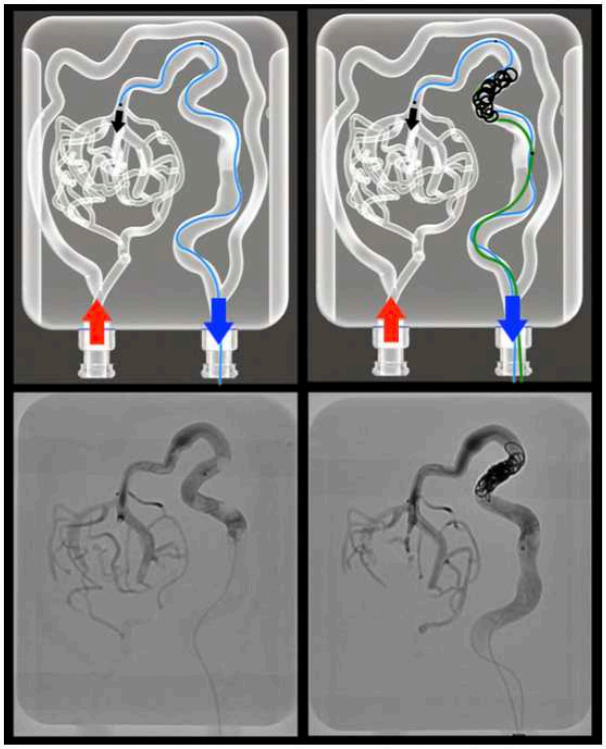

TVE technique was divided in two groups. A) Group 1 where retrograde embolization was done using a Apollo 1.5 30mm microcatheter. B) Group 2 the same position of Apollo 1.5 30mm and venous coils deployed with a Vasco+ microcatheter. C) X-ray vision after EVOH embolization of a group 1 case. D) X-ray vision after EVOH embolization of a group 2 case.

TVE= Transvenous embolization; EVOH=Ethylene Vinyl Alcohol

Table 1.

Group	Group 1	Group 2	Significance
Total Time (min:sec)	14:40	18:29	NS
Number of stops	13	15.5	NS
Total LEA (ml)	1.3ml	1.75ml	NS
Nidal LEA Volume (ml)	0.46 ml	0.49 ml	NS
Nidal occlusion %	57.6	61.95	NS

Nonparametric test for different variables between groups using Mann-Whitney test. NS=non-significant.

VII.4. Main Results and comments of article 3.

In this paper we were able to design and develop a functional 3D printed in vitro model for BAVM. It is an evolution from our second article achievement and the main improvement is the transfer from patient data to an in vitro model. This process is challenging, because nidal anatomy is still difficult to define and reproduce. Segmentation and definition of the small BAVM channels is still difficult, nevertheless, with some modifications and technical achievements we were able to create a realistic nidus, arteries and draining vein. Moreover, using a pulsatile pump we reproduced the anterograde flow inside the BAVM and we were able to access the nidus in an inverse way from the venous side.

We found that arterial pressure was a critical variable of contrast advance against flow from the venous side. A significant correlation was found between the two variables using Pearson correlation test ($p=0.001$). Better nidal penetration was higher with lower MAP values, a characteristic that has been tested in animal models and used in real TVE treatments. This is a key factor during TVE because the nidus should be filled as fast and complete as possible to avoid higher nidal pressure that could end in rupture and bleeding. Lowering the gradient of pressure inside the AVM and nidus has been a goal since the early Transvenous access animal models proposed by Massoud et al, where they confirmed that retrograde contrast filling of the nidus (Rete Mirabile in Swine model) was better and higher when using systemic or local hypotension, a technique they named TRENSH (Transvenous REtrograde Nidus Sclerotherapy under controlled Hypotension). They proposed that TRENSH could be used in the future for transvenous sclerosis of BAVM[41,42]. On the other hand, in clinical large series, MAP control and reduction for better nidal penetration has proved to be beneficial and has been obtained with different strategies: reducing the input flow (temporary balloon occlusion of the feeding

arteries), inducing systemic hypotension with drugs or by transient cardiac pacing with electric stimulation [44,49,91].

Transvenous embolizations were feasible in our model, and this is the first report of an in vitro model that achieved and described this procedure. Performance of the LEA was similar as real cases, allowing a plug and push technique, with an initial advance of the material, followed by reflux plug and then extra push and penetration to the BAVM. We compared two different techniques, trying to define the utility of coils at the venous side for better LEA penetration. This technique, that has been described and used by Pr. Mounayer in Limoges, known as "porcelain vein", allows higher nidal penetration with better control of LEA reflux to the vein. Group 1 was treated with no coils at the vein and in Group 2 coils were used to reduce flow on the output (Figure 44). We compared several variables as *total embolization time*, *total injected LEA*, *percentage of embolized nidus* and *number of stops* during the procedure. No differences were found between the two groups. This was unexpected because we thought that the coiling group would have a better nidal penetration and occlusion, less total time for procedure and less stops during treatment.

Figure 44. The transvenous embolization process at the model.
Images correspond to a case of group 2. A) Roadmap image of microcatheterization using an Apollo 1.5F. B) Deployment of a coil at venous side. C) LEA injection and partial retrograde filling of the nidus. D) Almost complete filling of the nidus with LEA.

The reasons that adding coils at the venous side did not have a relevant utility in our model could have been caused by: 1) no added thrombus within the coil (because we used NaCl 0.9% and no blood); and 2) we used a single coil in each case (with no multiple coils and compact filling) because of material availability.

Despite these limitations we achieved a great milestone of creating an in vitro BAVM model for TVE. The possibility of using real patient data for creating a model opens a huge new opportunity for rehearsal, training, and teaching for these often very complex cases, as it has been used in brain aneurysm simulations [63–68].

The article in perspective:

We developed the first in vitro BAVM model for TVE and this is the first literature report to our knowledge.

We were able to recreate a BAVM using real patient data and SLA 3D printing. The model allowed realistic retrograde transvenous embolizations using LEA. We proved that reducing systemic pressure can achieve a better nidal penetration.

The model opens a whole new era of training and testing for the TVE technique. Rehearsal could become a reality as it has been used in silicon or 3D printing models for brain aneurysms.

Chapter VIII. General synthesis, Discussion, and perspectives.

VIII.1. General synthesis and Discussion.

Brain Arteriovenous malformations are an infrequent but relevant disease that affects humans. Consequences of their rupture and bleeding could be catastrophic[10]. Although there is not a single ideal treatment, endovascular embolization has become one of the main management options for this disease. Its constant evolution and seeking for better and safer results have led to the development of the transvenous approach for BAVM embolization. This new technique has radically changed the treatment of BAVM with unprecedent curation rates and possibilities[44,49]. Nevertheless, because its technical needs and required skills practice, training and development of specific tools has become essential. The Neuroradiology Department at CHU Dupuytren at Limoges France under Prof. Mounayer leadership has become one of the main centers for BAVM treatment and one of the developers of the TVE strategy[45,48,92,93]. As a big and experienced center for BAVM treatment and training, it has faced the need and requirements of preparing physicians in this technique. We started this thesis with the main question of *how can we create a new BAVM model for TVE?*

In the first research part of the thesis, we performed a systematic scoping review of all BAVM models[94]. We used the PRISMA methodology proposed for scoping reviews[95,96] with an initial search of 942 articles and finally, after eligibility selection, we included and reviewed 177 articles. We found that BAVM models started focusing on surgical questions and using small rodents or cats for studying the normal perfusion pressure breakthrough[52]. Thus, later model research and development focused on genetic models with an interest in the understanding of the etiology mechanisms of BAVM and potential therapeutic targets[97,98]. Suitable models for

endovascular treatment have been mainly the RM in swine, because of its unique vascular structure near the brain. This structure is an arterial network with no venous side, and it could be modified and transformed in a functional AV shunt in different ways to a BAVM nidus like anatomy[61,62,99]. Although our group has used and developed several Swine rete mirabile models and has a complete animal lab angio suite[98,100], we were conscious of some limitations of using these experimental animals, as inability of moving the models to other sites, difficulties in preparing the models, and costs. Our exploration of in vitro models and their use for endovascular treatments, showed that they were not well developed: lacked angioarchitectural complexity, no nidal resemblance, and no generalized use[53,69–73,75,101]. Three-dimensional printing seemed interesting because of the capacity of rapid production, customization design and generalized use in other vascular diseases as brain aneurysms [63–68]. Thus, until our scoping review it has just been used for solid BAVM models, for surgical planning, anatomical demonstrations, or didactic use[102,103]. *We proposed to create a novel in vitro BAVM model for endovascular and TVE use with 3D printing.*

On the second experimental part of the thesis, we focused on developing an in vitro model for BAVM using 3D printing. We searched for the different 3D printing technologies, arriving to SLA technique. This type of 3D printing presented several properties that caught our attention as: high-definition printing, watertight products, minimum staircase effect; moreover, previous SLA use for brain aneurysms models and millifluidic chip production. Millifluidics were very important in defining our BAVM model because these micro laboratory structures have been using very small hollow channels and intricate designs, like a BAVM, to study fluid behaviors.

We proved this in our second article. We were able to create a novel in vitro BAVM model using SLA 3D printing with millifluidic techniques[104]. The structure of the model was designed with the three main components of a BAVM: arterial feeders, nidus and draining vein. Our

design was based on anatomical and clinical experience, together with the limitations of the printing technique. During the process of design, we faced the two main issues of creating BAVM 3D models: 1) recreation of the nidus structure is very challenging because there is insufficient anatomical data to really understand how vessels are organized at the BAVM. The lack of real structure comprehension comes from the resolution of actual image acquisitions, not sufficient to depicts nidus anatomy. Without clear image data, it is not possible to segment and digitally recreate these structures. 2) BAVM can have very small vessels and channels. Creation of 3D printing hollow channels is still challenging. In the case of SLA, channels are filled with uncured resin, which must be removed afterwards. Moreover, there are still technical restrictions to create submillimetric hollow channels.

After we went through these difficulties, we were able to create a viable BAVM model that we validated with different structural and functional tests. We reproduced LEA embolizations using EVOH (Squid 18) from the arterial side of the model, recreating conditions and operator's sensation like real embolizations. A qualitative questionnaire showed that operators felt that the model presented realistic embolization characteristics, and that it could be used for training, teaching, and testing tool for BAVM endovascular procedures.

In our third research part, we showed how we developed a more realistic BAVM model from real data ready for TVE. We were able to reproduce and segment a small BAVM and then recreated it with SLA 3D printing. The process led us to our next step of reproducing TVA and TVE. We created a flow circuit using the 3D model and we performed counter flow access, testing the effect of arterial pressure on the retrograde advance of contrast injections. This was an important simulation of the role of MAP in the successful penetration to the nidus seen in real cases during TVE. Thus, the main test was using LEA (Squid 18) for performing transvenous embolizations in the model. In this experiment we achieved the advance of LEA

retrogradely to the nidus, with the ability to navigate up to 2 microcatheters inside the vessel (group 2), in which we added coils to the venous side to try to increase nidal LEA penetration. Although we didn't find an extra advantage of using coils between groups in the model, we proved that we could manipulate devices and inject the LEA in a similar way as real cases. Our model showed that it was a functional reproduction of a BAVM that can be used for TVA / TVE.

Our work and final product it is far from perfection, and several limitations have been stated in this document. The printed models are rigid, with no flexibility as real vessels and no chances to recreate ruptures an important characteristic and complication during embolizations. Anatomy is still under development and evolution, and a 100% realistic anatomy transfer to the model is still no possible to recreate. Thus, can venture that definition and reproducibility will only be improving as technology advances. Finally, resin gives higher friction than real vessels, and although the sensation of material navigation could be different, it allows in our cases to use two simultaneous microcatheters for LEA embolization with no higher difficulties.

VIII.2. Work perspectives and collaborations.

Our work, during these years lead us to create a new in vitro model, that has not been described or reported, that can be used for different techniques in endovascular treatments. We were able to use SLA 3D printing to create our models. This is a very interesting technique, because 3D printing allows faster design process, quick iterations, and customization of the model creation.

We developed several contributions during the process of the thesis. The first and main collaboration was with Alvaro Cespedes at the Design and Manufacturing Department at

Universidad Técnica Federico Santa Maria in Valparaiso Chile. He helped us with all CAD designs of the model and translating our drafts and ideas into perfect computer designs.

Another important collaboration was created with Alvaro Valencia and Carlota Rivera from the Mechanical Engineering Department at Universidad de Chile. They were responsible of the computer flow dynamic analysis of models in article 2. With their work we were able to perform the structural validation and simulate how flow, pressure and velocity could behave inside the 3D printed BAVM.

A big part of this work, in part because of the COVID-19 pandemic and because of geographical distance, was done in two different settings: at the Neuroradiology Department in CHU Dupuytren Hospital in Limoges, and at the Neuroradiology Department of the Instituto de Neurocirugia Dr. Asenjo in Santiago Chile. This created a synergic collaboration between centers, that will continue in the future for further work.

We look forward to the continuous improvement of the model. We will keep advancing on realistic BAVM models. We should focus on creating smaller hollow channels, better image acquisitions to more accurate nidal recreation and modifiable flow variables to recreate different embolization conditions.

The work on this thesis has created a group with innovation interest and ready to create a StartUp from this project. We are applying to government grants (https://anid.cl/concursos/startup-ciencia-2024/) to advance in the elaboration of a product that could be commercialized in the near future. There is big interest in the field to have this model available in the market for training, teaching, and testing.

During the process of developing the model we ask for the advice from several entities about patenting the idea. This process has had no pragmatic result until the writing of this document. We are still working on the subject and although all presented data could not be patented due

to the previous exposition, we are on the way of developing a complete setting for TVE training that could be patented and protected.

We are ending this thesis and period with still more questions about TVE models and TVE that must be answered. We aim to continue our work in our group for improving the model and giving the answers regarding this topic.

Chapter IX. Conclusions.

Our work has created and validated a new in vitro BAVM model. We achieved to answer our initial question if it was possible to create a new BAVM model for TVE. Through a sequential and progressive process, we were able to achieve our objective.

The creation of a new in vitro BAVM model opens a new spectrum of possibilities in training, teaching, and testing. We hope that this model could play an important role in recreating endovascular treatments, for the training process of doctors around the world and helping them to get the necessary skills for patients' safety. Case specific models in BAVM has been a long-standing desire for this disease, and this model could become a revolutionary way of rehearsal, and teaching.

Finally, our in vitro model could be used to test new devices and materials for endovascular embolizations providing a newer, faster, and standardized process of creating new products.

Bibliography

1. Geibprasert S, Pongpech S, Jiarakongmun P, et al. Radiologic assessment of brain arteriovenous malformations: What clinicians need to know. *Radiographics* 2010; 30: 483–501.
2. Dalton A, Dobson G, Prasad M, et al. De novo intracerebral arteriovenous malformations and a review of the theories of their formation. *British Journal of Neurosurgery* 2018; 32: 305–311.
3. Lasjaunias P. A Revised Concept of the Congenital Nature of Cerebral Arteriovenous Malformations. *Interventional Neuroradiology* 1997; 3: 275–281.
4. Valavanis A, Yasargil MG. The Endovascular Treatment of Brain Arteriovenous Malformations. In: Cohadon F (ed) *Advances and Technical Standards in Neurosurgery*. 1998, pp. 132–204.
5. Sturiale CL, Puca A, Sebastiani P, et al. Single nucleotide polymorphisms associated with sporadic brain arteriovenous malformations: Where do we stand? *Brain* 2013; 136: 665–681.
6. Delev D, Pavlova A, Grote A, et al. NOTCH4 gene polymorphisms as potential risk factors for brain arteriovenous malformation development and hemorrhagic presentation. *J Neurosurg* 2017; 126: 1552–1559.
7. Thalgott JH, Dos-Santos-Luis D, Hosman AE, et al. Decreased expression of vascular endothelial growth factor receptor 1 contributes to the pathogenesis of hereditary hemorrhagic telangiectasia type 2. *Circulation* 2018; 138: 2698–2712.
8. Beijnum J van, Worp HB van der, Buis DR, et al. Treatment of Brain Arteriovenous Malformations A Systematic Review and Meta-analysis. *JAMA* 2011; 306: 2011–2019.
9. Al-Shahi R, Fang JSY, Lewis SC, et al. Prevalence of adults with brain arteriovenous malformations: A community based study in Scotland using capture-recapture analysis. *J Neurol Neurosurg Psychiatry* 2002; 73: 547–551.

10. Solomon RA, Connolly ES. Arteriovenous malformations of the brain. *New England Journal of Medicine* 2017; 376: 1859–1866.
11. Morris Z, Whiteley WN, Longstreth WT, et al. Incidental findings on brain magnetic resonance imaging: Systematic review and meta-analysis. *BMJ (Online)* 2009; 339: 547–550.
12. Brown RD, Wiebers DO, Torner JC, et al. Frequency of intracranial hemorrhage as a presenting symptom and subtype analysis: a population-based study of intracranial vascular malformations in Olmsted County, Minnesota. *J Neurosurg* 1996; 85: 29–32.
13. ApSimon HT, Reef H, Phadke R V., et al. A population-based study of brain arteriovenous malformation: Long-term treatment outcomes. *Stroke* 2002; 33: 2794–2800.
14. Gross BA, Du R. Rate of re-bleeding of arteriovenous malformations in the first year after rupture. *Journal of Clinical Neuroscience* 2012; 19: 1087–1088.
15. Kim H, Al-Shahi Salman R, Edin Charles McCulloch FE, et al. Untreated brain arteriovenous malformation Patient-level meta-analysis of hemorrhage predictors. *Neurology* 2014; 83: 590–597.
16. Mohr J, Parides MK, Stapf C, et al. Medical management with or without interventional therapy for unruptured brain arteriovenous malformations (ARUBA): a multicentre, non-blinded, randomised trial. *Lancet* 2014; 15: 614–621.
17. Keil F, Bergkemper A, Birkhold A, et al. 4D Flat Panel Conebeam CTA for Analysis of the Angioarchitecture of Cerebral AVMs with a Novel Software Prototype. *American Journal of Neuroradiology* 2022; 43: 102–109.
18. Houdart E, Gobin YP, Casasco A, et al. A proposed angiographic classification of intracranial arteriovenous fistulae and malformations. *Neuroradiology* 1993; 35: 381–385.
19. Raman A, Uprety M, Calero MJ, et al. A Systematic Review Comparing Digital Subtraction Angiogram With Magnetic Resonance Angiogram Studies in

Demonstrating the Angioarchitecture of Cerebral Arteriovenous Malformations. *Cureus*. Epub ahead of print 10 June 2022. DOI: 10.7759/cureus.25803.

20. Muller-Forell W, Valavanis A. How Angioarchitecture of Cerebral Arteriovenous Malformations should Influence the Therapeutic Considerations. *Mini Invas Neurosurg* 1995; 38: 32–40.
21. Spetzler RF, Martin NA. A proposed grading system for arteriovenous malformations. *J Neurosurg* 1986; 65: 476–483.
22. Lawton MT, Kim H, McCulloch CE, et al. A supplementary grading scale for selecting patients with brain arteriovenous malformations for surgery. *Neurosurgery* 2010; 66: 702–713.
23. Magro E, Gentric JC, Darsaut TE, et al. Responses to ARUBA: A systematic review and critical analysis for the design of future arteriovenous malformation trials. *J Neurosurg* 2017; 126: 486–494.
24. Patel SD, Saber H, Desai N, et al. Impact of ARUBA trial on trends and outcomes in symptomatic non-ruptured brain AVMs: A national sample analysis. *Journal of Stroke and Cerebrovascular Diseases*; 31. Epub ahead of print 1 December 2022. DOI: 10.1016/j.jstrokecerebrovasdis.2022.106807.
25. Fahed R, Batista AL, Darsaut TE, et al. The Treatment of Brain Arteriovenous Malformation Study (TOBAS): A preliminary inter- and intra-rater agreement study on patient management. *Journal of Neuroradiology* 2017; 44: 247–253.
26. Richling B, Killer M, Al-Schameri AR, et al. Therapy of brain arteriovenous malformations: multimodality treatment from a balanced standpoint. *Neurosurgery*; 59. Epub ahead of print 2006. DOI: 10.1227/01.NEU.0000237408.95785.64.
27. Morgan MK, Davidson AS, Assaad NNA, et al. Critical review of brain AVM surgery, surgical results and natural history in 2017. *Acta Neurochirurgica* 2017; 159: 1457–1478.
28. Doby T. Cerebral angiography and Egas Moniz. *AJR Am J Roentgenol* 1992; 159: 364–364.

29. Yasargil M. Operations on intracranial arteriovenous malformations. In: Yasargil M (ed) *Microsurgery. Applied to Neurosurgery.* New York, 1969, pp. 143–148.
30. Potts MB, Lau D, Abla AA, et al. Current surgical results with low-grade brain arteriovenous malformations. *J Neurosurg* 2015; 122: 912–920.
31. Darsaut TE, Magro E, Bojanowski MW, et al. Surgical treatment of brain arteriovenous malformations: clinical outcomes of patients included in the registry of a pragmatic randomized trial. *J Neurosurg* 2023; 138: 891–899.
32. Starke RM, Kano H, Ding D, et al. Stereotactic radiosurgery for cerebral arteriovenous malformations: Evaluation of long-term outcomes in a multicenter cohort. *J Neurosurg* 2017; 126: 36–44.
33. Starke RM, Kano H, Ding D, et al. Stereotactic radiosurgery for cerebral arteriovenous malformations: Evaluation of long-term outcomes in a multicenter cohort. *J Neurosurg* 2017; 126: 36–44.
34. Starke RM, Komotar RJ, Hwang BY, et al. A comprehensive review of radiosurgery for cerebral arteriovenous malformations: Outcomes, predictive factors, and grading scales. *Stereotact Funct Neurosurg* 2008; 86: 191–199.
35. Crowley RW, Ducruet AF, McDougall CG, et al. Endovascular advances for brain arteriovenous malformations. *Neurosurgery* 2014; 74: 74–82.
36. Zanetti PH, Sherman FE. Experimental evaluation of a tissue adhesive as an agent for the treatment of aneurysms and arteriovenous anomalies. *J Neurosurg* 1972; 36: 72–79.
37. Taki W, Yonekawa Y, Lwata H, et al. A New Liquid Material for Embolization of Arteriovenous Malformations. *AJNR* 1990; 11: 163–168.
38. Loh Y, Duckwiler GR. A prospective, multicenter, randomized trial of the Onyx liquid embolic system and N-butyl cyanoacrylate embolization of cerebral arteriovenous malformations: Clinical article. *J Neurosurg* 2010; 113: 733–741.
39. Saatci I, Geyik S, Yavuz K, et al. Endovascular treatment of brain arteriovenous malformations with prolonged intranidal Onyx injection technique: Long-term results in

350 consecutive patients with completed endovascular treatment course - Clinical article. *J Neurosurg* 2011; 115: 78–88.

40. Valavanis A, Pangalu A, Tanaka M. Endovascular treatment of cerebral arteriovenous malformations with emphasis on the curative role of embolisation. *Interventional Neuroradiology* 2005; 11: 37–42.
41. Massoud TF, Hademenos GJ. Transvenous retrograde nidus sclerotherapy under controlled hypotension (TRENSH): A newly proposed treatment for brain arteriovenous malformations - Concepts and rationale. *Neurosurgery* 1999; 45: 351–365.
42. Massoud TF. Transvenous retrograde nidus sclerotherapy under controlled hypotension (TRENSH): Hemodynamic analysis and concept validation in a pig arteriovenous malformation model. *Neurosurgery* 2013; 73: 332–342.
43. Nguyen TN, Chin LS, Souza R, et al. Transvenous embolization of a ruptured cerebral arteriovenous malformation with en-passage arterial supply: Initial case report. *J Neurointerv Surg* 2010; 2: 150–152.
44. Mendes GAC, Kalani MYS, Iosif C, et al. Transvenous Curative Embolization of Cerebral Arteriovenous Malformations: A Prospective Cohort Study. *Clin Neurosurg* 2018; 83: 957–964.
45. Mendes GAC, Iosif C, Silveira EP, et al. Transvenous Embolization in Pediatric Plexiform Arteriovenous Malformations. *Neurosurgery* 2016; 78: 458–465.
46. Choudhri O, Ivan ME, Lawton MT. Transvenous Approach to Intracranial Arteriovenous Malformations: Challenging the Axioms of Arteriovenous Malformation Therapy? *Neurosurgery* 2015; 77: 644–651.
47. Chen CJ, Norat P, Ding D, et al. Transvenous embolization of brain arteriovenous malformations: A review of techniques, indications, and outcomes. *Neurosurg Focus* 2018; 45: 1–7.

48. Kessler R, Riva R, Ruggiero M, et al. Successful Transvenous Embolization of Brain Arteriovenous Malformations Using Onyx in Five Consecutive Patients. *Neurosurgery* 2011; 69: 184–193.

49. Koyanagi M, Mosimann PJ, Nordmeyer H, et al. The transvenous retrograde pressure cooker technique for the curative embolization of high-grade brain arteriovenous malformations. *J Neurointerv Surg* 2021; 13: 637–641.

50. Murayama Y, Massoud TF, Viñuela F. Transvenous Hemodynamic Assessment of Experimental Arteriovenous Malformations. Doppler Guidewire Monitoring of Embolotherapy in a Swine Model. *Stroke* 1996; 27: 1365–1372.

51. Vollherbst DF, Hantz M, Schmitt N, et al. Experimental investigation of transvenous embolization of arteriovenous malformations using different in vivo models. *J Neurointerv Surg* 2022; neurintsurg-2022-018894.

52. Spetzler RF, Wilson CB, Weinstein P, et al. Normal Perfusion Pressure Breakthrough Theory. *Clin Neurosurg* 1978; 25: 651–672.

53. Kerber CW, Bank WO, Cromwell LD. Calibrated leak balloon microcatheter: A device for arterial exploration and occlusive therapy. *American Journal of Roentgenology* 1979; 132: 207–212.

54. Xu M, Xu H, Qin Z. Animal Models in Studying Cerebral Arteriovenous Malformation. *Biomed Res Int*; 2015. Epub ahead of print 2015. DOI: 10.1155/2015/178407.

55. Ardelean DS, Letarte M. Anti-angiogenic therapeutic strategies in hereditary hemorrhagic telangiectasia. *Front Genet* 2015; 5: 1–8.

56. di Ieva A, Boukadoum M, Lahmiri S, et al. Computational Analyses of Arteriovenous Malformations in Neuroimaging. *Journal of Neuroimaging* 2015; 25: 354–360.

57. Raj JA, Stoodley M. Experimental animal models of arteriovenous malformation: A review. *Vet Sci* 2015; 2: 97–110.

58. Herrmann AM, Meckel S, Gounis MJ, et al. Large animals in neurointerventional research: A systematic review on models, techniques and their application in

endovascular procedures for stroke, aneurysms and vascular malformations. *Journal of Cerebral Blood Flow and Metabolism* 2019; 39: 375–394.

59. Nielsen CM, Huang L, Murphy PA, et al. Mouse models of cerebral arteriovenous malformation. *Stroke* 2016; 47: 293–300.

60. Rivera R, Cruz JP, Merino-Osorio C, et al. Brain arteriovenous malformations: A scoping review of experimental models. *Interdiscip Neurosurg* 2021; 25: 101200.

61. Massoud TF, Ji C, Viñuela F, et al. Laboratory simulations and training in endovascular embolotherapy with a swine arteriovenous malformation model. *American Journal of Neuroradiology* 1996; 17: 271–279.

62. Massoud TF, Ji C, Vinuela F, et al. An experimental arteriovenous malformation model in swine: Anatomic basis and construction technique. *American Journal of Neuroradiology* 1994; 15: 1537–1545.

63. Spallek J, Krause D. Process Types of Customisation and Personalisation in Design for Additive Manufacturing Applied to Vascular Models. In: *Procedia CIRP*. Elsevier B.V., 2016, pp. 281–286.

64. Paramasivam S, Baltsavias G, Psatha E, et al. Silicone models as basic training and research aid in endovascular neurointervention - A single-center experience and review of the literature. *Neurosurg Rev* 2014; 37: 331–337.

65. Nawka MT, Spallek J, Kuhl J, et al. Evaluation of a modular in vitro neurovascular procedure simulation for intracranial aneurysm embolization. *J Neurointerv Surg* 2020; 12: 214–219.

66. Marciuc EA, Dobrovat BI, Popescu RM, et al. 3d printed models—a useful tool in endovascular treatment of intracranial aneurysms. *Brain Sci*; 11. Epub ahead of print 1 May 2021. DOI: 10.3390/brainsci11050598.

67. Pravdivtseva MS, Peschke E, Lindner T, et al. 3D-printed, patient-specific intracranial aneurysm models: From clinical data to flow experiments with endovascular devices. *Med Phys* 2021; 48: 1469–1484.

68. Yamaki VN, Cancelliere NM, Nicholson P, et al. Biomodex patient-specific brain aneurysm models: The value of simulation for first in-human experiences using new devices and robotics. *J Neurointerv Surg* 2021; 13: 272–277.

69. Kerber CW, Flaherty LW. A teaching and research simulator for therapeutic embolization. *American Journal of Neuroradiology* 1980; 1: 167–169.

70. Debrun GM, Vinuela F V., Fox AJ, et al. Two different calibrated-leak balloons: Experimental work and application in humans. *American Journal of Neuroradiology* 1982; 3: 407–414.

71. Bartynski WS, O'Reilly G V., Forrest MD. High-flow-rate arteriovenous malformation model for simulated therapeutic embolization. *Radiology* 1988; 167: 419–421.

72. Park S, Yoon H, Suh DC, et al. An arteriovenous malformation model for testing liquid embolic materials. *American Journal of Neuroradiology* 1997; 18: 1892–1896.

73. Inagawa S, Isoda H, Kougo H, et al. In-vitro simulation of NBCA embolization for arteriovenous malformation. *Interventional Neuroradiology* 2003; 9: 351–358.

74. Ishikawa M, Horikawa M, Yamagami T, et al. Embolization of arteriovenous malformations: Effect of flow control and composition of n-butyl-2 cyanoacrylate and iodized oil mixtures with and without ethanol in an in vitro model. *Radiology* 2016; 279: 910–916.

75. Vollherbst DF, Sommer CM, Ulfert C, et al. Liquid embolic agents for endovascular embolization: Evaluation of an established (Onyx) and a novel (PHIL) embolic agent in an in vitro AVM model. *American Journal of Neuroradiology* 2017; 38: 1377–1382.

76. Kaneko N, Ullman H, Ali F, et al. In Vitro Modeling of Human Brain Arteriovenous Malformation for Endovascular Simulation and Flow Analysis. *World Neurosurg* 2020; 141: e873–e879.

77. Mashiko T, Otani K, Kawano R, et al. Development of three-dimensional hollow elastic model for cerebral aneurysm clipping simulation enabling rapid and low cost prototyping. *World Neurosurgery* 2015; 83: 351–361.

78. Conti A, Pontoriero A, Iatì G, et al. 3D-Printing of Arteriovenous Malformations for Radiosurgical Treatment: Pushing Anatomy Understanding to Real Boundaries. *Cureus*. Epub ahead of print 29 April 2016. DOI: 10.7759/cureus.594.

79. Bae JW, Lee DY, Pang CH, et al. Clinical application of 3D virtual and printed models for cerebrovascular diseases. *Clin Neurol Neurosurg*; 206. Epub ahead of print 1 July 2021. DOI: 10.1016/j.clineuro.2021.106719.

80. Thawani JP, Pisapia JM, Singh N, et al. Three-Dimensional Printed Modeling of an Arteriovenous Malformation Including Blood Flow. *World Neurosurg* 2016; 90: 675-683.E2.

81. Chueh JY, Wakhloo AK, Gounis MJ. Neurovascular modeling: Small-batch manufacturing of silicone vascular replicas. *American Journal of Neuroradiology* 2009; 30: 1159–1164.

82. Waldbaur A, Rapp H, Länge K, et al. Let there be chip - Towards rapid prototyping of microfluidic devices: One-step manufacturing processes. *Analytical Methods* 2011; 3: 2681–2716.

83. Wurm G, Lehner M, Tomancok B, et al. Cerebrovascular biomodeling for aneurysm surgery: Simulation-based training by means of rapid prototyping technologies. *Surg Innov* 2011; 18: 294–306.

84. Wurm G, Tomancok B, Pogady P, et al. Cerebrovascular stereolithographic biomodeling for aneurysm surgery. *J Neurosurg* 2004; 100: 130–145.

85. Isoda K, Fukuda H, Takamura N, et al. Arteriovenous Malformation of the Brain. Histological Study and Micrometric Measurement of Abnormal Vessels. *Acta Pathol J p* 1981; 883–893.

86. Beauchamp MJ, Nordin GP, Woolley AT. Moving from millifluidic to truly microfluidic sub-100-μm cross-section 3D printed devices. *Anal Bioanal Chem* 2017; 409: 4311–4319.

87. Thome C. *Use of stereolithographic 3D printing for fabrication of micro and millifluidic devices for undergraduate engineering studies*. University of Tennessee, Chattanooga, https://scholar.utc.edu/honors-theses (2018).
88. Lee JM, Zhang M, Yeong WY. Characterization and evaluation of 3D printed microfluidic chip for cell processing. *Microfluid Nanofluidics* 2016; 20: 1–15.
89. Weisgrab G, Ovsianikov A, Costa PF. Functional 3D Printing for Microfluidic Chips. *Advanced Materials Technologies*; 4. Epub ahead of print 1 October 2019. DOI: 10.1002/admt.201900275.
90. Siekmann R. Basics and Principles in the Application of Onyx LD Liquid Embolic System in the Endovascular. *Interventional Neuroradiology* 2005; 11: 131–140.
91. Waqas M, Dossani RH, Vakharia K, et al. Complete flow control using transient concurrent rapid ventricular pacing or intravenous adenosine and afferent arterial balloon occlusion during transvenous embolization of cerebral arteriovenous malformations: Case series. *J Neurointerv Surg* 2021; 13: 324–330.
92. Mounayer C, Hammami N, Piotin M, et al. Nidal embolization of brain arteriovenous malformations using onyx in 94 patients. *American Journal of Neuroradiology* 2007; 28: 518–523.
93. Mendes GAC, Kalani MYS, Iosif C, et al. Transvenous Curative Embolization of Cerebral Arteriovenous Malformations: A Prospective Cohort Study. *Clin Neurosurg* 2018; 83: 957–964.
94. Rivera R, Cruz JP, Merino-Osorio C, et al. Brain arteriovenous malformations: A scoping review of experimental models. *Interdiscip Neurosurg*; 25. Epub ahead of print 2021. DOI: 10.1016/j.inat.2021.101200.
95. Peters MDJ, Godfrey CM, Khalil H, et al. Guidance for conducting systematic scoping reviews. *Int J Evid Based Healthc* 2015; 13: 141–146.
96. Tricco AC, Lillie E, Zarin W, et al. PRISMA extension for scoping reviews (PRISMA-ScR): Checklist and explanation. *Ann Intern Med* 2018; 169: 467–473.

97. Tual-Chalot S, Oh SP, Arthur HM. Mouse models of hereditary hemorrhagic telangiectasia: Recent advances and future challenges. *Front Genet* 2015; 5: 1–13.

98. Papagiannaki C, Clarençon F, Ponsonnard S, et al. Development of an angiogenesis animal model featuring brain arteriovenous malformation histological characteristics. *J Neurointerv Surg* 2017; 9: 204–210.

99. Massoud TF, Vinters H V., Chao KH, et al. Histopathologic characteristics of a chronic arteriovenous malformation in a swine model: Preliminary study. *American Journal of Neuroradiology* 2000; 21: 1268–1276.

100. Papagiannaki C, Yardin C, Iosif C, et al. Intra-arterial in-situ bevacizumab injection effect on angiogenesis. Results on a swine angiogenesis model. *Journal of Neuroradiology*. Epub ahead of print 2020. DOI: 10.1016/j.neurad.2020.03.003.

101. Kerber CW, Hecht ST, Knox K. Arteriovenous malformation model for training and research. *American Journal of Neuroradiology* 1997; 18: 1229–1232.

102. Dong M, Chen G, Li J, et al. Three-dimensional brain arteriovenous malformation models for clinical use and resident training. *Medicine*; 97. Epub ahead of print 2018. DOI: 10.1097/MD.0000000000009516.

103. Ye X, Wang L, Li K, et al. A three-dimensional color-printed system allowing complete modeling of arteriovenous malformations for surgical simulations. *Journal of Clinical Neuroscience* 2020; 77: 134–141.

104. Rivera R, Cespedes A, Cruz JP, et al. Endovascular treatment simulations using a novel in vitro brain arteriovenous malformation model based on three-dimensional printing millifluidic technology. *Interventional Neuroradiology*. Epub ahead of print 2023. DOI: 10.1177/15910199231184605.

Attention, ne supprimez pas le saut de section suivant (page suivante non numérotée)

Traitement Endovasculaire des Malformations Artérioveineuses Cérébrales par Voie Veineuse. Développement d'un Nouvel Modèle pour la Embolisation par Voie Veineuse

---

Les malformations artérioveineuses cérébrales (MAVC) sont des anomalies vasculaires rares mais significatives pouvant entraîner de graves conséquences neurologiques. Leur prise en charge a été un défi, et le traitement endovasculaire s'est imposé comme une approche essentielle. L'embolisation endovasculaire, impliquant l'utilisation de matériaux liquides qui se solidifient à l'intérieur des vaisseaux, peut partiellement ou complètement obstruer une MAVC. La voie artérielle a traditionnellement été le principal point d'accès pour traiter les MAVC. Cependant, ces dernières années, l'embolisation transveineuse (ETV) a révolutionné le traitement de certains cas, obtenant d'excellents résultats curatifs. Cette approche, impliquant l'embolisation endovasculaire du côté veineux de manière à contre-courant, exige des compétences avancées de l'opérateur.

Lorsque nous avons lancé cette étude, il n'existait aucun modèle de MAVC adapté à l'enseignement ou à la formation en ETV. L'objectif de notre thèse était de développer un nouveau modèle de MAVC pour l'ETV. Notre question de recherche centrale était de savoir s'il était possible de créer un nouveau modèle de MAVC pour l'embolisation transveineuse.

Dans une première partie de la thèse, nous avons mené des recherches approfondies, examinant systématiquement tous les modèles utilisés dans les études sur les MAVC. Nous avons observé que les modèles endovasculaires utilisaient principalement le rete mirabile chez le cochon, et que les modèles in vitro n'étaient pas largement utilisés à cette fin. L'impression 3D semblait être une technique attrayante pour créer de

nouveaux modèles, moins chère et plus accessible que les animaux ; cependant, aucun modèle efficace avec des canaux creux n'avait été développé en utilisant cette technologie.

Nous avons découvert qu'une technique d'impression 3D spécialisée appelée stéréolithographie (SLA) avait été utilisée pour créer des objets avec de petits canaux pour un domaine appelé millifluidique. Étant donné que la création de petits canaux creux était un défi technologique et une réalisation en millifluidique, nous avons choisi d'utiliser la SLA pour développer un nouveau modèle vasculaire. Nous avons commencé avec des conceptions de conteneurs simples, que nous avons appelées « puces », comportant des tubes internes creux. Au fil du temps, nous avons incorporé des courbes plus douces et des structures plus organiques pour simuler une MAVC, avec les éléments classiques des artères d'alimentation, du nidus et des veines de drainage.

Dans une deuxième phase de nos recherches, nous avons testé notre modèle initial de puce de MAVC en utilisant l'embolisation par voie transartérielle dans un circuit fermé et nous avons pu confirmer sa fiabilité structurelle et fonctionnelle. Cette étude a servi de preuve de concept que le modèle pouvait être utilisé pour la formation, l'enseignement et la recherche en embolisation de MAVC.

Grâce à un processus de conception itératif, nous sommes parvenus à la dernière évolution du modèle de MAVC, où nous avons pu transférer des données d'image de patients réels dans une conception informatique et l'imprimer en 3D. Ce modèle était connecté à un système avec une pompe, nous permettant de reproduire l'environnement vasculaire de l'embolisation transveineuse. Nous avons réussi à démontrer la faisabilité de l'ETV en utilisant des microcathéters et des agents

emboliques liquides. Cette réalisation a marqué la création et le test du premier modèle in vitro de MAVC pour l'ETV utilisant l'impression 3D, répondant ainsi avec succès à notre question de recherche.

Ce modèle unique et innovant ouvre de nouvelles possibilités pour l'enseignement, l'apprentissage, la formation et la recherche dans le traitement endovasculaire des MAVC.

Mots-clés : Malformations artério-veineuses cérébrales, impression 3D, modèles.

Transvenous Embolization of Brain Arteriovenous Malformations.

Development of a Novel Model for Transvenous Embolization

Brain Arteriovenous Malformations (BAVM) are rare but significant vascular anomalies that can lead to severe neurological consequences. Managing them has been challenging, and endovascular treatment has emerged as a cornerstone approach. Endovascular embolization, involving the use of liquid materials that solidify inside the vessels, can partially or completely occlude a BAVM. The arterial route has traditionally been the primary access point for treating BAVMs. However, in recent years, transvenous embolization (TVE) has revolutionized the treatment of selected cases, yielding excellent curative results. This approach, involving endovascular embolization from the venous side in a counterflow manner, demands advanced operator skills.

When we initiated this study, there were no BAVM models suitable for teaching or training in TVE. The objective of our thesis was to develop a new BAVM model for TVE. Our central research question was whether it was possible to create a new BAVM model for transvenous embolization.

As an initial part of the thesis, we conducted extensive research, were we systematically examined all the models employed in BAVM studies. We observed that endovascular models predominantly featured the utilization of the rete mirabile in swine, and that in vitro models had not been widely utilized for this purpose. Three-dimensional printing appeared to be an attractive technique for creating new models, cheaper and more accessible than animals; however, no effective models with hollow channels had been developed using this technology.

We discovered that a specialized 3D printing technique known as Stereolithography (SLA) had been used to create objects with small channels for a field called Millifluidics. Given that creating small hollow channels has been a technological challenge and achievement in millifluidic, we chose to utilize SLA to develop a novel vascular model. We began with simple container designs, which we referred to as 'chips,' featuring inner hollow tubes. Over time, we incorporated softer curves and more organic structures to simulate a BAVM, with the classical elements of arterial feeders, nidus, and draining veins.

On a second phase of our research, we tested our initial BAVM chip model using the transarterial route embolization within a closed circuit and we were able to confirm its structural and functional reliability. This study was used as a proof of concept that the model could be employed for training, teaching, and research in BAVM embolization.

Through an iterative design process, we reached the final evolution of the BAVM model, where we were able to transfer real patient image data into a computational design and 3D print it. This model was connected to a system with a pump, enabling us to replicate the vascular environment of transvenous embolization. We successfully demonstrated the feasibility of TVE using microcatheters and liquid embolic agents.

This accomplishment marked the creation and testing of the first in vitro BAVM model for TVE using 3D printing, successfully answering our research question.

This unique and innovative model opens new possibilities for teaching, learning, training, and research in endovascular treatment for BAVMs.

Keywords: Brain Arteriovenous Malformations, 3D Printing, Models.